Romanian Journal of
MINERAL DEPOSITS

continuation of

DARI DE SEAMA ALE SEDINTELOR INSTITUTULUI DE GEOLOGIE SI GEOFIZICA
COMPTES RENDUS DES SÉANCES DE L'INSTITUT DE GÉOLOGIE ET GÉOPHYSIQUE
(2. Zacaminte)

Founded 1910 by the Geological Institute of Romania

ISSN 1220-5648

VOL. 85
No. 2

CONTENT

- continued on the back cover -

Geological Institute of Romania
Society of Economic Geology of Romania
Bucharest – 2012

The authors are responsible for the ideas presented in the papers.

ISSN 1220-5648

Volume edited with the support of

SAMAX Romania S.R.L.

and

the “Munții Apuseni” Professional Association, Brad

A PRELIMINARY RAMAN AND FT-IR SPECTROSCOPIC STUDY OF SECONDARY HYDRATED SULFATE MINERALS FROM THE HONDOL OPEN PIT (METALIFERI MTS., ROMANIA)

Andrei Ionuț APOPEI[1,*], Gheorghe DAMIAN[1,2], Nicolae BUZGAR[1]

[1]"Alexandru Ioan Cuza" University of Iaşi, Faculty of Geography and Geology, Department of Geology, 20A Carol I Blv., 700505 Iaşi, Romania, *e-mail: andrei.apopei@geology.uaic.ro
[2]Tech Univ Cluj Napoca, North University Center of Baia Mare, 62A Dr. Victor Babeş Street, 430083 Baia Mare, Romania, damgeo@ubm.ro

Abstract Raman and infrared spectroscopy has been used to analyze three samples from the Hondol open pit, in order to identify and characterize these samples using vibrational features. The minerals found are secondary hydrated sulfate minerals associated with both the alteration of sulfide-bearing mine wastes and primary minerals. The minerals found by vibrational spectroscopy are: ferricopiapite $Fe^{3+}{}_{0.66}Fe^{3+}{}_4(SO_4)_6(OH)_2 \cdot 20(H_2O)$; coquimbite $Fe^{3+}{}_2(SO_4)_3 \cdot 9(H_2O)$; and epsomite $Mg(SO_4) \cdot 7(H_2O)$. The spectral features observed in these minerals allowed four distinct hydrous sulfates to be discriminated without conventional methods, such as XRD or chemical analyzes.

The study shows the potential of Raman and infrared spectroscopy to identify hydrous sulfates very fast, non-destructively, non-invasively, with a very small volume samples.

Both Raman and infrared spectra show the fundamental vibrational modes of SO_4 groups. Also, the spectral variations of the internal modes of sulfate tetrahedra were used to discriminate between minerals from the same group, where divalent or trivalent cations from the octahedral sites or H_2O in different proportions were the only differences.

Keywords: ferricopiapite, epsomite, coquimbite, Vibrational spectroscopy, hydrated sulfates, Hondol deposit

1. Introduction

Raman spectroscopy is regarded as a powerful technique for the characterization of minerals due to its intrinsic features: (i) requires little or no sample preparation; (ii) is highly specific like the chemical fingerprint of a material; (iii) Raman spectra are acquired quickly within seconds; (iv) Raman spectra can be collected from a very small volume (< 1 μm in diameter); (vi) non-destructive, non-invasive and does not interfere with H_2O. Furthermore, there are many other advantages over FT-IR, which is considered in many situations a complementary method because some vibrational modes that are observed in infrared spectra (IR active) are not observed in Raman spectra (Raman inactive) and vice versa. The major differences between these spectroscopic methods are as follows: (i) the infrared spectroscopy requires sample preparation (KBr pellets method) while Raman requires no sample preparation; (ii) the IR spectra are obtained from a mixture (it is not a punctual technique like Raman) and (iii) Raman is applicable to the surface analysis of each mineral (Buzgar et al., 2009a; de Veij et al., 2009; Frezzotti et al., 2012).

In the present study, three samples (see Table 1) have been analyzed using vibrational spectroscopy (Raman and infrared, without any chemical analysis) in the process of fast identification and in order to discriminate the minerals of the samples.

The minerals considered in this paper have been the subject of several studies of vibrational spectroscopy (Bishop, 2004; Makreski et al., 2005; Velasco et al., 2005; Wang et al., 2006; Lane, 2007; Locke et al., 2007; Ling and Wang, 2010; Kong et al., 2011; Frezzotti et al., 2012). Many of these studies focused on the fast and reliable discrimination of anhydrous and hydrous sulfates which occur on Mars' subsurface and in outcrops (Liu et al., 2009). Furthermore, some studies are focused on changes in spectral features caused by cation substitutions. (Lane, 2007; Kong et al., 2011).

2. Geology of the study area

The Hondol open pit is located at the southern extremity of the "Golden Quadrilateral", South Apuseni Mountains (Metaliferi Mts., Romania), approximately 15 km NE of Deva city and has been the focus of previous studies (Ianovici et al., 1976; Uduba a et al., 1982; Alderton et al., 1998; Ciobanu et al., 2004; Ageneau et al., 2006).

The Hondol deposit is broadly characterized by the intrusion of the Hondol andesite and includes the Hondol Carol and Coranda Mica zones. The surface geology of the Hondol open pit prospects is dominated by a highly altered intrusive andesite. The wedge of sediments is typically brecciated, is mineralized at depth and represents the fluid pathway for the Hondol mineralization (Forward et al., 2009). In the Hondol open pit, AMD forms by the dissolution of metal sulfide minerals. Sulfides such as pyrite are oxidized quickly to aqueous Fe^{2+} and $(SO_4)^{2-}$ when O_2 and H_2O are present.

3. Materials and methods

3.1. Sampling

At the bottom of the open pit site, the samples were collected from the surface and stored in polypropylene bags and flasks in order to avoid loss of water. The samples were prepared by hand picking under binocular stereo microscope (45x) in order to analyze them with Raman spectrometer. Also, they were finely powdered to allow the analysis with the FT-IR spectrometer.

3.2. Analytical methods

3.2.1. Raman analysis. The Raman spectra were obtained at room temperature with a Raman Spectrograph Horiba Jobin-Yvon RPA-HE 532 with a multichannel air-cooled (-70°C) CCD detector using an excitation source Nd-Yag laser 532 nm and a nominal power of 100 mW. The spectra were obtained in the spectral range between 210 and 3400 cm^{-1} with a spectral resolution of 3 cm^{-1}. The Raman system includes a "Superhead" optic fibre Raman probe for non-contact measurements, with a 50X LWD visible objective Olympus, NA = 0.50 WD = 10.6 mm. Sulphur and ciclohexane bands were used for the calibration of the wavenumbers of Raman spectra. Data acquisition was performed by 3-100 seconds exposure time (in most cases an exposure of 4-20 seconds was sufficient to obtain a good spectra), 10-100 acquisitions, at a laser magnification of 50-65% (50% - 3.90 mW; 60% - 7.37 mW; 70% - 14.3 mW; 80% - 22.9 mW; 90% - 35.8 mW; 100% - 53.6 mW) in order to improve the signal-to-noise ratio and also to avoid any photochemical and/or thermal degradation (see further discussion). Spectra manipulations consist of basic data treatment, such as smoothing adjustments and peak fitting (Lorentz function); however, some spectra are presented as acquired for a better interpretation.

3.2.2. Fourier-transform infrared analysis. The mid-IR spectra were collected with a Bruker Vertex 70 Fourier-transform infrared (FT-IR) spectrometer with a spectral resolution of 3 cm^{-1} and the spectral range between 370-4000 cm^{-1}. The measurements were taken at room temperature using a KBr pellet technique. The infrared spectra were analyzed with an OPUS 6.5 software and for the resulting spectra, we choose the type of absorption spectrum. The fitting procedure of the spectra was not used.

Table 1. Names and ideal chemical formulas for minerals identified in this study

Sample ID	Mineral name	General formula	Geographic coordinates
CH001A	Ferricopiapite	$Fe^{3+}_{0.66}Fe^{3+}_4(SO_4)_6(OH)_2 \cdot 20(H_2O)$	N 45° 59' 32.9" / E 23° 0' 26.2"
CH002A	Coquimbite	$Fe^{3+}_2(SO_4)_3 \cdot 9(H_2O)$	N 45° 59' 39.2" / E 23° 0' 22.0"
CH003A	Epsomite	$Mg(SO_4) \cdot 7(H_2O)$	N 45° 59' 32.6" / E 23° 0' 39.4"

4. Results and discussion

4.1. Fundamental Raman and IR vibrational modes of uncoordinated and coordinated sulfate species

Early Raman and infrared spectroscopic studies have shown that the sulfate anion $(SO_4)^{2-}$ in aqueous solution produces four fundamental vibrational features: (i) around 1104 cm^{-1}; (ii) ~981 cm^{-1}; (iii) ~613 cm^{-1} and (iv) ~451 cm^{-1} (Nakamoto, 1986; Bishop and Murad, 2005; Lane, 2007; Buzgar et al., 2009b). The vibrational bands in the 900-1300 cm^{-1} spectral range arise from the Raman active symmetrical (ν_1) and IR active asymmetrical (ν_3); both of these (ν_1 and ν_3) are stretching vibrational modes. The other two fundamental vibrational features (ν_2 and ν_4) are assigned to symmetrical bending modes (ν_2) around ~610 cm^{-1}, respectively to asymmetrical bending modes (ν_4) around ~450 cm^{-1}. But this is the case when $(SO_4)^{2-}$ tetrahedra vibrates freely in aqueous solution. While in sulfate mineral species (and not only in the case of sulfates) these vibrations are modified due to (i) the repeating molecular units and (ii) the influences of the symmetry changes when $O^{2-}/(OH)^-$ is shared with other sulfate tetrahedra or connects different types of cation sites (e.g. M = Ca, Mg, Fe, Al). Furthermore, in Raman and mid-IR spectra there also occur vibrational modes of hydroxyl and water molecules.

4.2. Raman and infrared results

From the bulk samples of Hondol open pit were obtained 25 preliminary spectral analyses. Generally, all the samples contain sulfate minerals in sufficient proportion to be easily identified by comparison with the reference spectra database (Downs, 2006; Buzgar et al., 2009a).

Raman and infrared analysis allowed the identification of a variety of salts including: ferricopiapite, coquimbite and epsomite.

Figs. 1 and 2 show three Raman and infrared spectra collected on the bulk samples. These spectra are split into three main spectral regions: from 210 to 1500 cm^{-1} corresponding to the region of SO_4 tetrahedra (internal and external vibrations), 1500 to 1800 cm^{-1} for water bending vibration and 2600 to 3800 cm^{-1} for water stretching vibrations, respectively.

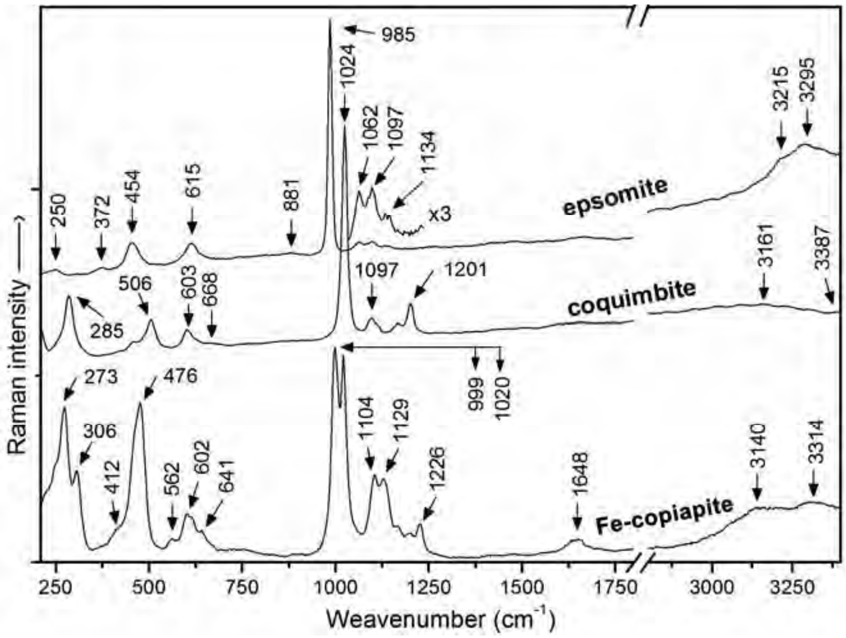

Fig. 1. Raman spectra of the sulfates found in the Hondol open pit. Spectra are offset for clarity.

4.2.1. Ferricopiapite. The Raman bands in the 980 – 1025 cm^{-1} region are due to the ν_1 symmetrical stretching mode of SO_4 groups. In the case of Raman spectrum of ferricopiapite, two strong bands arise at 999 cm^{-1} and 1020 cm^{-1}.

In accordance with Kong et al. (2011), a systematic peak shifting was observed in the copiapite group, where, from a crystallographic point of view, the structure consists of three distinct sites for the SO_4 tetrahedra, and these different sites generate multiple peaks for ν_1 mode. In the copiapite group there are two distinct octahedral sites: one is connected with $(SO_4)^{2-}$ by sharing O^{2-} and the other is isolated and occupies the space between the sheets formed by infinite chains. Because the octahedral sites are connected with SO_4 tetrahedra by sharing O^{2-}, the Raman bands shift due to the cations with different ionic radii, masses and charges. Furthermore, for the divalent copiapite species, an additional shoulder peak arises at ~1005 cm^{-1}, which is not the case for our spectra.

Based on the assumption made by Kong et al. (2011), the higher ν_1 mode of $(SO_4)^{2-}$ shifts from 1019 cm^{-1} for ferricopiapite (with Fe^{3+}) to 1026 cm^{-1} for copiapite (with Fe^{2+}). The Raman peaks at 1104, 1129, 1166 and 1199 cm^{-1} are assigned to ν_3; while the ν_2 and ν_4 modes arise at: 412 (sh), 476 cm^{-1} and 602, 641 cm^{-1}, respectively.

On the other hand, infrared spectrum of ferricopiapite (Fig. 2) reveals characteristic absorbance bands at 1000 cm^{-1} (ν_1 mode) and ν_3 mode of SO_4, which appears as a doublet at 1080 cm^{-1} and 1139cm^{-1}, respectively. The broad absorption bands, which appear in the 2800 – 3600 cm-1 spectral range (in all samples), are due to the presence of water in the chemical structure. Also, in this spectral domain, the OH^- stretching vibration occurs, but this vibration is mainly masked by water bands (only in the case of ferricopiapite with OH^- in crystal structure). The infrared absorption peaks around 1650 cm^{-1} are due to the water bending mode (Lane, 2007; Buzgar et al., 2009b).

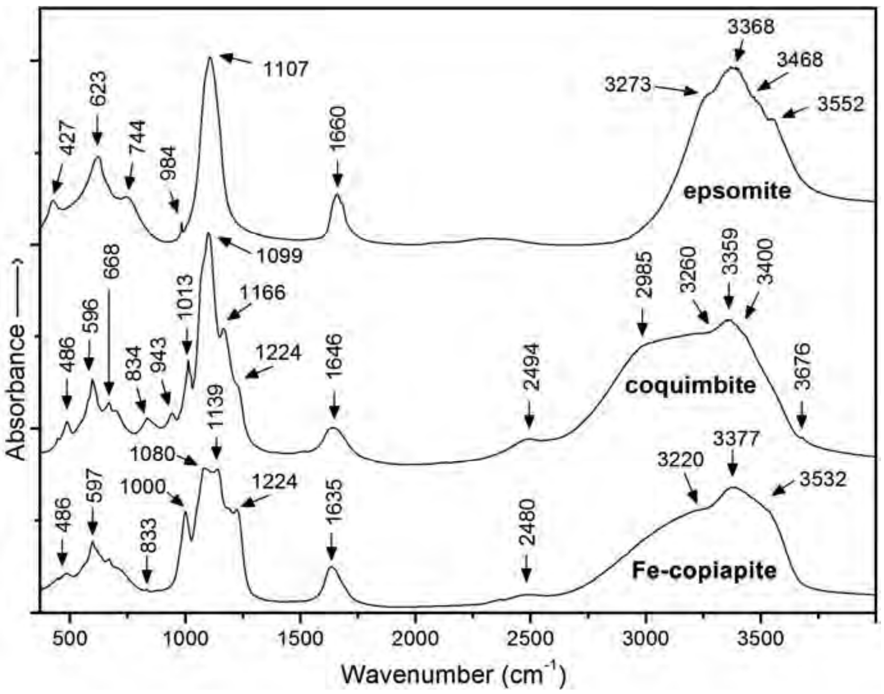

Fig. 2. FT-IR spectra of the sulfates found in the Hondol open pit. Spectra are offset for clarity.

4.2.2. Coquimbite. Coquimbite, $Fe^{3+}{}_2(SO_4)_3 \cdot 9(H_2O)$, and paracoquimbite, $Fe^{3+}{}_2(SO_4)_3 \cdot 9(H_2O)$, are both iron(III) sulfate nonahydrates (nine molecules of water). Bearing this in mind, the Raman spectra of coquimbite and paracoquimbite are quite similar, and it is very difficult to distinguish between them (Downs, 2006). The Raman bands (Fig. 1) found in samples of coquimbite from the Hondol open pit fit very well the literature values (Downs, 2006; Ling and Wang, 2010). The ν_1 peak of coquimbite appears as one sharp band at 1024 cm^{-1}. The peaks at 1097, 1112 (sh), 1168 and 1201 cm^{-1} are assigned to ν_3 while the ν_2 and ν_4 modes arise at: 458 (sh) cm^{-1}, 506 cm^{-1} and 603 cm^{-1}, 668 cm^{-1}, respectively.

Infrared spectrum of coquimbite (Fig. 2) is dominated by the fundamental vibrations of the SO_4 groups with the maxima at 1099 cm^{-1} and adjacent Raman peaks at 1076 (sh), 1166 and 1224 cm^{-1}, which are assigned to ν_3 mode. The other fundamental vibrations of the SO_4 groups are found in infrared spectrum of coquimbite at 1023 (sh) cm^{-1} assigned to ν_1; at 446 (sh) and 486 cm^{-1} assigned to ν_2 mode; and at 578 (sh), 596, 610 (sh), 668, 694 (sh) cm^{-1} due to the ν_4 vibrations. The absorption peaks observed in the infrared spectrum of coquimbite (Fig. 2) fit very well the literature data (Bishop, 2004; Downs, 2006; Lane, 2007; Ling and Wang, 2010).

4.2.3. Epsomite. The identification of the epsomite is confirmed by the analysis of its Raman spectrum (Fig. 1). Here, it should be pointed out that the very strong band at 985 cm^{-1} due to the ν_1 vibrational mode has also been observed by Lakshman (1941); Makreski et al. (2005); Buzgar et al. (2009b); and Frezzotti et al. (2012). The other fundamental bands of epsomite are found at: 454 cm^{-1} (ν_2); 1062, 1097, 1134 cm^{-1} (ν_3) and 615 cm^{-1} (ν_4). The Raman peaks at 250 cm^{-1} and 372 cm^{-1} were assigned to the vibrations of the Mg-O bond, where oxygen is from H_2O (Buzgar et al., 2009b). The broad band with two quite well resolved peaks at 3215 (sh) cm^{-1} and 3295 cm^{-1} was also reported by Lakshman (1941) due to the H_2O stretching vibrations.

The infrared spectrum of epsomite also reveals the characteristic peaks with maxima at 1107 cm^{-1} assigned to (ν_3); and the other fundamental vibrations at 984 cm^{-1} (ν_1); 427 cm^{-1} (ν_2) and 623 cm^{-1} (ν_4). Positions of the peaks are in a good agreement with the literature values (Makreski et al., 2005; Ruiz-Agudo et al., 2008).

5. Conclusions

The successful identification and characterization of the spectral features in the sulfates samples taken from the Hondol open pit allows the following conclusions to be drawn:

(1) The Raman and IR spectral results obtained on the sulfates from the Hondol open pit are in good agreement with other data; and were found all of the fundamental vibrational modes of sulfate anion (ν_1, ν_2, ν_3 and ν_4). Also, other spectral features identified in all the analyzed minerals (and in both type of spectra) are the vibrational modes of the H_2O and the translational modes between cation-oxygen.

(2) These minerals identified by vibrational spectroscopy are formed as a result of the oxidation of metal sulfides (such as pyrite, which quickly oxidize to aqueous Fe^{2+} and $(SO_4)^{2-}$ when O_2 and H_2O are present) and are due to the crystallization from the solution. The Neogene conglomerates can be the source of the magnesium, which is present in epsomite.

(3) Another conclusion is that the presence of the identified sulfates is a clear evidence of the impact of AMD on the surrounding environment.

(4) Raman is a punctual technique, while the infrared is a mixture technique (if some “undesired” mineral particles remain after the separation at binocular stereo microscope) and for this reason further measurements (X-ray diffraction) may be able to solve the uncertainties of the AMD crust composition for the other bulk samples (not included in this study).

Acknowledgments

The authors gratefully acknowledge the staff of S.C. DevaGold S.A. for access on the Hondol open pit and their support on the sampling site.

References

Ageneau M., Mastrodicasa L., Marton I., 2006. Magmatism and metallogeny of the Certej-Săcărâmb District, Apuseni Mts. Romania Field Trip SEG Student Chapters Uni Geneva - ETH Zürich - Uni Budapest - Uni Cluj.

Alderton D.H.M., Thirlwall M.F., Baker J.A., 1998. Hydrothermal alteration associated with gold mineralization in the southern Apuseni mountains, Romania: preliminary Sr isotopic data. Mineralium Deposita 33, 520-523.

Bishop J.L., Murad E., 2005. The visible and infrared spectral properties of jarosite and alunite. American Mineralogist 90, 1100-1107.

Bishop J.L.D., Lane M. D.; Banfield J. F., 2004. Spectral identification of hydrated sulfates on Mars and comparison with acidic environments on Earth. International Journal of Astrobiology 3, 275-285.

Buzgar N., Apopei A., Buzatu A., 2009a. Romanian Database of Raman Spectroscopy (http://rdrs.uaic.ro).

Buzgar N., Buzatu A., Sanislav I.V., 2009b. The Raman study on certain sulfates. Anal. Şt. Univ. “Al. I. Cuza” Iaşi, Geologie LV, 5-23.

Ciobanu C., Cook N.J., Damian G., Damian F., Buia G., 2004. Telluride and sulphosalt associations at Săcărâmb. Gold-Silver-Telluride Deposits of the Golden Quadrilateral, South Apuseni Mts., Romania. Guidebook of the International Field Workshop of IGCP project 486, Alba Iulia, Romania, 31st August - 7th September 2004.

de Veij M., Vandenabeele P., De Beer T., Remonc J.P., Moens L., 2009. Reference database of Raman spectra of pharmaceutical excipients. Journal of Raman Spectroscopy 40, 297-307.

Downs R.T., 2006. The RRUFF Project: an integrated study of the chemistry, crystallography, Raman and infrared spectroscopy of minerals. Program and Abstracts of the 19th General Meeting of the International Mineralogical Association in Kobe, Japan. O03-13.

Forward P., Liddell N., Jackson T., 2009. Certej Updated Definitive Feasibility Study Summary Technical Report. European Goldfields Limited.

Frezzotti M.L., Tecce F., Casagli A., 2012. Raman spectroscopy for fluid inclusion analysis. Journal of Geochemical Exploration 112, 1-20.

Ianovici V., Borco M., Bleahu M., Patrulius D., Lupu M., Dimitrescu R., Savu H., 1976. The Geology of Apuseni Mountains (Geologia Munților Apuseni). (In Romanian). Editura Academiei Republicii Socialiste România, Bucharest. 605 pp.

Kong W.G., Wang A., Freeman J.J., Sobron P., 2011. A comprehensive spectroscopic study of synthetic Fe^{2+}, Fe^{3+}, Mg^{2+} and Al^{3+} copiapite by Raman, XRD, LIBS, MIR and vis-NIR. Journal of Raman Spectroscopy 42, 1120-1129.

Lakshman R.B., 1941. Raman spectra of some crystalline nitrates and sulphates. Proceedings of the Indian Academy of Science A 14, 49-54.

Lane M.D., 2007. Mid-infrared emission spectroscopy of sulfate and sulfate-bearing minerals. American Mineralogist 92, 1-18.

Ling Z.C., Wang A.L., 2010. A systematic spectroscopic study of eight hydrous ferric sulfates relevant to Mars. Icarus 209, 422-433.

Liu Y., Wang A., Freeman J.J., 2009. Raman, MIR, and NIR spectroscopic study of calcium sulfates: gypsum, bassanite, and anhydrite. 40th Lunar and Planetary Science Conference.

Locke A.J., Martens W.N., Frost R.L., 2007. Natural halotrichites - An EDX and Raman spectroscopic study. Journal of Raman Spectroscopy 38, 1429-1435.

Makreski P., Jovanovski G., Dimitrovska S., 2005. Minerals from Macedonia XIV. Identification of some sulfate minerals by vibrational (infrared and Raman) spectroscopy. Vibrational Spectroscopy 39, 229-239.

Nakamoto K., 1986. Infrared and Raman Spectra of Inorganic and Coordination Compounds. 4th ed. Wiley-Interscience, New York. 484 pp.

Ruiz-Agudo E., Putnis C.V., Rodriguez-Navarro C., 2008. Interaction between epsomite crystals and organic additives. Crystal Growth & Design 8, 2665-2673.

Udubaşa G., Istrate G., Vălureanu M., 1982. Metallogenesis of Coranda - Hondol region, Metaliferi Mountains (Metalogeneza regiunii Coranda - Hondol, Munții Metaliferi). (In Romanian). D.S. Inst. Geol. LXVII/2, 197-232.

Velasco F., Alvaro A., Suarez S., Herrero J.-M., Yusta I., 2005. Mapping Fe-bearing hydrated suphate minerals with short wave infrared (SWIR) spectral analysis at San Miguel mine environment, Iberian Pyrite Belt (SW Spain). Journal of Geochemical Exploration 87, 45-72.

Wang A., Freeman J.J., Jolliff B.L., Chou I.M., 2006. Sulfates on Mars: A systematic Raman spectroscopic study of hydration states of magnesium sulfates. Geochimica Et Cosmochimica Acta 70, 6118-6135.

RAMAN AND INFRARED STUDIES OF WEATHERING PRODUCTS FROM BAIA SPRIE ORE DEPOSIT (ROMANIA)

Andrei BUZATU[1,*], Gheorghe DAMIAN[1,2], Nicolae BUZGAR[1]

[1]University "Al. I. Cuza" of Iaşi, Department of Geology, 20A Carol I Av., 700505 Iaşi, Romania. *e-mail: andrei.buzatu@geology.uaic.ro

[2]Tech Univ Cluj Napoca, North University Center of Baia Mare, 62A Dr. Victor Babeş Street, 430083 Baia Mare, Romania, damgeo@ubm.ro

Abstract Preliminary investigations were carried out on secondary minerals formed by weathering in the Minei Hill open pit (Baia Sprie deposit, Romania). Several samples were analyzed using vibrational spectroscopy (Raman and FT-IR) in order to identify the mineral species formed by the weathering of the main ore minerals. The Raman spectra revealed the presence of hydrated iron sulfate – rozenite ($FeSO_4 \cdot 4H_2O$) and a hydrated zinc sulfate – either bianchite $(Zn,Fe)SO_4 \cdot 6H_2O$ or goslarite ($ZnSO_4 \cdot 7H_2O$). The IR spectra of the weathering product indicated the presence of rozenite and goslarite. These two minerals are products of sphalerite and pyrite weathering. No lead sulfates were identified in Raman or IR spectra. The presence of rozenite and goslarite can represent a source for environmental contamination.

Keywords: Baia Sprie; Raman Spectroscopy; IR; rozenite, goslarite.

1. Introduction

The Baia Sprie ore deposit is situated on the southern part of Oaş-Gutâi-Țibleş volcanic chain (Romania), and is genetically linked with the Minei Hill andesite structure, which evolved on an area of 2 km x 360 m (Stanciu, 1973). Geologically, the Baia Sprie deposit is placed in sedimentary formations (argillaceous marls) of Pannonian age, and is related to pyroxene-andesites of Pontian age (Jereapăn), which in turn are considered to be a dyke or a complex effusive volcanic body associated with pyroclastic lava flows (Borcoş et al., 1973). Later papers interpreted the compartment as a graben with volcanic rock filling (Iştvan et al., 1996).

The Baia Sprie ore deposit is epithermal, of low-sulfidation type (Damian et al., 2003). The mineralogy of the deposit is very complex and presents a wide range of paragenesis of native elements (S, As, Au, Ag), common metallic sulfides, sulfosalts, arsenides, oxides, antimonides, carbonates, sulfates, wolframates, silicates, phosphates. The most frequent minerals are pyrite, chalcopyrite, sphalerite, galena, stibnite, quartz, barite, dolomite, adularia, calcite, chlorite, wolframite (Borcoş et al., 1973). In the upper part (Minei Hill) the deposit occurs as branched veins and stockwork-type ores (Damian et al., 2003). Locally contains also voltaite – the former monsmedite (Johan et al., 2009; Kovács-Pálffy et al., 2011).

The mining activity that took place in the past at the Baia Sprie left behind at the surface the sulfide-bearing material, which under atmospheric conditions can lead to the formation of secondary minerals, such as metal-bearing sulfates. These minerals are very soluble and can release the metals in the environment, during the complex process of acid mine drainage. Thus, it is important to know the mineral species that form through weathering in such mining sites and how they can affect the environment.

Fig. 1. The appearance of secondary minerals in the field (Minei Hill open pit)

2. Materials and methods

2.1. Sampling

Several samples of weathering products were studied using Raman and infrared spectroscopy. The samples were collected from the Minei Hill open pit, in the eastern part of the Baia Sprie ore deposit. The weathering product is developed on the surface of mineralized (sphalerite and galena) areas and occurs as a white fine deposition material (Fig. 1).

2.2. Experimental

The Raman spectra were acquired using a Horiba Jobin–Yvon RPA–HE 532 Raman Spectrograph with a multichannel air cooled (–70°C) CCD detector, using a frequency doubled NdYag laser at 532 nm and a nominal power of 100 mW. The spectral range was 200–3400 cm^{-1}, and the spectral resolution of 3 cm^{-1}. The Raman system includes a "Superhead" fibre optic Raman probe for non-contact measurements, with a 50X LWD Olympus visible objective. Sulphur and cyclohexane bands were used for the calibration of the frequencies of the Raman spectra.

The mid-IR spectra were collected with a Bruker Vertex 70 Fourier transfrom infrared (FT-IR) spectrometer with a spectral resolution of 3 cm^{-1} and the spectral range between 370-4000 cm^{-1}. The measurements were taken at room temperature, using a KBr pellet technique. The infrared spectra were analyzed with the OPUS 6.5 software and for the resulting spectra, the absorption spectrum was chosen.

3. Results and discussion

The weathering products collected from the open pit, in the east part of Minei Hill, are present as a white fine material coating the massive mineralized areas with galena and sphalerite (Fig. 1). These secondary minerals have been studied through Raman and infrared spectroscopy.

3.1. Raman spectroscopy

The Raman spectra (Fig. 2) revealed two distinctive minerals. One interesting aspect was found during the experiment. Under the laser excitation, the sample revealed one spectrum in the first seconds of exposure, and in less than two minutes, the spectrum was changed to a different one. The first type of Raman spectrum is characteristic to rozenite ($FeSO_4 \cdot 4H_2O$), showing the typical Raman bands for sulfate minerals, namely the four fundamental vibration modes. The symmetric stretching ν_1 is observed at 992 cm^{-1}, the symmetric bending ν_2 at 480 cm^{-1}, the asymmetric stretching ν_3 and bending ν_4 at 1080 and 1153 cm^{-1}, and 611 cm^{-1} respectively. Several authors reported these values for rozenite (Chio et al., 2007; Downs, 2006). The second type of Raman spectrum is showing the ν_1 mode shifted at higher wavenumbers (1024 cm^{-1}), the vibrations assigned to ν_2 are found at 427 and 506 cm^{-1}, ν_4 mode at 626 cm^{-1} and the ν_3 modes at 1080 and 1191 cm^{-1}. These peaks were found to correspond to hydrated zinc sulfate, bianchite ($(Zn,Fe)SO_4 \cdot 6H_2O$) or goslarite ($ZnSO_4 \cdot 7H_2O$) (Buzgar et al., 2009; Downs, 2006). These two minerals have very similar Raman spectra due to the same type of structure, which makes the identification difficult.

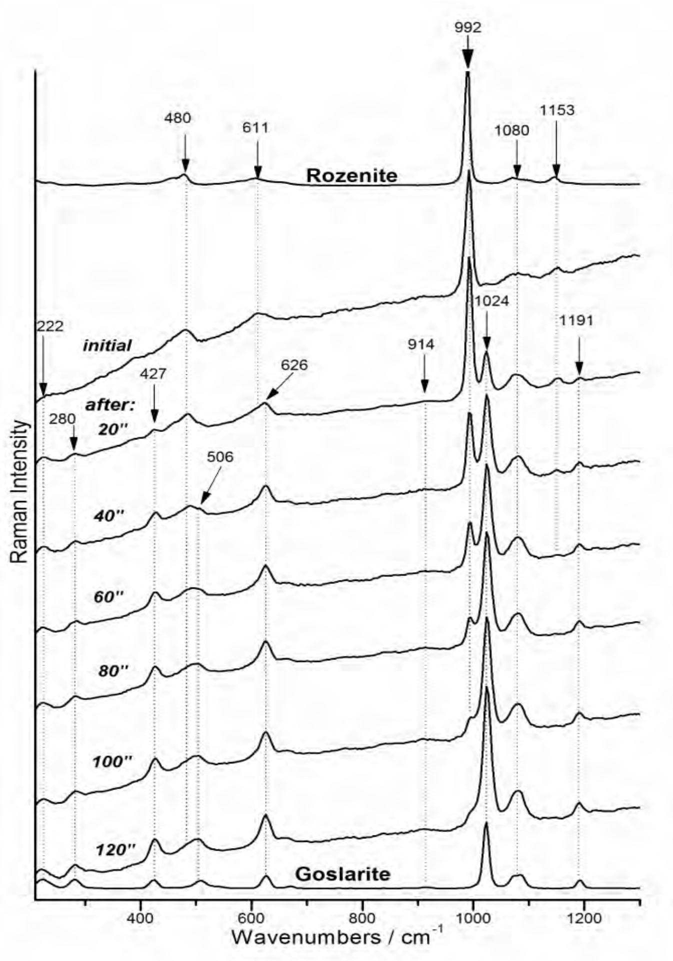

Fig. 2. The Raman spectra acquired on weathering product sample and rozenite (Downs, 2006) and goslarite (Buzgar et al., 2009) standards

The changes that take place during the Raman analysis were observed at laser intensity higher than 60% (7.37 mW). Thus, it is possible that these changes are due to laser radiation, which at 100% intensity gives a power on the sample surface of 53.6 mW. It is possible that rozenite is unstable under laser irradiation, due to the oxidation of Fe^{2+} to Fe^{3+}. Less Raman signal is received from rozenite during the lattice destruction, and thereby the hydrated zinc sulfate, which was masked by rozenite, dominates the Raman spectrum.

3.2. Infrared spectroscopy

The IR spectrum confirms the presence of goslarite in the sample (Fig. 3). The ν_1 vibrational mode of SO_4 is observed at 1009 cm^{-1}, at 459 cm^{-1} is present the ν_2 mode, at 1108, 1157 and 1267 cm^{-1} – ν_3 modes, and the ν_4 vibration modes are shown at 610, 632 and 655 cm^{-1}. The bending of O-H bonds is observed at 758 and 882 cm^{-1}, while the stretching mode at 577 cm^{-1}. The band at 985 cm^{-1} is assigned to the liberation modes of water molecules. The bending of H_2O appears at 1616 cm^{-1} and the strong stretching vibrations are observed at values higher than 2800 cm^{-1}. These IR bands were also reported by Saha and Podder (2011) for goslarite, except for the ν_3 modes, where a value of 1090 cm^{-1} was indicated. The intense ν_3 bands from this study can be assigned to rozenite spectrum, which is overlapped by the goslarite bands. An IR band was reported at 1100 cm^{-1} for rozenite and at 1149 cm^{-1} for szomolnokite ($FeSO_4 \cdot H_2O$). The presence of szomolnokite could be possible since rozenite can dehydrate readily (Lane, 2007). The other characteristic IR bands of the hydrated iron sulfate are mostly the same and overlapped by the goslarite bands, such as: 1680, 1220, 992, 760, 660 and 645 cm^{-1} (Lane, 2007).

Goslarite and rozenite have been observed as sphalerite and pyrite oxidation products. These minerals can hydrate, dehydrate, dissolute and recrystallize with seasonal variations in temperature and rainfall (Anderson et al., 2005). The iron content is provided by the sphalerite which can reach up to 3.8% Fe (Manilici et al., 1965) together with the presence of pyrite and chalcopyrite in smaller amounts.

The presence of these minerals represents a source for environmental contamination, through dissolution of the soluble sulfates with high concentrations of metals (Anderson et al., 2005).

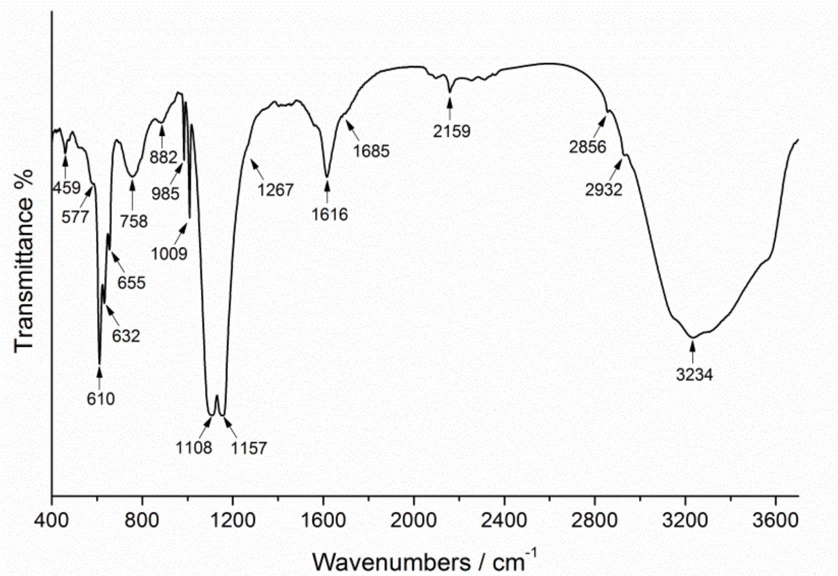

Fig. 3. The IR spectrum obtained on the weathering product sample

4. Conclusions

The weathering product samples collected from the upper part of the Baia Sprie deposit, in the open pit from Minei Hill, were successfully analyzed by Raman and infrared spectroscopy. These techniques allowed a fast and easy identification of the secondary mineral species present in the samples.

The Raman spectra show the presence of rozenite ($FeSO_4 \cdot 4H_2O$) and a hydrated zinc sulfate - either bianchite ($(Zn,Fe)SO_4 \cdot 6H_2O$) or goslarite ($ZnSO_4 \cdot 7H_2O$). The clear distinction between these last two minerals can be difficult due to the very similar Raman spectra. It was observed that rozenite is very unstable in the samples, and a clear Raman spectrum can be obtained only at laser powers less than 7.37 mW. The infrared spectra also revealed the characteristic four fundamental vibration modes in sulfates, as in the case of Raman spectra. The presence of goslarite and rozenite was observed.

The source of these secondary sulfates can be explained by the weathering of sphalerite and pyrite, which are subject to atmospheric conditions. The observed minerals are unstable and can contribute to the retention and release of metals to the environment in the process of acid mine drainage.

References

Anderson J. L., Peterson R. C., Swainson I. P., 2005. Combined neutron powder and X-ray single-crystal diffraction refinement of the atomic structure and hydrogen bonding of goslarite ($ZnSO_4 \cdot 7H_2O$). Mineralogical Magazine, 69, 259-271.

Borcoş M., Lang B., Boştinescu S., Mîndroiu V., Volanschi E., 1973. Considerations on metallogenetic activity associated with pontian pyroxene andesites from Gutîi mountains. Institutul Geologic Român - Studii tehnice şi economice, 9, 108.

Buzgar N., Buzatu A., Sanislav I. V., 2009. The Raman study on certain sulfates. Analele tiinţifice ale Universităţii "Al. I. Cuza" Iaşi, Geologie, LV-1, 5-23.

Chio C. H., Sharma S. K., Muenow D. W., 2007. The hydrates and deuterates of ferrous sulfate ($FeSO_4$): a Raman spectroscopic study. Journal of Raman Spectroscopy, 38, 87-99.

Damian G., Damian F., Cook N. J., Ciobanu C. L., 2003. Ag-Sulphosalts in upper parts of the Baia Sprie deposit (Romania): microanalyses and implications for the deposit zonality. Studia Universitatis Babeş-Bolyai Cluj-Napoca, Seria Geologia, Special Issue, 37-39.

Downs R.T., 2006. The RRUFF Project: an integrated study of the chemistry, crystallography, Raman and infrared spectroscopy of minerals. Program and Abstracts of the 19th General Meeting of the International Mineralogical Association in Kobe, Japan, O03-13.

Iştvan D., Halga S., Vârşescu I., Grancea L., Chiuzbăian C., 1996. New data on the upper part of the Baia Sprie deposit, East Carpathians, Romania. Analele Ştiinţifice ale Universităţii "Al. I. Cuza" Iaşi, Geologie, XLII - supliment 101-110.

Johan Z., Udubaşa G., Zemann J., 2009. “Monsmedite”, a discredited potassium thallium sulphate mineral from Baia Sprie and its identity with voltaite: The state of the art. Neues Jahrbuch für Mineralogie - Abhandlungen, 186, 63-66.

Kovács-Pálffy P., Muske J., Földvári M., Kónya M., Homonnay Z., Ntaflos T., Papp G., Király E., Sajó I., Szilágyi V., Bozsó G., 2011. Detailed study of „monsmedite” specimens from the original (1963) find, Baia Sprie, Baia Mare ore district (Romania). Carpathian Journal of Earth and Environmental Sciences, 6, 321-330.

Lane M.D., 2007. Mid-infrared emission spectroscopy of sulfate and sulfate-bearing minerals. American Mineralogist, 92, 1-18.

Manilici V., Giuşcă D., Stiopol V., 1965. Study of Baia Sprie ore deposit (in Romanian). Memoriile Comitetului Geologic, Institutul Geologic Bucuresti, VII, 1-95.

Saha J. K., Podder J., 2011. Crystallization of zinc sulphate single crystals and its structural, thermal and optical characterization. Journal of Bangladesh Academy of Sciences, 35, 203-210.

Stanciu C., 1973. The hydrothermalism in Herja and Baia Sprie ore deposits (in Romanian). Institutul Geologic Român - Studii tehnice şi economice, 9, 73-92.

MĂNĂŞTUR SALT DEPOSITS (CLUJ-NAPOCA) – PRELIMINARY INVESTIGATIONS

Dana Monica SAVA[1], Aura CEHLAROV[2], Gheorghe C. POPESCU[3], Antonela NEACŞU[3], Iulia NEGREA[3]

[1] F&R Worldwide, 2, D. Danielopolu Street, Bucharest, msava@fandr.ro
[2] University Oil- Gas Ploiesti, 39, Bucuresti Blvd., 100680 Ploiesti
[3] Dept of Mineralogy, Faculty of Geology and Geophysics, University of Bucharest, 1, N. Bălcescu Blvd., 010041 Bucharest, ghpop@geo.edu.ro, antonela.neacsu@gmail.com, iulia_biri@yahoo.com

Abstract: In the Transylvanian Basin, almost all the salt occurrences occupy negative landscape forms, placed in floodplains at confluence of watercourses, or at higher altitudes, within terraces or piedmont. Unexpectedly, a salt layer was encountered in some of the drill holes of the eastern part of Cluj-Napoca - Mănăştur perimeter.

Keywords: halite lithofacies, decreasing degree of recrystallization, biphasic fluid inclusions, cracking pressure, halokinesis

1. Introduction

During the geotechnical works occasioned by building an oil reservoir in the eastern part of Cluj-Napoca – Mănăştur perimeter (Fig. 1), a salt layer was found in some of the drill holes, starting at a depth of 13 m. In the drill hole no. 13 salt was encountered between 13–16.7 m, in the drill hole no. 8 between 15-18 m, and in the boring no. 3 between 18-22 m in depth (Fig. 2).

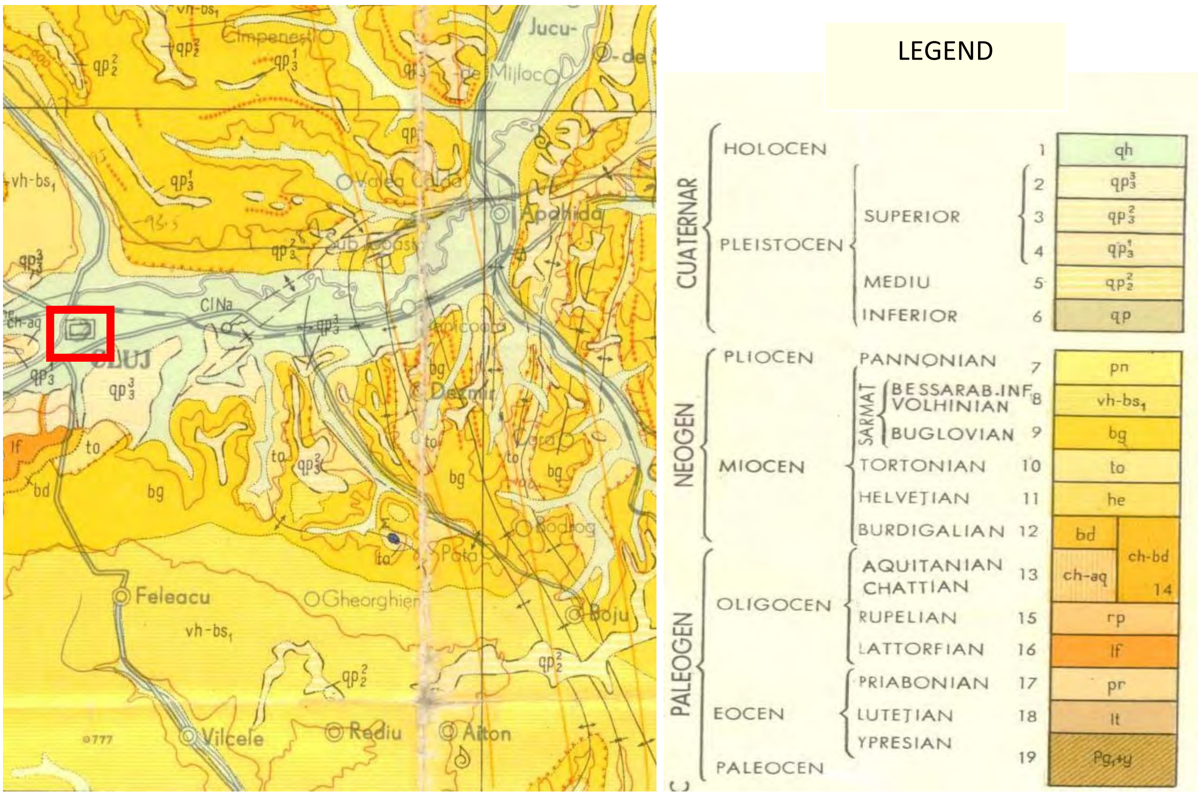

Fig. 1. Geological map of the Cluj - Apahida area (Dumitrescu, 1968) with the indication of Mănăştur investigated area

2. Mesoscopic, structural, textural and microscopic analyses of salt

The analyzed material was presented as salt cores, and is differentiated by colour; in the drill hole no.8 it shows blue–gray colour with white translucent intercalations; in the drill hole no. 13, the colour of salt is generally white, with glassy–gray separations; and in the drill hole no. 18 it is white-translucent. Therefore, this material presents common characters and can be assigned to evaporite petrofacies, a halite lithofacies, and can be seen as recrystallized halite. The textural character is idiotopic and hipidiotopic with linear contacts, showing macrocrystalline features. This structural character is the result of a chemical precipitation and of some diagenetic transformations, manifested by a decreasing degree of recrystallization (Fig. 3).

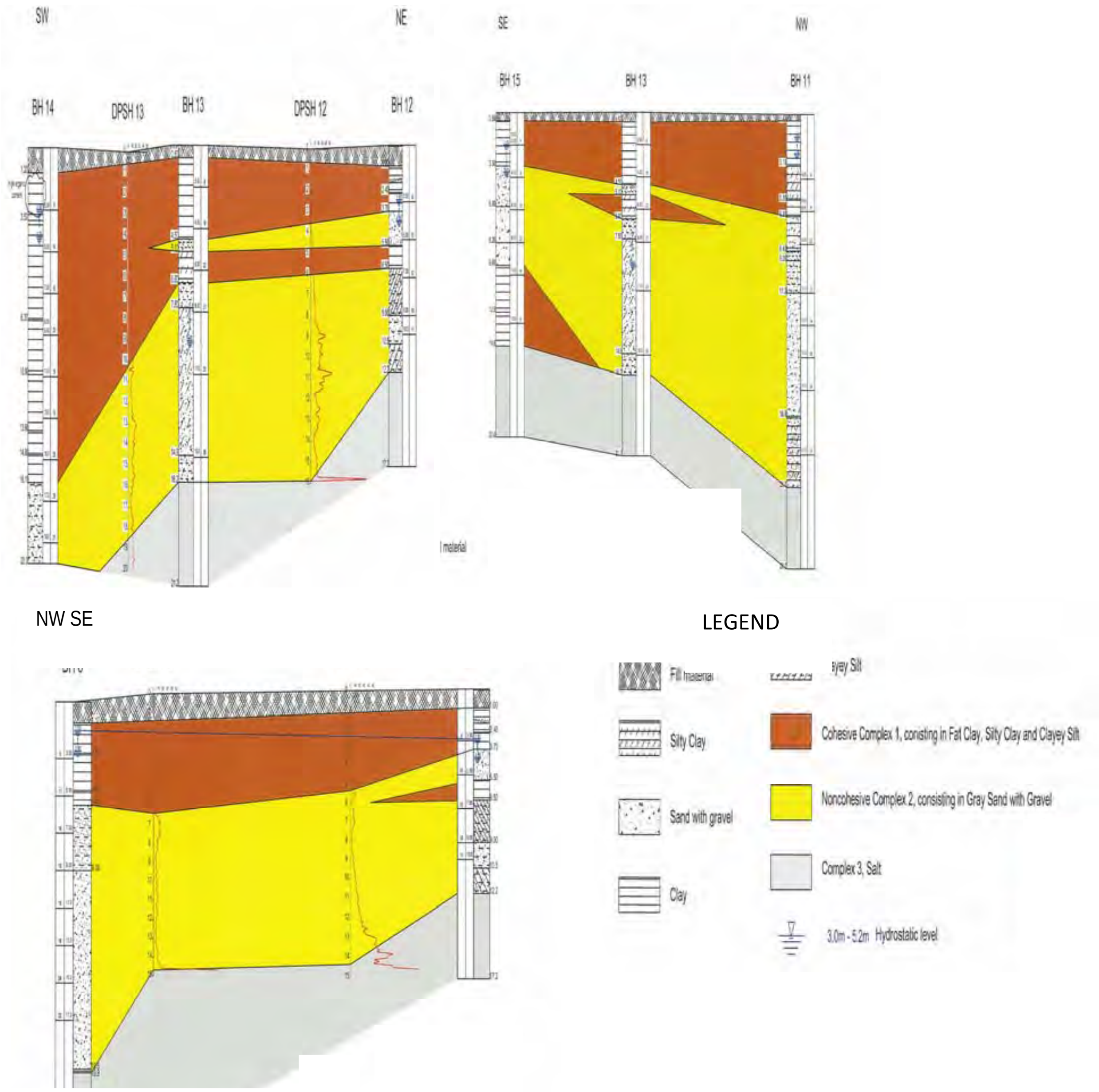

Fig. 2. Geological sections through the salt lens of Mănăştur encountered in drill holes no. 8, 11,12,13,14, and 15

Fig. 3. Mesoscopic image of a sample from the drill hole no. 13

From the mesoscopic point of view, the crystallized material is composed by large, translucent, nested crystals, locally sugar–white and dark–gray in some parts. The comparative microscopic analyses (immersion liquid, nitrobenzene, and refraction index 1.5503 – 1.5523) from the white and gray portions, does not present significant differences. Both sectors present halite as clear crystals, with anhydrite inclusions, and accidentally very small red biotitic lens are found.

In thin sections, the microscopic analyses mainly show a percentage over 95% of halite, less contaminated with clayey material; completely subordinate is the presence of anhydrite ($CaSO_4$), arranged as isolated prismatic crystals or rarely as clusters of prismatic crystals (Annex 1, Fig. B-C). It should be noted that the salt from the drill hole no. 13, sampled at a depth of 15-18m, contains a high percentage of anhydrite, and the salt from the drill hole no. 18, sampled at a depth of 13-15m, contains less anhydrite. Anyway, anhydrite presents rectangular crystals, with no homogenous halite, being grouped in certain sectors. The crystals dimensions (ϕ) are around of 0.0372 mm. An obvious microscopic characteristics of salt is the very good cleavage after the cube face (Annex 1, Fig. B), and the presence of biphasic fluid inclusions. These are present in geometric (quadratic) frames, with a dimension (ϕ) of 0.722 mm, with CO_2 and rarely methane (CH_4 - gas) fluid inclusions. Also, they rarely present twisted forms, and, in this case, gas bubbles are observed (Annex 2, Fig. A-B). Optic anomalies with anisotropic character were detected, due to the deformation of cubic cell because of the pressure. In support of this consideration is the fact that these anomalies are more frequent in the samples collected from higher depths (*e.g.*, sample from drill hole no. 18), and also can be correlated with the salt diagonal cracks (See Annex 1, Fig. A).

In textural terms, halite is idiotopic to hipidiotopic, and anhydrite is macrocrystalline and paurocrystalline. From the structural point of view, there is a depositional chemical material, post-depositionally modified through digenesis process (recrystallization).

We consider that the Mănăştur Salt presents the same geological position as the Someşeni Salt (drill hole no. 1), meaning that it is situated right below the Quaternary deposits, without any brecciate aspect, which usually accompanies diapirs; breccias are situated between the core and the complex salt dome, known as “hat salt” or “cap-rock” salt. This leads to the hypothesis of a non-tectonic origin of this structure, stated by Lachmann since 1911, meaning an “autoplastic” movement from the areas of maximum pressure to the areas of minimum pressure.

3. Brief history

The Someşeni anticline, in relation with which is related the salt of Mănăştur, is mentioned by I. Szadeczky (1917) and it is described in details by V. Dragoş (1963); it is located at Băile Someşeni, with a small ejection character, where the flanks gradients are of 20^0-30^0. Stratigraphically, the salt is in a normal position, with the top slightly arched, but undiapirised. The drill hole performed on the salt anticline has crossed the salt layer on a depth of 20-128 m. From the lithological column belonging to the drill hole no. 1 Someşeni, some facts can be observed: empty march between 0-15 m, terrace boulders between 15–18.5 m, and breccias between 18.5-20 m. There is only salt starting here at a depth of 128 m. After crossing the salt a package of approximately 4-5 m of evaporites was encountered, containing an abundant debris material. For the first time, the evaporite sequence was revealed by the drill hole no. 1 Someşeni - Cluj: limeschist (mentioned for the first time by M. Paucă, 1967), primary gypsum and rock salt. Below evaporites the Dej tuff was not encountered, as other drill holes showed till then. The performed chemical analyses on salt revealed the presence of iodine and bromine ions and of small hydrocarbon quantities. The absence of K and Mg ions from the salt mass indicates a less advanced stage of water concentration. So, the Transylvanian Basin was not an ordinary lagoon, but an enclosed epicontinental sea, with a depth of 300-400 m, leading to a subsidence movement. Salt is disposed as transgressive formations on an early Miocene relief.

4. The salt deposits of Transylvanian Depression

In the Transylvanian Depression, salt occupies an area of approximately 16,206 km^2, with an average thickness of about 250 m, reaching the thickness of 1000-2000 m in diaper blocks. On the western frame of depression and Mureş corridor the evaporitic facies of Upper Badenian is represented by gypsum (Stoica, Gherasie, 1981).

In some areas, the salt layer is very thin till extinction (to south), and in the others, it forms salt domes that are found up to 4000m below the Sarmatian-Pliocene deposits. There were identified two main diapirs alignments on the east and west sides of the basin. Domes and marginal folds affected only the upper formation of salt deposits. The age of deformation is Pontian or much younger, and the particularities are generated by the salt tectonics combined with the convergent molasses movements (Drăgănescu, 1997).

The evaporitic level corresponds to Wielician (Middle Badenian) correlated with the upper part of Langhian (Săndulescu, 1984). Arguments are based on the superposition principle and also regional correlations, with regard to the planktonic microfauna of the Dej tuff.

From the morphologically point of view, almost all occurrences of salt in Transylvania occupy negative landforms, being placed in floodplains at the confluence of watercourses, whether they are situated at higher altitudes, in the terrace or piedmont. It is not known salt deposits, which integrally occupies a positive landform (Maxim, 1961).

It is considered that the salt from Transylvania was formed in a lagoon like the current bay of Kara-Bugaz (Marinescu and Mărunțeanu, 1990). According to the same authors, the Badenian salt formation is clayey, often marly, including a quasicountinuous salt layer whose average thickness varies between 250 and 300 m (only few drill holes, situated in the center of the Transylvanian Basin, did not cross this layer). The excessive thickness in some regions is a consequence of diapirism: *e.g.*, Praid, Sovata, Ocna Mureş, Ocna Sibiu, Ocna Dej, Someşeni,Turda, Jabenița, Sovata (Stoica, Gherasie, 1981).

5. Halokinesis problem

In 1957-60 Trushein introduced in the literature the *halokinesis* notion in relation with the meaning of isostatic hypothesis in the German Basin, where the cause of salt domes was assumed to be the positive difference between density of roof salt deposits and density of salt. A movement of subsurface salt that involves mainly tangential compressive stress is called *halotectonism.*

Salt tectonics is a general term that includes concepts of salt flow, transstratal displacement of salt, pillowing and diapirism. L. Mrazec has defined *diapirism* in 1906, after the Greek word *diaperin* (to push). In 1916, Mrazec, Macovei and Baptist stated that "till now, no one could see the salt placed on its origin or the rocks in which was sedimented; because all the salt massifs appear only on strong dislocation alignments".

In a historical perspective it was shown that salt tectonics can be divided into three parts: the pioneer's stage (1856-1933), the fluid stage (1933-1989) and the construction stage (1995), in which diapirism is recognized as one of the most important mechanism of salt flow (Warren, 1999).

Salt tectonics – halotectonism concerns to the tectonic deformation involving halite or other evaporites as a subsurface or as source layer. Halokinesis is a form of salt tectonics in which the salt flow is driven by unleashing the potential of gravity outside the major lateral tectonic forces (Warren, 1999).
There have been proposed several mechanisms of halokinesis that are combinable (Jackson and Talbot, 1986): *e.g.*, halokinesis caused by emerging, gravitational expansion, thermal convection, halotectonic contraction and halotectonic expansion.

Overall, from the seismic stratigraphy data, the distribution of diapir alignment from Transylvanian Basin can be in connection with the mechanisms of the combined gravitational expansion and compression stress due to the Styric movements in the adjacent basin zones. The structural imaging assembly of the salt horizon emphasizes the areas of lifting and lowering due to its movement, and also to the no homogeneities of the Ante Badenian formation (Colțoi, 2011).

References

Colțoi O., 2011. Processes of formation and evolution of slide structures and their role in hydrocarbon accumulation. PhD thesis (in Romanian). University of Bucharest.

Dragoş V., 1969. Contributii la cunoasterea genezei evaporitelor din Bazinul Transilvaniei. St. Cerc. Geol., Geof., Geogr., Seria Geologie, T.14, nr.1, Bucuresti, p. 163-180.

Drăgănescu L., 1997. Originea sării şi geneza masivelor de sare. S.C. Grafica Prahoveană, Ploieşti, 226 p.

Dumitrescu I., 1968. Geological map of Romania, scale 1: 200 000, Cluj sheet. Ed. by Geol. Inst. Rom. Bucharest.

Jackson M.P.A., Talbot C., J., 1986. External shapes, strain rates and dynamics of salt structures. Geological Society of America Bulletin, v. 97, p. 305-323.

Marinescu F., Mărunțeanu M., 1990. La paléogéographie au niveau du sel Badenien en Roumanie. Geol. Carpathica, Bratislava, p. 49-58.

Maxim I., A., 1961. Câteva observații asupra aspectelor morfologice ale locurilor de apariție a masivelor de sare din Transilvania. Studia, Series II, Fasc.1, Geol. Geogr. Cluj, p. 21-33.

Paucă M., 1967. Contribuții la geneza zăcămintelor de săruri miocene din România. D.S. Inst. Geol. Rom, vol. LIII (1965 - 1966), p. 159-164.

Săndulescu M., 1984. Geotectonica României, Ed. Tehnică, 335 p.

Stoica C., Gherasie I., 1981. Sarea. Ed. Tehnică, Bucuresti, 250 p.

Warren J., 1999. Evaporites. Blackwell Science, London, p.438

Annex 1: Halite and anhydrite microscope images
(A) Quasiperfect cleavage after (100) and diagonal pressure cracking Nll, x42
(B) Perfect cleavage after (100) for halite Nll, x42
(C) Anhydrite crystal with perfect prismatic cleavage, the drill hole no. 13, N+, x120
(D) Association of anhydrite crystals, the drill hole no. 8, N+, x250

A 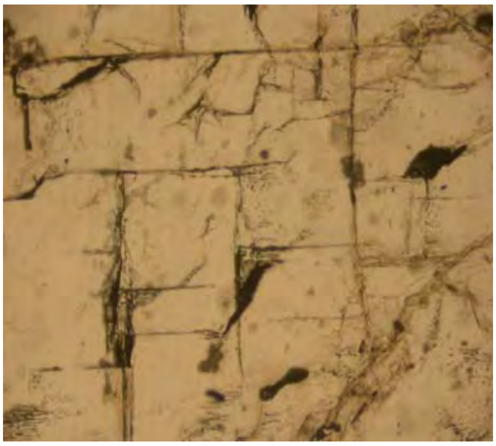 B 

C 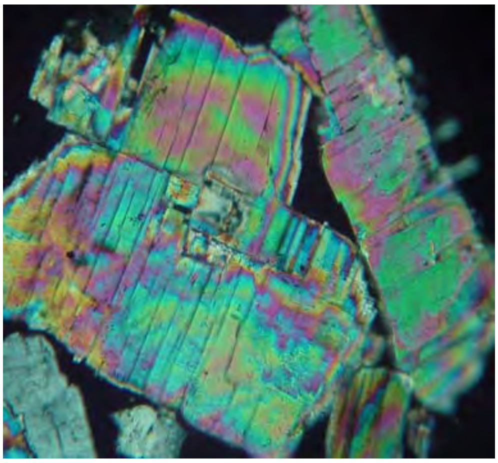 D 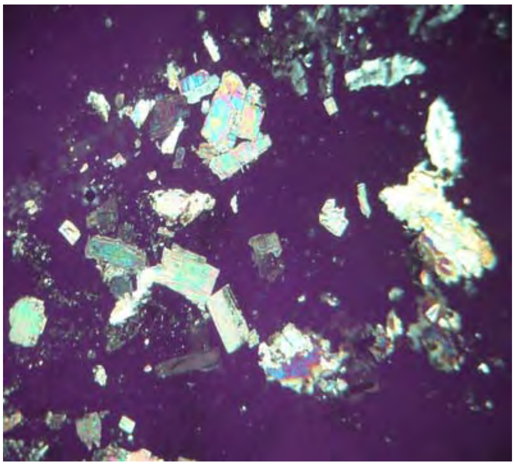

Annex 2: Microscopic images of fluid inclusions in salt
A) CH_4 inclusions arranged on (111) direction, N||, x42
B) CO_2 inclusions in inequigranular cubic cavities, N||, x60

A 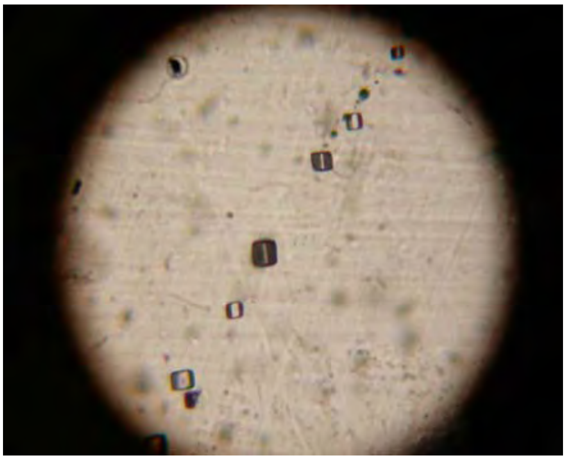 B 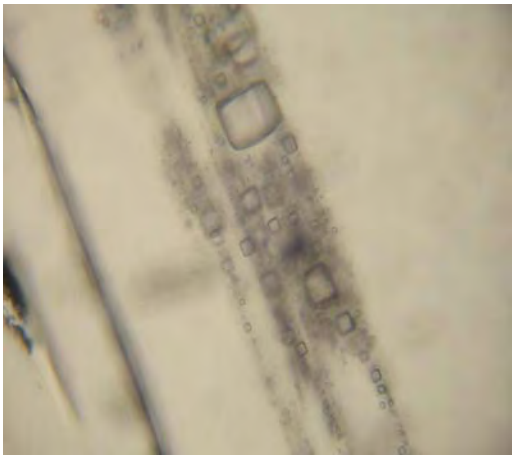

THE SALITRE CAVE KARST IN THE QUARTZITE ROCKS OF DIAMANTINA, MINAS GERAIS, BRAZIL

Heinrich Adolf HORN[1], Essaid BILAL[2], Hernando BAGGIO [3], W. TRINDADE[4], André RODET[5]

[1] IGC-UFMG, Universidade Federal de Minas Gerais, Belo Horizonte-MG

[2] UMR CNRS 5600 EVS-ENSMSE-Géosciences et Environnement F 42, France. bilalessaid@gmail.com

[3] Universidade Federal dos Vales de Jequitinhonha e - UFVJ,

[4] Universidade Montes Claros, Pirapora-MG,

[5] UMR 6143 CNRS, Laboratoire de Géologie de l'Université de Rouen, France,

Abstract This work presents the main morphological characteristics of the Salitre Cave, located in the municipal district of Diamantina - MG and formed in quartzite rocks of the Espinhaço Supergroup, Sopa-Brumadinho Formation as an example of a well-developed karst system. This system now supported by two to three independent small seasonal rivers and displays well-developed dissolution and breakdown structures, as a result of intense intemperance activity. This karst formed, probably before the beginning of Quaternary taking advantage of a system of fractures, normal and thrust faults caused by Espinhaço and Brasiliano events in the Middle to Late-Cambrian. This work attempts at presenting an integrated view of the investigated area and at emphasizing its importance for the understanding of the processes, which occurred in the in carbonatic, quartzitic and silico-carbonatic rocks of Rio San Francisco and Rio Jequitinhonha Basins among the chain of the Espinhaço Range on east and the river valley of San Francisco on the west.

Keywords: Noncarbonatic karst, Salitre Cave, Espinhaço Range, Diamantina-MG

1. Introduction

The study of karsts in non-carbonate environments corresponds to a recent theme in the world of karstological sciences, which make it possible to understand weathering processes in silicate regions in the same way as in carbonate terrains. Therefore, it is important to emphasize that the study of the karstic processes "in situ" are in the center of the speleological discussions.

In this context, debates are included also for the revision of the concept of "pseudo-karsts" and its exclusion from use due to its morphologic significance, which ignores of dynamic facet of the processes involved, such as the physiographic characteristics and the dissolution process.

Several studies carried out in countries of Africa, Venezuela and others demonstrate the existence of karsts morphologies in non-carbonate lithologies and show that the genesis in these environments corresponds to the same processes taking place in carbonate rocks. Those works show the fingerprints of dissolution of the rock and features which are observed in carbonate substrates. This demonstrates that the karsts morphologies originated by the dissolution processes should not be considered "pseudo karsts".

In Brazil, the studies of the non-carbonate karsts are more recent and the main references are Borghi & Moreira (2002), Hardt (2009), Auler (2004), Willems et al. (2008), and Rodet et al. (2009).

These studies investigate mainly karsts developed in sandstones and quartzites in São Paulo, Tocantins, Mato Grosso, Minas Gerais, and Rio Grande do Sul and Roraima States. These works contributed to an increased knowledge in non-carbonate karst environment research and to an enlarged speleological heritage. The justification of the present study is that the massif of Salitre is a well-defined body of silicate clastic rocks showing all features of an evolving karst. The research is been carried out together with European experts, within a multinational and interdisciplinary context. This study also has the objective to present the main characteristics of the karst morphology of the Salitre Cave, located in the municipal district of Diamantina - MG, developed in silicatic rocks of Espinhaço Supergroup, Sopa-Brumadinho Formation.

2. Location and physiographic characterization of the studied area

The municipal district of Diamantina is located in it is upper Jequitinhonha Valley, approximately 292 km from Belo Horizonte - MG. The access to the region is made by the federal highways BR-259 and BR-367. The Massif of the Salitre Cave is located 9 km southeast of the city of Diamantina - MG, between the coordinates UTM 0687393E and 7962317S (Fig. 1). The access to the site is made by a local secondary road.

3. Geological context

The cave is situated in the units of the Espinhaço Supergroup, especially in the Sopa-Brumadinho formation, southeast of Diamantina, near Extração (Fig. 2). The geological profile of the whole supergroup with a zoom of the cave situated part of the Sopa-Brumadinho Formation, is given in Fig. 3.

This is the most important part of the whole Espinhaço Supergroup, due to its widespread distribution and the content of diamond placers. The typical sequence is found northern of the city of Guinda, where the formation has three members: Datas, Caldeirões e Campo Sampaio (Almeida-Abreu, 1993) consisting of metapelites, a wide variety of quartzites, polymictic metaconglomerates, with local intercalations of volcano-sediments, basic volcanites and levels of hematite phyllites.

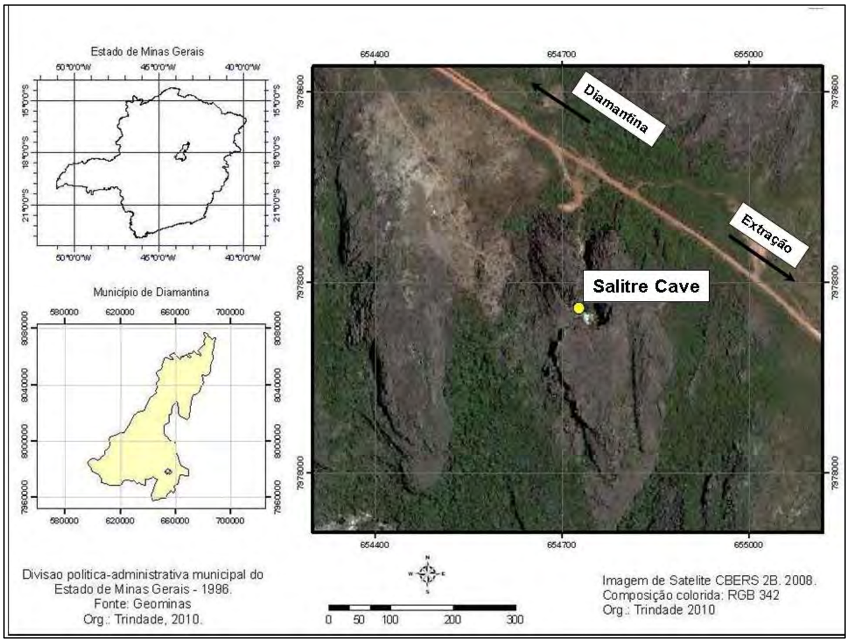

Fig. 1. Location of the Massif of the Salitre Cave (Gruta do Salitre) between Diamantina and Extração (Souza et al. 2010, modified). The cave is part of a lixiviated fracture system situated in a N-S direction on the both side of the road, which cut the figure from E to W (Souza et al. 2010).

3.1. Stratigraphy

The investigated region encompasses only the middle part of Espnhaço Supergroup, the Sopa-Brumadinho Formation, together with younger sedimentary covers (Fig. 2).

Datas Member: The base of the formation is formed by a 30-40m stack of quartzites, phyllite and mica rich quartzites with fluvial structures, cross beddings, laminations and a wide variety of facies, suggesting a sedimentation in low energy environments like subsident flat platforms (Schöll, 1980; Garcia & Uhlein, 1987).

Caldeirões Member: This is the more developed unit with 100-200m of an extreme variety of sediments, hosting the Salitre Cave. This unit is predominately formed by quartzites, discontinuous mono- or polymictic metaconglomerates, with a N-S trend (Schöll, 1980). In the mining area, the formation is dominated by medium of fine-grained quartzites, sometimes with microconglomeratic aspect and very rich in iron oxides (hematite) or mica matrix, accompanied by mono- to polymictic conglomerates, hematite-phyllite and dykes of grey and green schists and centimetric m to metric levels with rare fragments from the basement. These sediments suggest marine-coastal ore continental-close environments and are abundant in tabular, channel- and cross-bedding structures (Schöll, 1980).

Campo Sampaio Member: This upper unit of normally 2-3m up to 50m can be observed in the western part of the map (Fig. 2) and show N-S orientation (Fogaça & Almeida-Abreu, 1982). This unit is formed principally by metapelites (phyllites and siltites) and some fine grained quartzites at the top, close to the erosive contact with the overlaying units. This unit has a very high content of iron oxides and contains intercalated polymictic breccias formed by angular quartz and hematite fragments, with numerous typical lacustrine to shallow water and coastal sediment structures, such flaser, channels, cross layering, fishbone-structures and wave and ripple marks.

3.2 Structural geology

The area is characterized by important fault-zones with mainly N-S orientation, accompanied by an open W-vergent fold system. In the studied area, the fault zones are well-expressed and cross-cut earlier folds. The important direction of foliation S_n is between N5°W and N10°E diving to E (~70^o) and intersected by another West vergent fold system S_{n+1} with centimetric to metric amplitudes and by a final system S_{n+2}, responsible for the formation of anticlines and synclines such as the one containing the Salitre Cave (Fig. 4). An opening of the fracture system by tensional forces and the erosion of the overlain sediments is clearly visible in the composition of all the quartzites of all formations of the Supergroup. The structural evidences suggests a evolution with one compression maxima N10°E and N20°E, plans (N10°E and N20°E) and another one of N60-70°W orientation, all diving nearly to E.

4. Geomorphological context

The Espinhaço Range is the hydrographic divisor between the São Francisco basin on the West and Jequitinhonha basin on the East. The Espinhaço Range is characterized by a sequence of plateaus oriented N-S. According to Saadi (1995), the denomination "range" obscures, however, the physiographic reality and would be better defined by the term "highlands". The Espinhaço Range is built up by the compartments of a median and a western range with a general SSE-NNW and SSW-NNE orientation separated by a well-expressed NW-SE depression area originating in the same tectonic processes, but lithologically differentiated. The southern compartment, which includes the study area, starts in the East near the springs of the Cipó river, close to Belo Horizonte and extends to the city of Couto of Magalhães. The average altitude varies around 1200 m , with Itambé Mountain summit at about 2062 m.

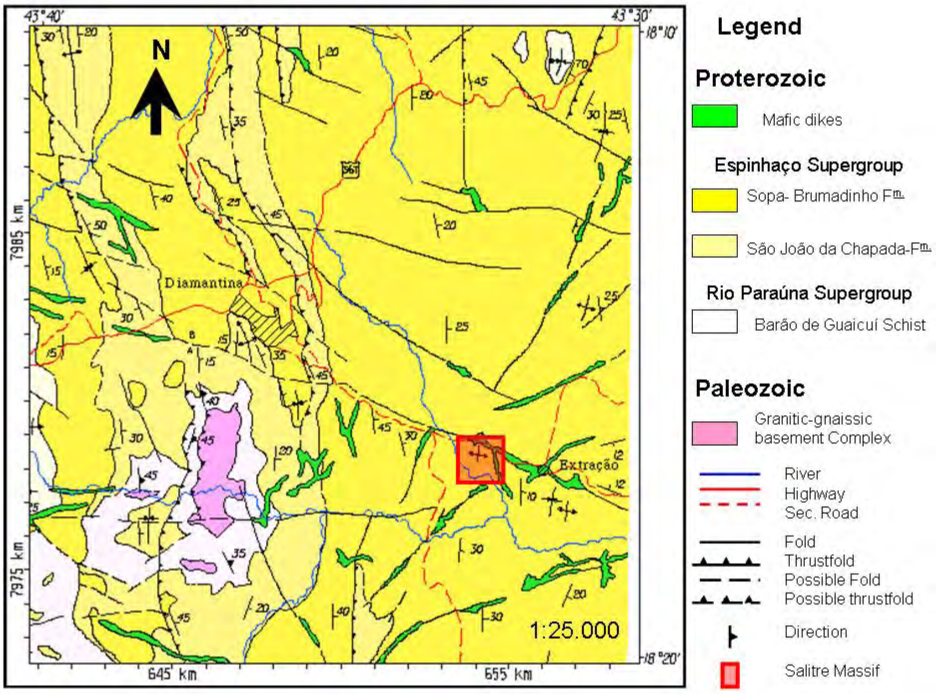

Fig. 2. Geological map of the investigated area. The Salitre Cave is situated in the red quadrangle, between two small rivers. (Fogaça, 1997).

The southern Espinhaço Range is mainly characterized by the absolute predominance of quartzites that, over the whole extension of the area, describe a rigid covering, but intensively fractured and sheared. The relief is formed by crests, scarps and deep valleys as a result of fluvial dissection, oriented in the most part, by old tectonic directions. It is to restate, that the geomorphological evolution of the Espinhaço Range was exclusively determined by structural, morpho-structural, morpho-tectonic patterns and subordinately, by climatic factors. The leveled paleo-surfaces are represented by plateaus with crest alignments and with the presence of quartzite "monadnocks".

5. The quartzite Karst of the Salitre Cave

The Salitre Cave is a natural cavity, developed in the quartzite rocks of the Sopa-Brumadinho Formation and oriented NW-SE. Fig. 2 shows the main morphological and evolutional compartments of this cave.

The canyon allows access to the Poljé of the Salitre Cave, to the Halls and to smaller cavities. The canyon of the Salitre Cave is an important structural feature and possesses beside the geological, geomorphological and biological importance, a historical relevance, because rebelling slaves used the canyon to take refuge among the rocky mazes. The canyon of the Salitre Cave is formed in the direction of a brittle N-S fault, with an extension of approximately 125m in length and 10 to 15 m in width. The scarps of the canyon show tectonic structures like folds and faults, locally reaching 50m in height. Horizontal and vertical systems of "karrens" may also be observed (Hardt et al. 2010). The canyon of the

Salitre Cave does not have a specific superficial drainage; however, the exuberant arboreal and herbaceous vegetation demonstrates the existence of a active subsurface hydrological system, formed by two to three small sectional rivers.

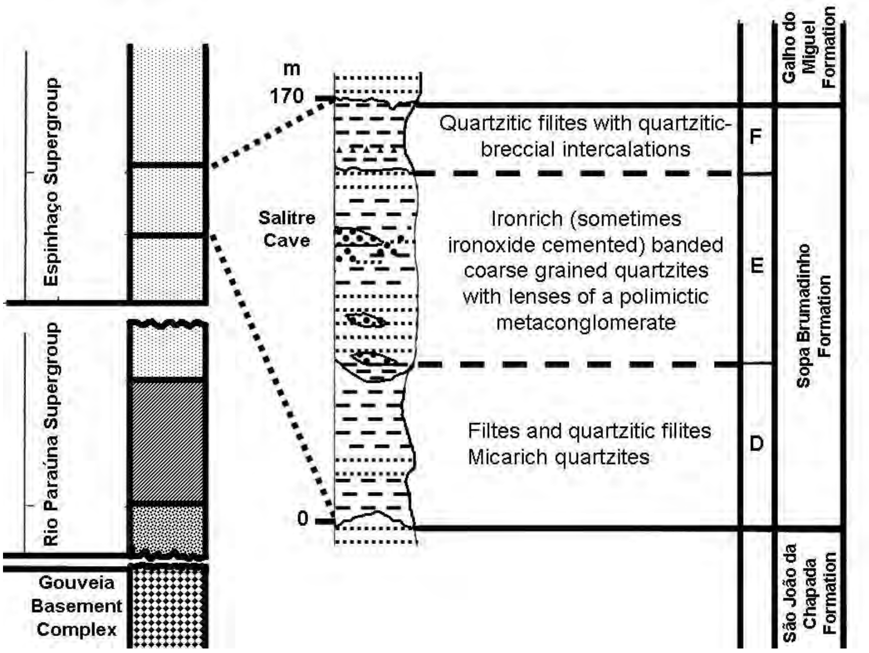

Fig. 3. Simplified geological profile of the Espinhaço Supergroup. The right side details the Sopa-Brumadinho formation. The middle part shows the host formation of the cave (after Fogaça, 1997). D: Datas; E: Caldeirões; F: Campo Sampaio.

Fig. 4. Satellite image of Salitre Cave region. Some structures are indicated: 1. The canyon and 2. Poljé (red dashed line); First halls (red dotted line); Inner hall (brown dotted line); Traverse (green ring); the continuation (yellow dotted line); The blue arrows show he supposed water directions from the regional rivers. Picture from www.googleearth.com.br, modified.

The tectonic evolution of the Salitre canyon is linked directly to the Espinhaço Rift System, whose sedimentation began in the late Paleo-Proterozoic (± 1,75 Ga), lasting till the Meso-Proterozoic (± 1,4 Ga) and the Brasiliano Event at the limit between the Pre-Cambrian and the Mesozoic. The middle part of this canyon is covered by blocks and sand and hosts one important water system.

6. The Poljé of the Salitre Cave

The Poljé of the Salitre Cave is directly connected to the canyon and it is characterized by a semicircular form, which appears as a closed depression. The floor of the depression is locally formed by scarce white medium to coarse-grained sand and by a wide variety of quartzite blocks from the breakdown of the walls and roofs. In the areas close to the rocky blooming, however, the floor is covered by a layer of clay from desilicification processes. The walls of the Poljé are more than 80m high and are intersected by several planes and groups of fractures, sometimes of significant dimensions (from cm to meters) and developing in a variety of directions controlled by old tectonic processes.

In the right corner of the Poljé, when looking from the canyon to the outer halls of the cave, a well-expressed fault of 40 to 100cm of width and 18m of length, may be observed. The fault was opened by the breakdown of a giant block. Fig. 4 displays a part of this fault and of the fracture system visible here. The wall rocks are characterized by systems of alveoli of various dimensions, which may be directly related to the karst genesis (Rodet & al. 2009) which is also responsible for the forming of halls and other cavities, using faults, fractures, and heterogeneities of the massif. The Salitre Cave Saltpeter possesses two external main halls and three internal ones, located at different paleo-levels. The presence of those paleo-levels is a consequence of the change in the local base-level which also modified the dynamics of rock dissolution. The paleo-level 1 includes the external main hall, which is easily accessible; the paleo-level 2 is less accessible and corresponds to the secondary external hall connected to a deeper and smaller hall by passages between irregular blocks.

The upper main hall (1) of the Salitre Cave has is funnel shaped with front semicircular opening. The main access of this cavity is N-E oriented and has an angular profile of oval-semicircular form with a W-E extension of 120-30m and 70m depth. Several microspeleological features on the floor and the roof demonstrate that the genesis of the Salitre Cave is mainly a result of the dissolution process in the quartzite rock often along heterogeneities with subsequent breakdown of rock blocks.

The floor is dominated by deposits formed in a collapsed block, with clastic sediments and karst microfeatures that are concentrated in less accessible areas, thus fortunately inhibiting any human intervention.

The roof is covered in a thin mineral film, described by Willems (2008) as pyrolusite (MnO_2). is the coating is concentrated mainly on the left area of the hall (looking the entrance) and hosts also various iron minerals (e.g. $Fe_2O_{3;}$ $FeO(OH)_2$), nitrates and organophosphate compounds.

The entrance of the secondary lower hall is located on the right deeper side of the entrance of the upper main hall. The access is difficult due to the inclination, steep slopes and a high amount of depressed blocks. The traverse part of the entrance to the secondary hall is very irregular, and is 2m wide and 1.5m high. The interior of the hall has an elliptic form with its inner part enlarged to 25m wide and 15m long (Fig. 5). The hall is characterized by the presence of oxidic and argillitic deposits up to 10cm, several speleological micro features that also prove the process of dissolution of the quartzite rocks. "Tafoni" in different stages of evolution can be seen in all parts of the cave and in the host rock. Various speleothems are still visible in the more internal parts of the cave, probably due to the difficult access. The hall continues down with a small tubular syphon and with the W-E passage of a small river.

Fig. 5. The upper, first main hall of the Salitre Cave with blocky material on the ground and microstructures located in its roof. The red material is composed by argillites, iron oxides and a slightly violet phosphate of organic origin (guano). Dissolution effects are visible on the roof and on the collapsed blocks.

The karst is still active and there are underground drainages at the bottom of the two internal halls located close to the hall floor. The first drainage begins in the canyon and occupies the lower part of the first internal hall; the second comes from the opposite direction and flow into the most internal hall. During the dry periods, the first drainage reaches 0.5m wide and 0.5m deep; the water is clear and the flow is fast. A thick pyrolusite layer is visible inside the drainage. The second drainage seems to be smaller, it lacks pyrolusite but shows instead, cave clay and gravel.

The floor is ornamented by several karst microstructures, formed on the white fine sand and in the areas of influence of the river where red sediments develop. The walls and the roof of the internal halls are covered by variously colored microfeatures: with ash-grey, white, yellow and red tones standing out. The presence of coral structures indicates the interception of groundwater level and indicates active karst processes. From this hall, a small passage goes down to the South leading to a small fracture.

7. Final considerations

The Salitre Cave is a natural cavity developed in quartzite rocks. Its genesis is the result of the same physico-chemical processes developed in carbonate rocks, and is in this way related to the dissolution process, which occur along fissures, fractures and layers. This karst system is segmented in three main physiographic units: the canyons, the Poljés and underground drainages represented by the halls and floors.

The speleological characteristics in the quartzite system suggest the actuation of dissolution process all over the Salitre Massif, but concentrated along old tectonic structures. This is supported by the existence of a group of features that are typical to karst environments formed by dissolution, e.g. the horizontal and vertical "karren"; the benches or warts; the towers; the alveoli; the coral type hairs, the interconnected halls, the canyons and the Poljés and various types of microspeleothems on the roofs and floors. The peculiarity of the form and surface of the wall rocks of the halls together with secondary drainage systems show that this is still an active karst system.

During its evolution, the energy level has lowered at least two times thus leading to the formation of halls in distinct levels and collapsed forms in the inner hall. All this pleads for a more detailed speleological study aiming at the creation of a Conservation Unit (UC) that will secure the preservation of this area.

Acknowledgements We thank the UFMG, FVMJ and UNIMONTES for technical support.

References

Almeida-Abreu P.A., 1993. A Evolução Geodinâmica da Serra do Espinhaço Meridional, Minas Gerais, Brasil. Doct. dissertation, Geowiss. Fakultät. Universidade de Freiburg, Freiburg, 150 p.

Auler A.S., 2004. Quartzite caves of South America. In: Gunn, J.. (Org.). Encyclopedia of Cave and Karst Science. New York: Taylor and Francis, v. , p. 617-619.

Borghi L. and Moreira M.I.C., 2002. A região da caverna Aroe Jari, Chapada dos Guimarães, MT - Raro exemplo de caverna em arenito. In: Schobbenhaus, C.; Campos, D.A.; Queiroz, E.T.; Winge, M.; Berbert-Born, M.L.C.. (Org.). Sítios geológicos e paleontológicos do Brasil. Brasília: Departamento Nacional da Produção Mineral - DNPM / Serviço Geológico Nacional -CPRM, 2002, v. , p. 481-490.

Fogaça A.C.C. 1997. Geologia da Folha Diamantina. In Projeto Espinhaço em Cd-Rom ed. Grossi-sad, j. h.; Lobato, l. m.; Pedrosa-soares, a. c. and Soares-filho, b. s. Belo Horizonte, COMIG - Companhia Mineradora de Minas Gerais. p. 1575-1665.

Fogaça A.C.C. and Almeida-Abreu P. A., 1982. Depósitos de planícies de marés na Formação Sopa Brumadinho (Proterozóico Inferior), Cordilheira do Espinhaço, Estado de Minas Gerais, Brasil. Actas, Anais 5UºU Congresso Latinoamericano de Geologia, Buenos Aires. Vol. 2, p. 373-388.

Garcia A.J.V. and Uhlein A., 1987. Sistemas deposicionais do Supergrupo Espinhaço na região de Diamantina (MG). Anais, Simpósio sobre Sistemas Deposicionais do Pré-Cambriano, Soc. Bras. Geologia, Núcleo MG, Bol. 6, Ouro Preto, p. 113-136.

HHardt R.H, Rodet J., HPinto S.A.F.H, 2010. O carste, produto de uma evolução ou processo? Evolução de um conceito. Revista de Geografia (Recife), v. 3, p. 100-111, 2010.

HRodet M. J.H, Rodet J., Horn A.H. 2008. Sistema geomorfológico e sistema antrópico pré-histórico no Brasil Central. Exemplo do estado de Minas Gerais. In: 7a Simposio Nacional de Geomorfologia, 2008, Belo Horizonte. Anais do 7a SINAGEO. Belo Horizonte: ABG, 2008. v. 1. p. 1-10.

Rodet J., Willems L., Brown J., Ogier S., Bourdin M., Viard J. P., 2009. Morphodynamic incidences of the trepanning of the endokarst by solution pipes. Examples of chalk caves in Western Europe (France and Belgium). In: 15th International Congress of Speleology, 2009, Kerrville (Texas). Proceedings of the 15th International Congress of Speleology. Huntsville (Alabama) : National Speleological Society, 2009. v. 3. p.

1657-1661.
Saadi A. 1995. A Geomorfologia da Serra do Espinhaço de Minas Gerais e de suas margens. Geonomos. v.3. n. 1. p.41-63. 1995. HYPERLINK: http://www.igc.ufmg.br/geonomos-3_1_41_63_Saadi.pdf. Acesso em: 15/10/2009.
Souza F.C.R.de, Baggio H., Trindade W.M., 2010. Carste em rochas quartzíticas da gruta do salitre, diamantina - MG. 1º Cong. Org. Espaço. X. Sem. Pós-Grad. Geograf., UNESP, *ISBN: 978-85-88454-20-*, Anais, SP. P: 4982-4991
Scholl W.U., 1980. Estratigrafia, sedimentologia e paleogeografia da região de Diamantina (Serra do Espinhaço, Minas Gerais, Brasil). Munst. Forsch. Geol. Pal. 51, p. 223-240.
Willems L., Rodet J., Pouclet A., Melo S., Rodet M.J., Compére P.H., Hatert F. and Auler A.A., 2008. Karst in sandstones and quartzites of Minas Gerais, Brazil. Cadernos Lab. Xeólóxico de Laxe. Belgium: Corunã. 33. p.127-138. 2008.

MIOCENE EVAPORITES FROM THE SOUTHERN PART OF EASTERN CARPATHIANS – SEDIMENTOLOGICAL APPROACH

Dumitru FRUNZESCU*

* Universitatea Petrol-Gaze din Ploieşti, Calea Bucuresti nr. 39, cod 100680, dfrunzescu@yahoo.com

Abstract This paper presents the diagnosis and the interpretation of the evaporitic facies from the southern side of Carpathians Foredeep, in Badenian deposits at Valea Rea (Istrița Hill, Buzău county) and Piatra Verde (Slănic-Teişani, Prahova county).

Keywords: sulphatic evaporites, sulphatic facieses, Miocene, southern side of Eastern Carpathians

The paper proposes the study of sulphatic evaporites in Miocene formations that appear between Valea Buzăului and Valea Teleajenului, geotectonically positioned in Tarcău and Subcarpathians units and the inner-folded flank of Carpathians Foredeep (Săndulescu M., 1989) in the Southern part of the Eastern Carpathians arch bend. We sedimentologically detailed (in more outcrops) the *medium subformation (with tuff and gypsum)* and the *upper subformation (with calcareous shales and sulphur)* from ***Doftana Molasses***, respectively, the *striped formation* in the ***Low Molasses*** (= Doftana Mollases) of the Subcarpathian unit as well as the *lower subformation* (*with tuff and gypsum*) of lower Badenian from ***Slănic Molasses*** (Ştefănescu, Mărunțeanu, 1980), respectively *Cosmina Breccia formation (upper salt breccia formation)* in the lower Molasses of the Subcarpathian unit. Theoretical considerations were extrapolated concerning other adjacent formations.

Sulphatic evaporitic type facies (defined, especially, according to the structural criterion) as well as siliciclastic facies (defined by the compilation of granofacies information, structofacies, petrofacies) are codified in tables (Figs. 1, 2) theoretically described and interpreted (Figs. 3, 4) for field examples reference. Facies models are as well typized and described, giving priority to the sedimentological criterion, not to the geographic one in the classification of evaporitic settings (permanently considered as being in transition, as a result of the variation of control factors): continental, basin margin, basin center. They will also represent a reference basis for the interpreted settings that we met in the field. By integration we obtained the basin evolution.

The molasses realm that integrates the sulphatic formations represents an accumulation resulted from progradation of a siliciclastic coast line, which imposes the approach of type models: shallow-water, with a moderate basin energy. The succession of processes group peritidal facies in a parasequence = succession of shallowing-upward trend settings. A parasequence has variable thickness (decimeter-meter rank) and, ideally speaking, component lithofacies may be grouped in three limit units (mesosequences): for Doftana Molasses: 1. subtidal, 2. intertidal, 3. supratidal, with or without terrestrial horizon at top; for the subformation in Piatra Verde: 1. of proximal slope, 2. of distal slope, 3. of basin bottom; for salt breccia formation from Valea Rea: 1. deep salinas = marine, 2. subtidal, 3. intertidal.

The contacts between units may be gradational or net when they are the proof of a local synsedimentary erosion. According to Walther law the decoding of units in parasequences allow resetting of a mosaic of environment succession. There are the characteristic features: (1) limit unit may be referred to at a large spectrum of settings or (2) may admit between them intermediary stages with their own, mixed facies, (3) parasequences may be cut at bottom, at top or in the middle – as total different environments are put in contact, or in another order than shallowing upward. They may be explained by erosion, non-depositing, being tied to the big changing speed, which is otherwise typical for the evaporites. Generally (depending on the climate), the parasequences shallowing upward may be: of low energy (1) subtidal: burrowed lutite over siltoarenites with intraclasts, (2) intertidal: thin, wavy carbonatic siltolutites, algal mats; sulphatic nodules; (3) supratidal: in mud of laminitic algal mats with mud cracks, with fenestral structures, with thin intraclasts and arenitic laminae levels; sulphatic nodules) or (2) of high energy (beach type) (1. subtidal: burrowed lutite (marl-clay) over siltoarenite with intraclasts; 2. intertidal: crusts, oblique or cross lamination of a small angle, sandstones with bioclasts; biolaminites with mud cracks. 3. supratidal: bio-laminites (with sulphatic nodules) with mud cracks, hardgrounds, crusts, paleo-sols). The contact of parasequences is marked by dissolution, erosion contacts (the erosion may be subaerial or underwater from the initiation of the next cycle). Shallowing upward para-sequences may be explained in three ways: 1. as progradations wedges; 2. as simultaneous agradation wedge; 3. as a mosaic of insular tidal flats. Stocking of parasequences can be: asymmetrical (as shallowing upward successions ABC, ABC, etc. where A= subtidal, B= intertidal, C= supratidal), or symmetric (as deepening upward succes-sions

CBABC type) and it is related to the flooding speed. (1) At gradual flooding: there is time for wave erosion of the top of the previous C member (a hiatus separating the parasequences: ABC-ABC-ABC…); (2) At rapid flooding, the previous C member is rapidly sunk, B member has no time for accumulation.

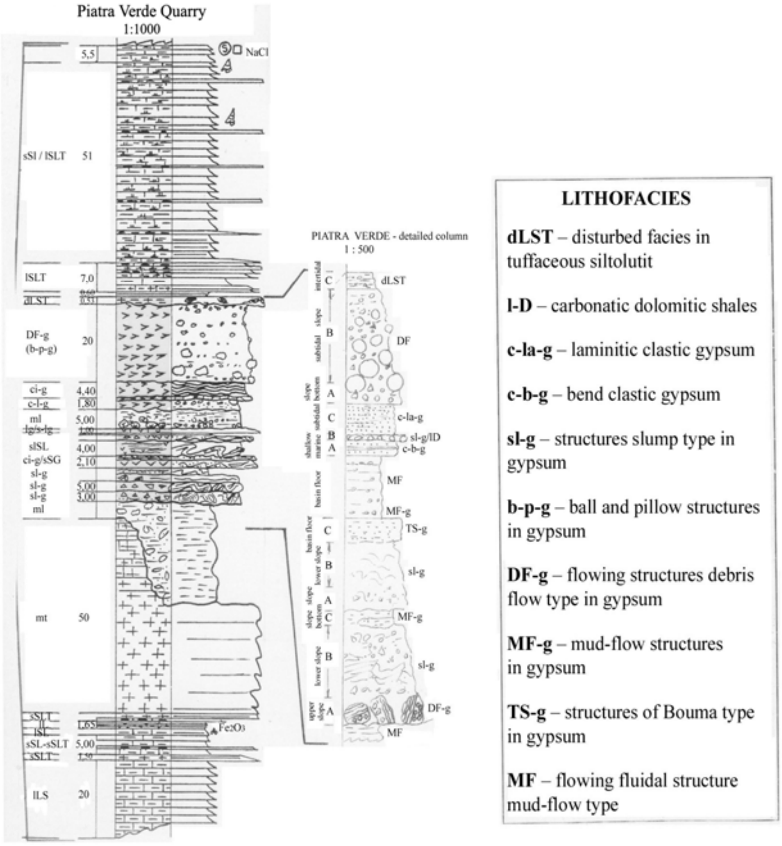

Fig. 1. Primary data and lithofacies identified in the column of Piatra Verde outcrops

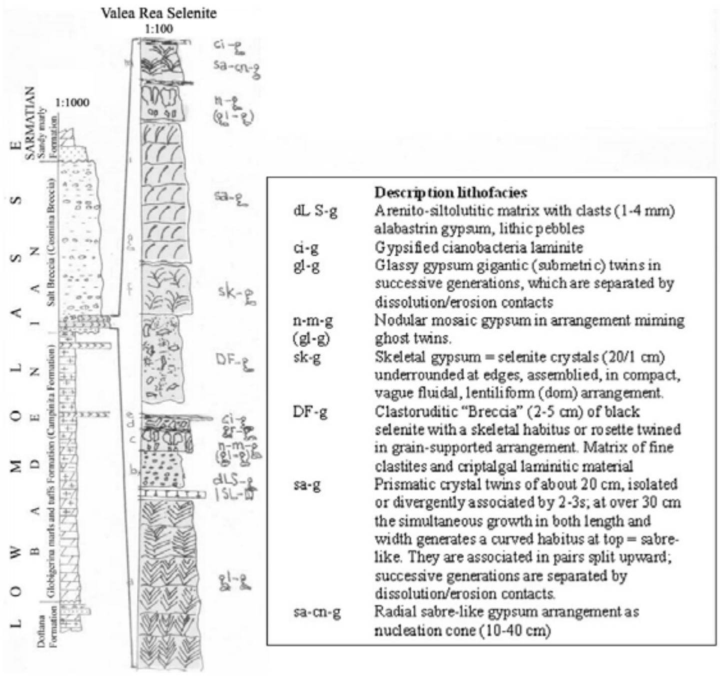

Fig. 2. Primary data and lithofacies identified in the column of Valea Rea outcrops

The evaporitic successions are rhythmical recurrences of submetric shallowing upward parasequences (ABC, ABC, ABC). The accommodation for such parasequences may result in: (1) allocyclic – by eustatism, (2) autocyclic – by changes of high frequency (specific to evaporites) eustatism overlapped. According to some authors (Algeo & Wilkinson, 1988), a parasequence covers a timespan of 10,000–100,000 years. Yet hiatus have a notable importance during this time. For a static or low variation marine level - progradation (by vertical accretion) slows down and stops. At a higher level, the prograded plain segment will become again subtidal, and after immersion, the cycle appears again. The island tidal flats may partially prograde and agrade by hydrographic changes. For a static marine level or in the case of slow level increase the evaporitic production decreases and stops. The appearance of accretion once again, after a break, with a long supratidal exposure necessitates a new accumulation space. At high level and long-term marine expansion the space of accu-mulation is renewed by coming back to insular peritidal units (laterally discontinuous). The extrinsic factors (subsidence and eustatism) intervene, especially on a high scale modelling. In order to explain metric or decimetric parasequences we must resort to marine level changes of high frequency, and reduced amplitude, as well as IVth rank cycle (=paracycle with the duration of 100,000-500,000 years) with depositional correspondent in parasequences (= macrosequences) or Vth rank (orbital cycle Milancovitch with the duration of 20,000 to 100,000 years, with a correspondent in sets of strata of cm-m growth (= mesosequences).

At this scale, a metric marine increase determines a time and accommodation opportunity window for a single shallow upward succession. The deposition is made at marine level rising (by any of the three styles: the progradation wedge of tidal flats, the simultaneous agradation or tidal insular mosaic sheet) and at its apex and it stops when the marine level falls. The control of parasequence coming back may be: (1) rhythmical eu-static change, or/ and (2) spasmotic subsidence (in seismically active areas, on listric faults, in passive margin areas).

Approaching the eva-poritic model through peritidal sequential strati-graphy, we must underline the difficulty of incorporating the peritidal deposits in peculiar systems tracts, be-cause there are many varia-bles that control the tidal flats development (climate, plat-form circulation, wind pat-terns, tidal amplitude func-tion of the platform evolution stage and/or platform con-figuration). The separation of sequences and systems tracks in tidal flat deposits may be finalized in understanding the two objectives: long-term changes of the marine level may suggest the geographic position on the platform of tidal flats; stocking models of upward shallow para-sequences may suggest changes at a larger scale in the accumulation space. (1) The tidal flats may be the first facies disposed over a boundary sequence when the rate of marine level decreases and the sea slowly floods the platform to the continent. On a cyclic variation of IIIrd rank (500,000-1,000,000 years) of marine level the strand line will migrate. The tidal flat deposits that were developed in fringes, fringing the continent will mark the position of coastal onlap. (2) Parasequence stocking (upward shallow = ABC, generated by progradation tidal flat wedges) may be seen as associations of modulations IV-th and V-th rank of a cycle of III-rd rank of variation of relative marine level. The long cycle (III-rd rank) fluctuation would carry the microcycles (and respectively the opportunity window of decimetric-metric parasequences formation) backwards and forwards on the platform. The progradation tidal flats parasequences will be geogra-phically redeposited in an agradation, back stepping shingled offlap (Fig. 5).

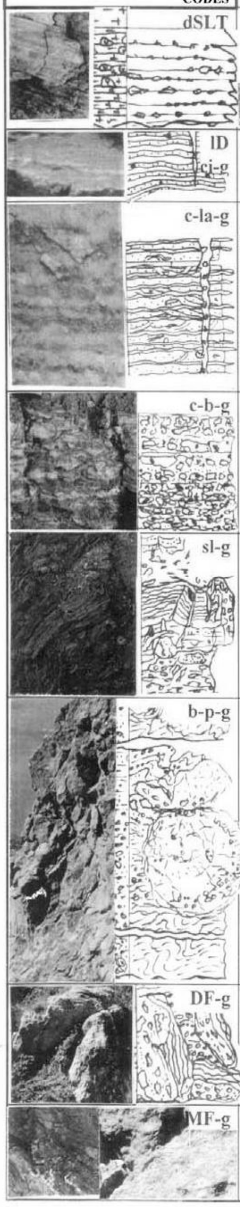

PIATRA VERDE CODES	DESCRIPTION	LITHOFACIES INTERPRETATION
dSLT	Microruditic clastes of alabastrin gyspum in tuffaceous siltic marly-clays vaguely stratified	Periodically flooded sabkha. The tuffaceous siltolutit from the start of the flooding influx conservates the products of the previous arid cycle: chips, sulphatic nodules, lithic pebbles, tuff enclaves
lD ci-g	Gypsified/dolomitic/terrigene disturbed algal mats: wavy, crinkled, broken, thrust	Resedimentation on salinas slope of a algal mats material from the adjacent sabkha, periodically flooded
c-la-g	Cyanobacteria laminae (<1 mm) disturbed by emersion and laminae (>1 cm) of recrystallized alabastrin gypsolutit with current flow or fold structures; parallel erosion/dissolution contacts; succession affected by fill fisures that separate creep trends piles	Accumulation in very shallow settings of weathering sabkha products (fine size) periodically flooded, or salinas in the last stage of clogging
c-b-g	Cyanobacteria laminae (<1 mm) very disturbed and lithones (<1 dm) of sulphatic clastorudites (1-3 cm) = algal mats crusts; current flow structures, channel filling, flaser, which are diagenetically blurred	Accumulation in deeper settings (salinas) of aeolian/underwater weathering sabkha products (coarse size) periodically flooded
sl-g	Algal/clastic sulphatic rhythmical alternations with the initial stratification a primarly disturbed (tectiform folds, small faults, thrusts, breccifications, convolute and fluidal structures	Mass rearranging of some accumulations of c-la-g or c-b-g type sabkha (in their turn c-la-g or c-b-g type of are sabkha weathering products). Increasing batimetry by tectonic and eustatic causes with seismic shock/storm/overloading mass flow prime
b-p-g	Ellipsoidal or spheroidal concretions (meganodules 10-40 cm diameter size) of nodular mosaic or alabastrin gypsum in sulphatic clastoruditic matrix (c-b-g); there are frequent gravity flow structures and loss water fluidal structures	Algal mats material (siliciclastic = sulphatic nodules) resedimentated and affected by overloading (ball & pillow structures). After, duet o erosion, transport, resedimentation by debris flow in an increasing basin slope batimetry (salinas/marine basin). The diagenetic growth of sulphate is large in meganodules in small in the clastoruditic matrix
DF-g	Metric blocks made up of two lithons (gypsorudites c-b-g type and cianobacteria laminites ci-g types) in clastoruditic matrix	Deposit of gravity flow on a short distance toward the slope bottom of a previous accumulation (c-b-a type followed by ci-g initially supplied by the adjacent sabkha
MF-g	Claly matrix with rare polimictic clastes or exclusively sulpahtic clastes (breccia aspect). Massive structure which is vaguely fluidal	Deposit of gravity flow at increasing batimetry towards the slope bottom

Fig. 3. Description and interpretation of lithofacies recorded at Piatra Verde outcrops

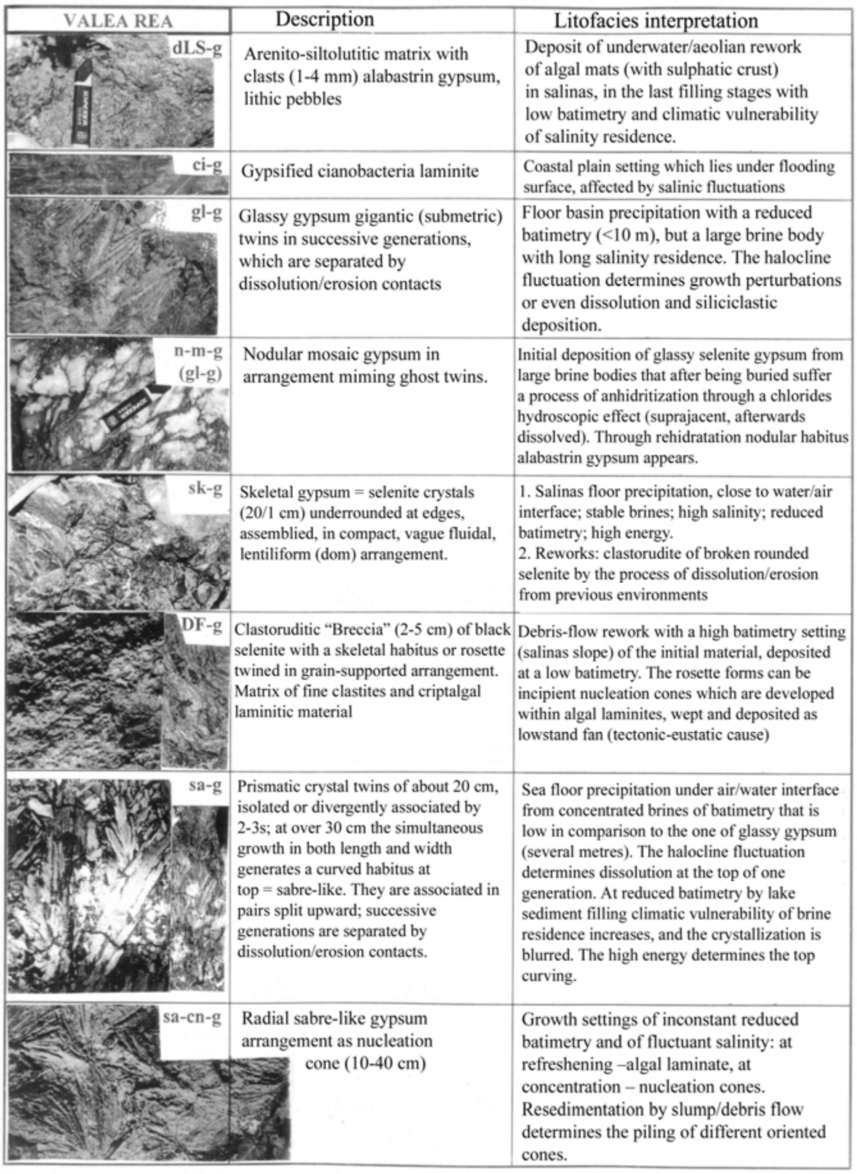

VALEA REA	Description	Litofacies interpretation
dLS-g	Arenito-siltolutitic matrix with clasts (1-4 mm) alabastrin gypsum, lithic pebbles	Deposit of underwater/aeolian rework of algal mats (with sulphatic crust) in salinas, in the last filling stages with low batimetry and climatic vulnerability of salinity residence.
ci-g	Gypsified cianobacteria laminite	Coastal plain setting which lies under flooding surface, affected by salinic fluctuations
gl-g	Glassy gypsum gigantic (submetric) twins in successive generations, which are separated by dissolution/erosion contacts	Floor basin precipitation with a reduced batimetry (<10 m), but a large brine body with long salinity residence. The halocline fluctuation determines growth perturbations or even dissolution and siliciclastic deposition.
n-m-g (gl-g)	Nodular mosaic gypsum in arrangement miming ghost twins.	Initial deposition of glassy selenite gypsum from large brine bodies that after being buried suffer a process of anhidritization through a chlorides hydroscopic effect (suprajacent, afterwards dissolved). Through rehidratation nodular habitus alabastrin gypsum appears.
sk-g	Skeletal gypsum = selenite crystals (20/1 cm) underrounded at edges, assemblied, in compact, vague fluidal, lentiliform (dom) arrangement.	1. Salinas floor precipitation, close to water/air interface; stable brines; high salinity; reduced batimetry; high energy. 2. Reworks: clastorudite of broken rounded selenite by the process of dissolution/erosion from previous environments
DF-g	Clastoruditic "Breccia" (2-5 cm) of black selenite with a skeletal habitus or rosette twined in grain-supported arrangement. Matrix of fine clastites and criptalgal laminitic material	Debris-flow rework with a high batimetry setting (salinas slope) of the initial material, deposited at a low batimetry. The rosette forms can be incipient nucleation cones which are developed within algal laminites, wept and deposited as lowstand fan (tectonic-eustatic cause)
sa-g	Prismatic crystal twins of about 20 cm, isolated or divergently associated by 2-3s; at over 30 cm the simultaneous growth in both length and width generates a curved habitus at top = sabre-like. They are associated in pairs split upward; successive generations are separated by dissolution/erosion contacts.	Sea floor precipitation under air/water interface from concentrated brines of batimetry that is low in comparison to the one of glassy gypsum (several metres). The halocline fluctuation determines dissolution at the top of one generation. At reduced batimetry by lake sediment filling climatic vulnerability of brine residence increases, and the crystallization is blurred. The high energy determines the top curving.
sa-cn-g	Radial sabre-like gypsum arrangement as nucleation cone (10-40 cm)	Growth settings of inconstant reduced batimetry and of fluctuant salinity: at refreshening –algal laminate, at concentration – nucleation cones. Resedimentation by slump/debris flow determines the piling of different oriented cones.

Fig. 4. Description and interpretation of lithofacies recorded at Valea Rea outcrops

At reduced rates of long-term change of relative marine level (at lowstand or early highstand = low accommodation) the geographic position of the opportunity windows = successive parasequences is close (position 1, respectively position 3 in Fig. 5) and the correspondent growths are thin, the rate of increasing accommodation being low. When the rate long term change of relative marine level is big, the opportunity window of parasequence would be placed backwards and forwards over the shelf (positions 2, and respectively 4 in Fig. 5). Either thick tidal fault succession will result (at a marine level rise = transgressive system tracts - position 2) or relatively thin shingled successions (at a marine level fall = late highstand system tracts or early lowstand – position 4). The progradation distance in each case will be specified at each peritidal accumulation on each shelf. The long term marine level rise would emphasize the short term rises and would suppress the short term falls; on the other hand, the long term fall would emphasize the short time falls and would suppress the short term rises. Therefore, the relative distribution of subtidal, intertidal and supratidal facies in shallowing upward parasequences will change function of the accommodation – resultant from the interference of long term and short term cycles. The long term cycle of III-rd rank can be connected to the evolution of the Lower Molasses (Doftana Molasses) or Slănic Molasses. The sulphates of upper salt formation (tuff and gypsum subformation of lower Badenian from Piatra Verde –Slănic and the salt breccia with selenite formation of Medium Badenian from Valea Rea, in Istrița Hill) are parts of a unique type sequence, which is here and there entirely developed and which appears quoted in the geological literature in the Northern Carpathian Foredeep. The diagnosed lithofacies units compare the megasequence with selenite from Valea Rea to the low side of the sulphatic Badenian type succession and Piatra Verde gypsum megasequence to the upper side (Fig. 6). Valea Rea lithofacies are made up of parasequences from the setting series: A = shallow underwater (gigantic selenite twins, skeletal gypsum debris, skeletal gypsum domal packages) – B = very shallow underwater to subtidal (sabre-like selenite, banded selenite + carbonatic laminites + grass-like type selenitic clastorudites – C = intertidal-subtidal (laminitic cryptalgal gypsum, nucleation cones of sabre-like gypsum within cianobacteria mats) (Figs. 7, 8).

Piatra Verde lithofacies (Figs. 7, 9) are made up of parasequences of deeper settings being dominated by clastic gypsum through resedimentation of a previous or a contemporary adjacent sulphatic material. The bathymetry of parasequences is included in the series: A = basin bottom (salinas or coast salinas) (mudflows with rare clasto-rudites of alabastrin gypsum, gypsiturbidite)- B=distal, proxi-mal slope (debris-flows, slumps)- C=subtidal, tidal mouth creek, intertidal (banded clastic gypsum, clastic laminitc gypsum, associated with flaser, disturbed facies structures). Some parasequences reveal deepening upward tendencies.

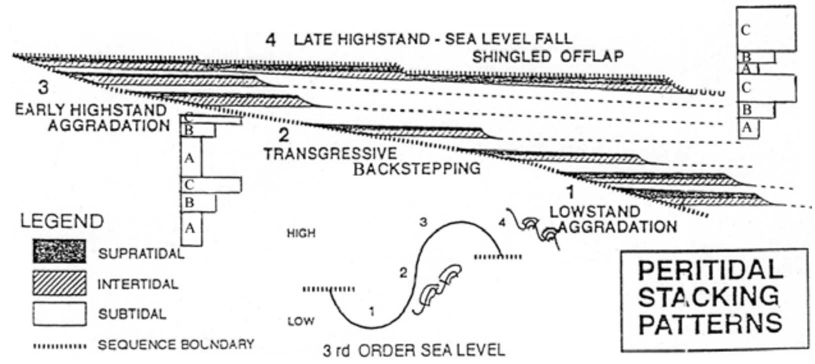

Fig. 5. Tilted shelf with a hypothetical stratigraphy of metric-decimetric peritidal parasequences between sequence limits. Each parasequence has been formed by progradation that took place in the opportunity window produced by short-time fluctuations of IV-th and V-th rank during a rise or a fall of long-time sea level of III-rd rank. The slow movement of III-rd rank of the seashore will dictate where tidal shelf areas will develop (modified after Walker and James (1992).

The basin paleogeography at the debut of the sulphatic accumulation is marked by tectonic balances with uplifts in Carpathian areas and the transgression of water over foreland cliffs in the outer side, with the generalization of a system of interconnected salinas, separated by insular barriers and accumulative shoals barriers. To the inner side, there are emergent area crests of Lera-Văleni-Buştenari or Homorîciu spurs and to the outer side there are sills marked by islands. The slopes are reduced, the morphology being blurred by previous highstand accumulation of tuff, siliciclastics or Lithothamnium (reefs) limestones. The morphology may be also produced by the erosion of these deposits at a lowstand successive episode, which was contemporary to the formation of evaporites. The evolution of sulphatic sedimentation is different and here and there diachronic between the border sectors (of foreland) and the inner sectors. The parasequences correspond to the lowstand system tracts of a III-rd and IV-th rank cycle. They are characterized by the increase of the low and medium term in comparison with the upper term and they have an agradation stocking for the low package and a regressive stocking for the upper

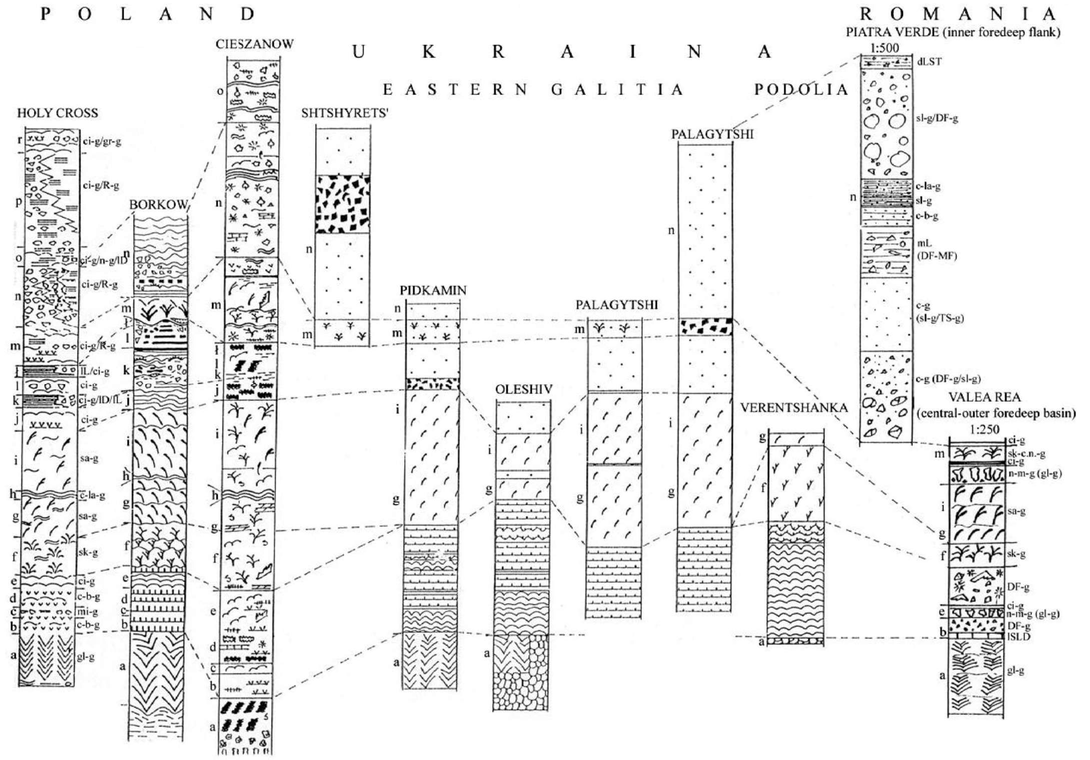

Fig. 6. Correlation of lithostratigraphic units in sedimentological columns of Badenian gypsum in the Northern Carpathic foredeep (Poland, Eastern Galitia, Podolia) and the Southern part of Eastern Carpathians

package. The parasequences from Valea Rea follow the way of evolution from a deep brine body, which is stable, with big brine residence to a body of reduced bathymetry due to the sediment filling. This bathymetry generates vulnerability at variable climatic conditions, determining the alternation of thin lithons of top variable composition, with biolaminites of intertidal facies. After the repetition of several parasequences, the bathymetric fall with a lowstand effect (erosion and regression of coast line with accumulation of slope wedges) determines the destruction of the megasequence top and, afterwards, the destruction of the entire succession and even the destruction of its carbonatic (algal) substratum.

Piatra Verde megasequence is dominated by allochtonous gypsum. On the innerly emersed ridges sulphatic evaporites periodically flooded sabkha type appears. Disturbed facies clasts, multiply reworked are accumulated at the border of the basin (salinas/playa) such as laminitic clastic gypsum, or banded clastic gypsum. The rapid accretion, but especially the instability of old stiric post-phase tectonic balance generates effects of drastic erosion on basin margins and accumulation basin bathymetry increase of low stand wedges. The flows are primed by seismic or storm mechanic shock. We may speak about all the series of gravity flows: from incipient stages or a small scale of laminae or lithon, which starts by creep, slide, slump, debris-flow, mud flow, to the last stage of turbidites. Flaser or load structures are associated. The flowing effects are emphasized by the differential tectonics horst/graben – which is visible in the fallen sector, Slănic. At megasequence top collapse breccia are noticed. The megasequence presents two packages: a low one with accumulation on the deep marine realm, and an upper one with accumulation in the subtidal/intertidal realm. The source area exists in the emergent spur Lera-Văleni-Buştenari. In the Northen margin of Carpathian influence, contemporary to the evaporitic flows alluvial cone ruditic deposits are accumulated: Bătrâni conglomerates, Vârful Benii conglomerates (Grujinschi, 1972).

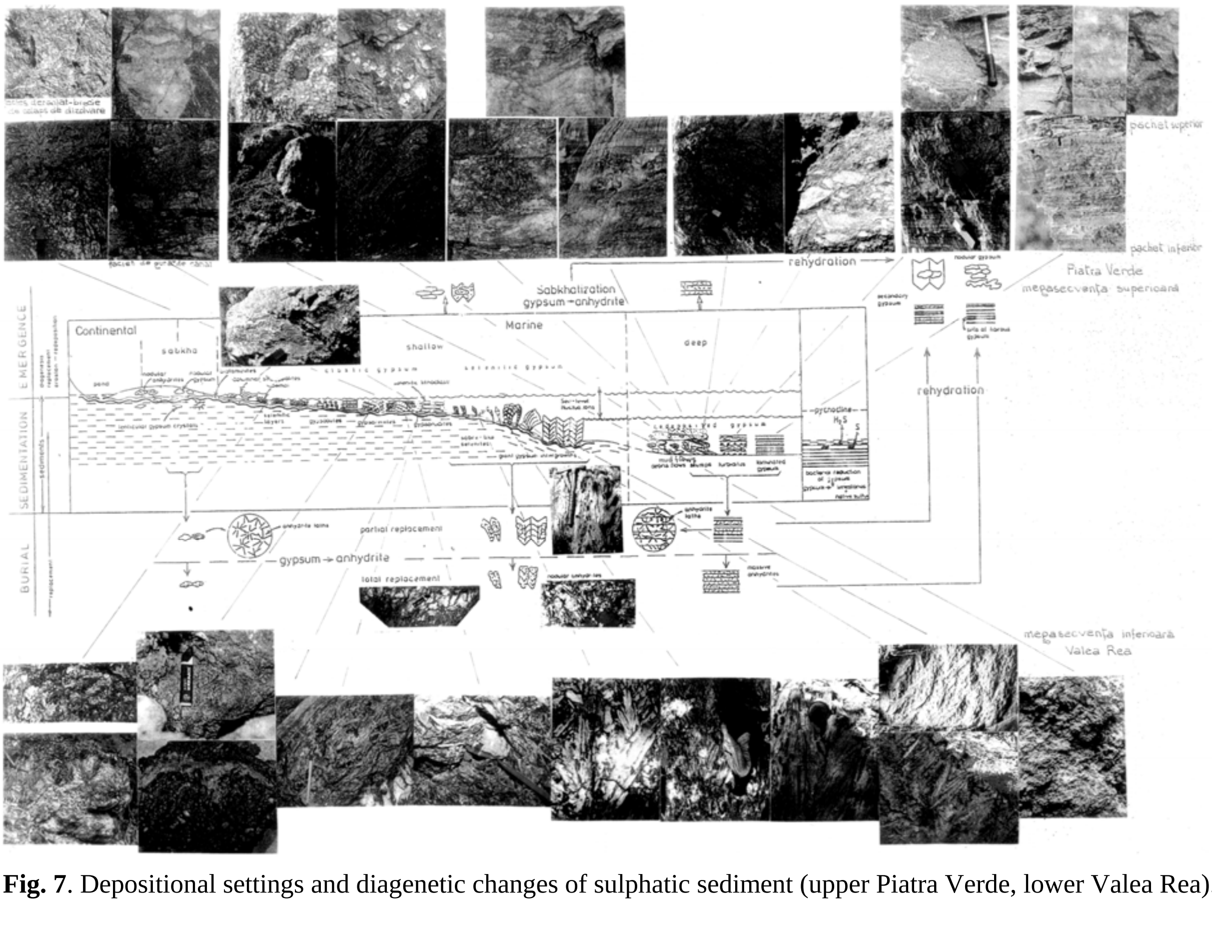

Fig. 7. Depositional settings and diagenetic changes of sulphatic sediment (upper Piatra Verde, lower Valea Rea).

The lack of the selenitic low part of the typical succession from Piatra Verde megasequence is related to the non-depositing on emergent areas, but especially to the lowstand drastic erosion, which affects lower than the evaporites level, respectively the marine sequence with Lithothamnium limestone and even the globigerina marl and tuff formation.

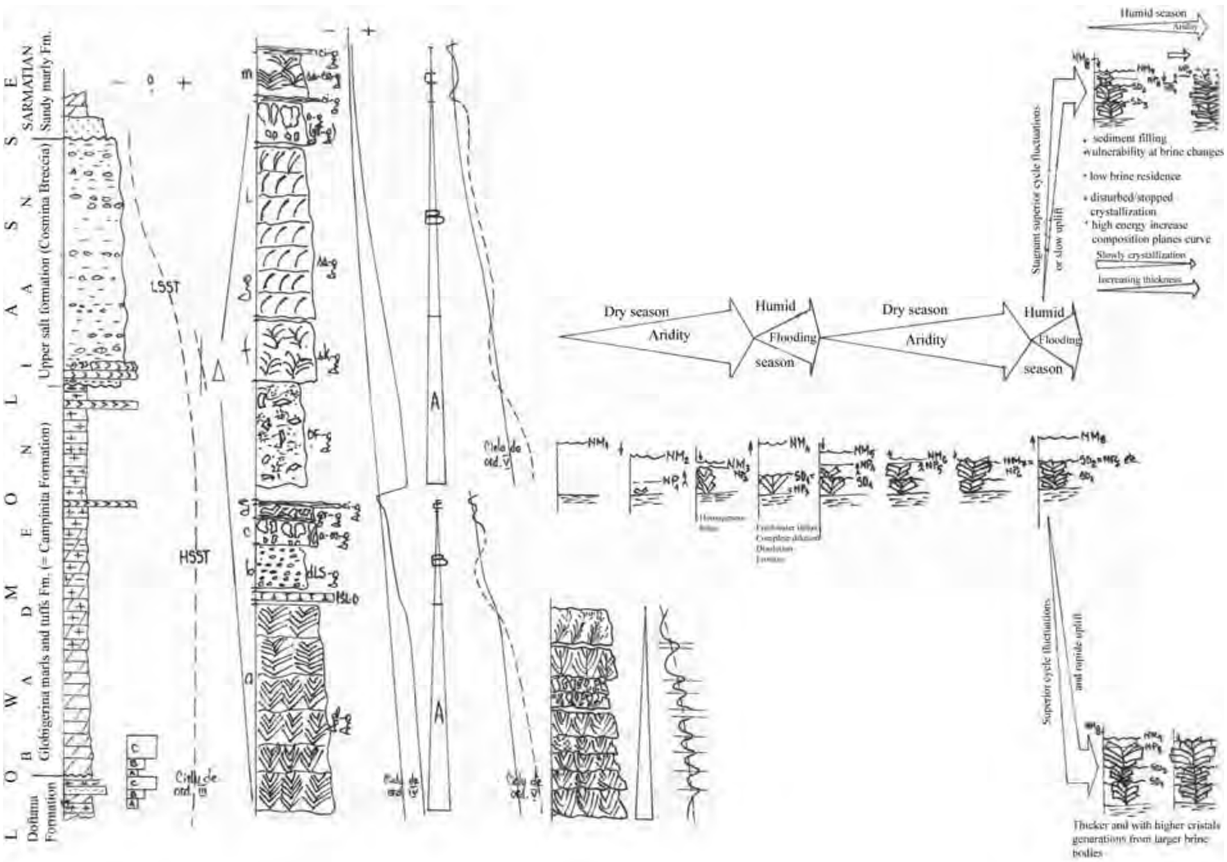

Fig. 8. The cycle hierarchy of a basin evaporitic environment of salinas coastal type from Valea Rea (Badenian).

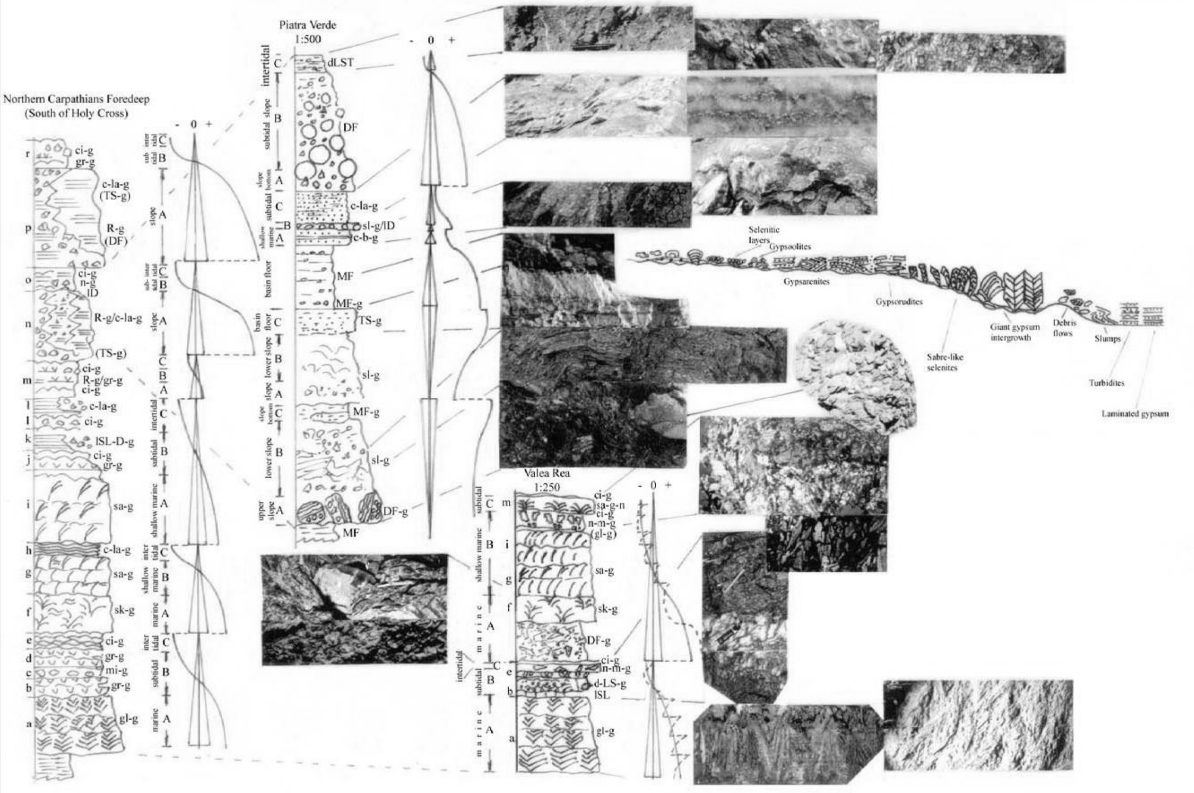

Fig. 9. Facies successions; typical parasequences of the Badenian gypsum and the depositional correspondent of component lithofacies

The obvious diagnosis of sulphatic units and the remarkable continuity allows the comparison of megasequences from Piatra Verde and Valea Rea and their correlation with the type sequence in the Northen Carpathian Foredeep (Poland, Ukraine, Bukovina, Galitia) (Figure 6). If we date as lower

Badenian the sulphatic megasequence from Piatra Verde and if we consider Valea Rea selenite megasequence as older, we may extend the stratigraphic content of salt breccia from Valea Rea from middle Badenian (as it was considered in literature) to lower Badenian.

References

Walker G.R., James P.N., 1992. Facies Models response to sea level change, Geol. Assoc. of Canada, Newfoundland.

Frunzescu D., Anastasiu N., Popa M., 1995. Clastic Evaporite events in the Lower Neogene of the Pericarpatian Unit, Romanian Journal of Stratigraphy, 76, *7*, X-th R.C.M.N.S. Congress, Bucharest.

Frunzescu D., 1998. Stratigraphic and sedimentologic study of the Miocene evaporites between Buzău Valley and Teleajen Valley, Ph.D. Thesis, Bucharest University.

LES WILDFLYSCHS ALPINS DES CARPATHES ROUMAINS REPRÉSENTENT DES MÉLANGES DU TYPE FRANCISCAIN – EXEMPLES: LES WILDFLYSCHS DES TRANSYLVANIDES DES CARPATHES ORIENTALES ET DES MONTS APUSENI

Mircea MUREŞAN

Institutul Geologic al României – str. Caransebeş 1, Sector 1, 012271 Bucharest 32
e-mail: muresenii@yahoo.com

Abstract: In the Romanian Carpathians, there are several stratigraphic entities of wildflysch type, of Mesozoic, Paleogene and early Miocene. Considering the strong resemblance of these wildflysch formations with the mélange associations, we argue that these wildflysch formations can be mélanges, parts of accretionary prisms, which could indicate the presence of subduction zones. In this article, we approach the cases of the wildflysch from the Transylvanides of the Eastern Carpathians and from the Apuseni Mountains.

Key words: East Carpathians, Apuseni Mountains, Eastern Transylvanides, Western Transylvanides, Alpine overthrust nappes, mélange; Alpine subduction

1. Introduction

Le mélange de la Formation franciscaine (mise en évidence et décrite dans la période 1968-1974, représente (selon Bleahu, 1983 et références citées) une formation chaotique qui renferme des blocs sédimentaires et des fragments de roches ophiolitiques, ainsi que des blocs de métamorphites. Tous ces éléments sont englobés dans une matrice pélitique fortement déformée. Le mélange franciscain, d'âge crétacée, est lié par la zone de subduction de la Plaque Pacifique sous la Plaque Nord-Américaine. Ultérieurement, une partie du mélange formé dans la zone de subduction a été expulsée, étant inclus dans la zone orogénique Sainte Lucie (en Californie). Aujourd'hui, des mélanges ont été décrits dans presque toutes les chaînes alpines du monde, partout ayant une signification d'un faciès tectonique, étant lié par les zones de subduction. Fréquemment, les mélanges participent à la constitution des prismes d'accrétion, liés par les mêmes zones de subduction. Ainsi, ce faciès tectonique, a coté d'autres caractéristiques, représente un trait très répandu et significatif des zones de subduction qui ont achevé leur activité.

Dans les Carpathes roumains, il y a des plusieurs entités décrites comme des formations sédimentaires du type wildflysch, qui ont été attribuées aux Mésozoïque, Paléogène et Miocène inférieur. Voyant tant la grande ressemblance des ces wildflyschs avec le mélange du type franciscain que leurs contextes géotectoniques, nous sommes convaincu que ces wildflyschs représentent des mélanges, participant fréquemment à la constitution des prismes d'accrétions. Cette conception change l'image structurelle des quelques importantes unités tectoniques des Carpathes.

Le concept de « Transylvanides » a été introduit et développé par Săndulescu (1975, 1984). Selon cet auteur, les Transylvanides « représentent la suture majeure téthysienne dans l'espace carpathique ». Parmi les Transylvanides, Săndulescu (1975) a distingué « les Nappes des Métallifères simiques » (logées dans la partie méridionale des Monts Apuseni) et « les Nappes transylvaines » logées dans la Zone Cristallino-Mésozoïque (ZCM) des Carpathes Orientales; là, l'auteur a inclut dans les unités transylvaines les trois nappes (la Nappe d'Olt, la Nappe de Perşani, la Nappe de Hăghimaş) associées au Wildflysch de Perşani-Hăghimaş (WfyPeHg), celui-ci étant considéré la formation supérieure de la pile bucovinienne. Ces unités (y compris le WfyPeHg) nous les dénommons « **les Transylvanides Orientales** ». Les Nappes des Métallifères simiques nous les redénommons « **les Transylvanides occidentales ».**

2. Transylvanides Orientales

Nous allons présenter le cas du Wildflysch de Perşani-Hăghimaş, développé dans la **ZCM** des Carpathes Orientales. **Le WfyPeHg,** le plus connue wildflysch des zones carpathiques roumaines, a été considéré antérieurement par Săndulescu (1984) comme une entité sédimentaire bucovinienne.

La ZCM, la plus interne unité tectonique majeure des CO, constitue, dans le nord, **le Compartiment Tisa-Ciuc** (le plus grand, étant développé entre les Monts Ciuc et les Massifs Rahov et Civcin) et, dans le sud, **le Compartiment Perşani**. Dans la ZCM, Săndulescu (1984) a décrit trois nappes alpines bucoviniennes (de cisaillement) superposées: **la Nappe bucovinienne (NBu), la Nappe subbucovinienne (NSBu) et les Nappes infrabucoviniennes (NIBu).**

 Le WfyPeHg (barrémien-albien – Săndulescu, 1975), affleure dans le les deux compartiments principaux de la ZCM. Dans le Compartiment Tisa-Ciuc, le WfyPeHg est logé principalement dans l'aire de la NBu et participe à la constitution des Synformes Hăghimaş et Rarău. Le WfyPeHg a été excellemment décrit dans la région Hăghimaş par Săndulescu (1975). Selon cet auteur, cette entité est constituée par une matrice argileuse (ou marneuse), dans laquelle il y a des éléments de roches magmatogènes basiques et ultrabasiques (des basaltes amigdaloïdes, des péridotites serpentinitisées), ainsi qu'une multitude des éléments et des blocs (de quelques centimétres cubes jusqu'a quelques dizaines milles de mètres cubes) faites en les mêmes roches mésozoïques des trois nappes transylvaines, associées au WfyPeHg (nappes mises en évidence et décrites par Săndulescu, 1984): **la Nappe d'Olt - NOt** (qui englobe, à coté de dépôts triasiques, jurassiques inférieures et supérieures, des ophiolites – ultrabasites, basaltes), **la Nappe de Perşani (NPe)** (en majeure partie, faite en dépôts triasiques) et **la Nappe de Hăghimaş - NHg** (principalement, faite en roches calcaires du Tithonique-Néocomien). Dans le WfyPeHg du Compartiment Tisa-Ciuc, il y a aussi des blocs métriques et des fragments plus grands (même kilométriques en longueur) faits en brèches à débris de métamorphites; aujourd'hui, celles-ci nous les considérons comme partie du WfyPeHg, étant formée par les mêmes processus tectoniques qui ont donné naissance au ce wildflysch:.

Le WfyPeHg et la Nappe bucovinienne sont couvertes d'une manière transgressive par les Conglomérats de Bîrnadu (Vraconien ? – Cénomanien), séparés et cosidérés par Săndulescu (1975) comme la couverture post-autrichienne dans la Zone Cristalino-Mésozoïque.

Le charriage du wildflysch, logé tant dans le Compartiment Perşani que dans le Compartiment Tisa-Ciuc a été soutenu tant auparavant que récemment (Balintoni, 1997; Mureşan, 2002, 2006, 2008). Les deux auteurs ont soutenu que les trois nappes transylvaines mentionnées ont été transportées solidairement par le wildflysch pendant son charriage. La Nappe du WfyPeHg a été représentée pour la première fois (Mureşan, 2008) sur la Carte géologique des Monts Hăghimaş. Selon notre conception, sur cette carte, le WfyPeHg et les trois nappes transylvaines mentionées (NOt, NPe, NHg) sont figurées comme une seule entité tectonique: **la Nappe du WfyPeHg,** considéré comme une unité de couverture transylvaine qui est charriée sur les dépôts mésozoïques anté-crétacées supérieurs des différentes nappes de charriage de couverture alpines (Mureşan, 2008) associées au Nappe bucovinienne. Pour cette situation, un bon exemple est la région des Monts Hăghimaş, où la succession tectoniques c'est la suivante (de bas en haut): **(1) La Nappe de Lacul Roşu-Licaş – NLRL** (Mureşan, 2008) est constituée par des dépôts permiens continentaux et des formations mésozoïques en faciès bucovinien (des successions attribuees aux Séisien, Campilien-Anisien, Trias supérieur, Lias, Dogger, Callovien-Oxfordien, Kimméridgien. La NLRL est charriée sur les mésotamorphites protérozoïques du Groupe Bretila: La NLRL a été reprisée tant dans la Nappe subucovinienne que dans les .les Nappes infrabucoviniennes (Mureşan, 2006). La NLRL est la plus developpée unité tectonique qui a un contenu lithostratigraphique du type bucovinien. **(2) Nappe de Lunca** (Mureşan, 2006) renferme les Couches de Lunca (Thitonic-Valanginien – Săndulescu, 1975) qui, vers le nord, supporte en transgression les Conglomérats de Chicera (hauterevien ? – cf. Săndulescu, 1975). Selon nous, la Nappe de Lunca constitue l'Antiforme Lunca, qui se trouve dans le prolongement vers le sud de la « Crête de Dămuc », faite pricipalement en métamorphites. La Nappe de Lunca est charriée sur la NLRL et supporte le charriage de la NWfyPeHg. **(3) La Nappe de Sălămaş** (Mureşan, 2008) renferme „le flysch gréseux-calcaire et calcarénitique" – hauterevien, séparé par Patrulius et al. 1969). La Nappe de Sălămaş est charriée sur la Nappe de Lunca et se dispose sous la NWfyPeHg. Toutes ces unités ; qui sont logées dans la partie méridionale du Compartiment Tisa-Ciuc de la ZCM, se développent sous la Nappe du Wildflysch de Perşani-Hăghimaş. Nous mentionnons que, plus au nord, tant dans la Compartiment Tisa-Ciuc que dans le Compartiment Perşani, il y a aussi des nappes de couverture sous le même WfyPeHg (Mureşan, 2008).

Au-dessus de WfyPeHg, dans le Compartiment Persani, se développe **la Nappe de Piscul Remeții** (auparavant dénomée par Mureşan – 2006, la Nappe du flysch à orbitolines et des dépôts calcaires, les deux entités étant d'âge aptien supérieur – cf. Patrulius et al. 1966).

3. Réinterprétations et des conclusions concernant le Wildflysch de Perşani-Hăghimaş

(1) Les suivants aspects nous démontrent que le WfyPeHg représente un mélange du type franciscain: **(a)** La structure chaotique du ce wildflysch, montrée par l'impossibilité d'établir une lithostratigraphie d'ensemble du celui-ci. **(b)** La présence d'une matrice argilo-marneuse qui présente une foliation tectonique pénétrative; c'est-à-dire il s'agit d'une matrice cisaillée. **(c)** La composition du WfyPeHg: dans sa matrice cisaillée il y a des blocs très variés: des éléments des magmatites basiques et ultrabasiques, des roches sédimentaires mésozoïques anté-cénomanienes et des brèches à métamorphites. **(2)** Selon nous, **le Mélange de PeHg (MePeHg),** représentant l'ancien Wildflysch de Perşani-Hăghimaş, provient sûrement par la trituration tectonique d'une unité transylvaine mésozoïque, une épreuve étant la présence de la multitude éléments rencontrés dans ce mélange, qui sont identiques avec les formations englobées dans les trois nappes transylvaines mentionnées (la NOt, la NPe, la NHg). Cette situation montre l'association très étroite du ce mélange, avec les trois nappes transylvaines (NOt, NPe, NHg); en ce cas, il en résulte que le mélange analisé s'associe avec des grands volums de formations à grandeurs des nappes de charriage. **(3)** L'ancien WFyPeHg étant d'origine tectonique, il ne peut pas appartenir d'une succession lithostratgraphique. **(4)** Ainsi, cet ensemble représente un faciès tectonique, formé dans une zone de subduction alpine, liée par les mouvements autrichien; c'est-à-dire l'âge du Mélange de PeHg MePeHg est mesocretacé. **(5)** Le MePeHg et les trois nappes de charriage du type transylvaine (la NOt, la NPe, la NHg) représent **le Prisme d'accretion de Perşani-Hăghimaş. (6)** Les nappes de couverture à formations du type bucoviniennes, englobées dans la Nappe bucovinienne – Mureşan, 2008 (**Nappe de Lacul Roşu-Licaş, la Nappe de Lunca, la Nappe de Sălămaş)** se développent sous le Mélange de Perşani-Hăghimaş. Dans ce cas, nous constatons que dans la ZCM, il y a tant des unités allochtones d'origine transylvaine (le MePeHg, la NOt, la NPe, la NHg) que des nappes de charriage à formations du type bucovinien. Les dernières unités se trouvant sous les premières, nous pouvons supposer que la mis en place des celles-ci est plus ancienne que la mis en place des entités d'origine transylvaine. Pendant leur charriage, les deux catégories ont été transportées de l'ouest vers l'est. On a observé qu'il y a des similitudes en ce qui concerne les contenus des Transylvanides Orientales et des Transylvanides occidentales (pour les deux catégories, voir les paragraphes dédiés aux Transylvanides occidentales) fait qu'indique leur possible origine commune. La présence des ophiolites dans quelques transylvanides montre que celles-ci représentent les vestiges d'une croûte océanique de la Mer Téthys. D'autre part, les nappes de couverture bucoviniennes associées au Nappe bucovinienne (voir le cas de la région Hăghimaş) présententent des similitudes par leurs contenus lithostratigraphiques avec les formations mésozoïques des Nappes de Biharia des Monts Apuseni (nappes de cisaillement qui contient aussi de métamorphites). Pour les détails concernant ces nappes, voir Ianovici et al. (1976).

4. Les wildflyschs des Transylvanides occidentales

Les Transylvanides occidentales sont charriées sur le Système des Nappes de Biharia des Monts Apuseni. Quoi que il y a plusieurs classifications des Transylvanides occidentales, présentées par Ianovici et al, (1976) et par Balintoni (1997), une réalité s'impose: les séquences à wildflysch crétacé sont très fréquentes. Voilà, par exemple, la classification faite par Săndulescu (1984) concernant les Transylvanides occidentales et leurs contenus. Selon cet auteur, les Transylvanides occidentales se groupent dans deux segments: l'un occidental et l'autre oriental. **Le segment occidental** renferme les Nappes: de Criş; de Groşi de Techereu-Drocea (dans cette unité est englobé le plus grand volume des ophiolites des Transylvanides occidentales), de Căbeşti et de Bejani. Dans ces entités, à coté d'autres formations sédimentaires et magmatogènes ophiolitiques, il y a des wilflyschs d'âge Aptien supérieur ou Albien. **Le segment oriental** englobe les Nappes suivantes: de Feneş, de Curechiu-Stănija, de Trascău et de Fundoaia s.str, parmi lesquelles, seulement la première unité renferme aussi de wildflysch d'âge Aptien supérieur ou Albien. Les indices suivants montrent que l'ensemble des Transylvanides occidentales représente un prisme d'accrétion, lié par une zone de subduction alpine: **(1)** l'existence des séquences de wildflysch, dans la majorité des celles-ci, qui, dans notre conception, représentent des mélanges. Nous mentionnons que, dans la Nappe de Techereu-Drocea, il y a une séquence faite en mélange, mis en évidence par Savu (1984); selon cet auteur, cette entité est formée par une matrice pyroclastique dans laquelle sont logés des blocs de roches basiques; **(2)** l'existence des roches ophiolitiques (parfois démembrées ou brèchifiées), présentes dans quelques nappes; **(3)** la présence du métamorphisme alpin (Russo-Săndulescu & Berza, 1976) dans les roches calcaires mésozoïques de la Nappe de Fundoaia s. str.

Vers le sud, les Transylvanides occidentales sont développés dans les Monts Drocea et dans le profondeur (dans le soubassement du Bassin de Transylvanie), sont interrompues et déplacées fortement vers l'ouest par la Ligne Sud-Transylvaine (pour cette fracture, voir Săndulescu, 1984), ainsi se continuant avec la Zone de Vardar, comme a montré Kräutner (1996). Pour souligner la liaison spatiale initiale entre le deux segments de la suture téthysienne, Kräutner (1996) la dénommé « **la Suture Transylvanie-Vardar** ».

Bibliographie

Balintoni I., 1997. Geotectonics of the metamorphic terranes from Romania (in Romanian). Editura Carpatica, 176 pp., Cluj-Napoca.

Bleahu M., 1983. Global Tectonics (in Romanian). Editura ştiinţifică şi enciclopedică, vol. I, 624 pp., Bucharest.

Ianovici V., Borcoş M., Bleahu M., Patrulius D., Lupu M., Dimitrescu R., Savu H., 1976. Geology of Apuseni Mountains (in Romanian). Editura Academiei, 631 pp. Bucharest.

Kräutner H.G., 1996. Alpine rifting, subduction and collision in the Romanian Carpathians. Abstract VI, Symposium fur Tectonik-Struktur- und Kristallingeologie, Salzburg, April 1996, p. 230-234.

Mureşan M., 2002. La Nappe alpine de Rarău. (structure interne; minéralisations) dans la Zone cristallino-mészoïque des Carpathes Orientales. Romanian Journal of Mineral Deposits, 80, 97-100, Bucharest.

Mureşan M., 2006. Rédéfinition de la Zone cristalino-mésozoïque des Carpathes Orientales et son charriage post-autrichien sur la Zone du flysch. Anuarul Institutului Geologic al României, 74 (Special Issue), 153-159, Bucharest.

Mureşan M., 2008. Nappes de charriage de couverture alpines dans la Zone cristallino-mésozoïque des Carpathes Orientales. Un exemple: la région des Monts Hăghimaş. Anuarul Institutului Geologic al României, 75 (Special Issue), 32-36, Bucharest.

Patrulius D., Dimian-Popa Elena, Popescu-Dimitriu Ileana, 1966. The Mesozoic series and the Transylvanian slide nappe around Comăna (Perşani Mountains) (in Romanian). Anuarul Comitetului de Stat pentru Geologie, 35, 397-444, Bucharest.

Patrulius D., Popa Elena, Popescu Ileana, 1969. Structure of the Bucovinian Nappe in the southern part of the Moldavian cristalline massif (Eastern Carpathians) (in Romanian). Anuarul Comitetului de Stat pentru Geologie, 37, 71-117, Bucharest.

Russo-Săndulescu Doina, Berza T., 1976. The Boierişte tectonic window from the Valea Muntelui Colţeşti (Trascău Mountains) (in Romanian). Dări de seamă ale Institutului de Geologie şi Geofizică, 62/5, 141-148, Bucharest.

Savu H., 1984. The Mélange with pyroclastic matrix associated with the southern island arc of the Mureş Zone (in Romanian). Academia Republicii Socialiste România, Studii şi cercetări de geologie, geofizică, geografie, series Geologie, 29, 36-43, Bucharest.

Săndulescu M. (1975). Geological study of the central and northern parts of the Hăghimaş Syncline (Eastern Carpathians) (in Romanian). Anuarul Institutului de Geologie şi Geofizică, 45, 5-200, Bucharest.

Săndulescu M. (1984). Geotectonics of Romania (in Romanian), Editura Tehnică, 334 pp., Bucharest.

PRISME D'ACCRÉTION ET ET DES MÉLANGES DANS L'OROGÈNE CIMMÉRIEN NORD-DOBROGÉEN – SITUATION DES MINÉRALISATIONS TRIASIQUES BARYTINIFÈRES ET DE SULFURES DU CELUI-CI

Mircea MUREŞAN

Geological Institute of Romania – str. Caransebeş 1, Sector 1, 012271 Bucharest
e-mail: muresenii@yahoo.com

Abstract The North Dobrogea orogen includes Cimmerian thrust nappes. These were formed during the late Cimmerian movements, which represent the main Alpine tectogenetic event in the North Dobrogean Orogen. The main thrust nappes in North Dobrogea are (from top to bottom): Măcin Nappe, Consul Nappe, Niculiţel Nappe, Tulcea Nappe, Denis Tepe Nappe and Subegisian Nappe. The Consul, Niculiţel, Tulcea and Denis Tepe nappes constitute the Egissian nappes (from Aegissus, the ancient name of Tulcea town) – Cimmerian cover units. We consider that all the Egissian nappes represent an accretionary prism (expelled during the end-Jurassic closure of the subduction zone). Our main argument is the presence of tectonic melange facies of Bogza type in each Egissian nappe and melange of Trestnic type in the Niculiţel Nappe.

Keywords: North Dobrogea Orogen, overthrust nappes, cimmerian subduction; mélange; accretionary prism, ophiolitic suture, Mississippi Valley type

1. Introduction

Les mélanges représentent des faciès tectoniques associés avec les zones de subduction, étant décrites presque dans toutes les chaînes alpines du monde. Typiquement, ces entités sont constituées par des fragments de roches sédimentaires, de roches magmatiques du type ophiolitiques et, parfois, de roches métamorphiques, toutes ces roches étant distribuées dans une manière chaotique dans une matrice pélitique fortement déformée.

Les prismes d'accrétion (constitués par des unités allochtones du type de nappes de charriage) sont liés aussi par les zones de subduction, étant expulsés pendant la fermeture des celles-ci.

Dans cet article, nous allons montrer que des mélanges et un prisme d'accrétion se développent aussi dans l'Orogène Nord-Dobrogéen (OND), lié par les mouvements cimmériens nouveaux.

2. Limites et l'extension de l'Orogène Nord-Dobrogéen (OND)

La position géotectonique de la Dobrogea dans l'avant pays des Carpathes a été examinée par Visarion et al. (1990). Săndulescu (1980) a déchiffré les relations de la Dobrogea avec les chaînes alpines autour de la partie occidentale de la Mer Noire. L'auteur a démontré que l'OND représente le prolongement vers l'est de la chaîne alpine développée dans la Crimée.

Auparavant, la Dobrogea Centrale (DbC) était attribuée en totalité à la Plate-forme Moésienne, renfermant tant le Groupe des Schistes Verts (GSV) – d'âge briovérien (Mirăuţă, 1969) que la pile mésométamorphique du Protérozoïque moyen du Groupe Altîn Tepe (séparé par Mureşan, 1971); par conséquent, le contact entre la DbC et l'Orogène Nord-Dobrogéen était considéré la Faille Peceneaga-Camena (FPC), qui représentait en même temps la limite entre la Plate-forme Moésienne et cet orogène. Par contre, selon nous (Mureşan, 2005, 2006), la Dobrogea Centrale renferme tant la partie septentrionale de la Plate-forme Moésienne (représentée par les roches briovériennes faiblement métamorphisées de la pile du GSV) que la partie méridionale de la Nappe de Măcin de l'OND (représentée par la pile du Groupe Altîn Tepe). **(1) La limite méridionale** à jour, de l'OND est logée au sud de FPC, étant représentée par le Charriage istrien (Mureşan, 1971) du GSV sur la pile de l'AT, la plus méridionale partie, à jour, de l'OND (représenté par la Nappe de Măcin du celui-ci – voir le paragraphe II A concernant cette unité). Le Charriage Istrien du GSV sur la pile de l'AT signifie en effet le charriage de la Plate-forme Moésienne sur l'OND. **(2) Vers le nord**, l'OND est limité par la Faille Sfântu Gheorghe (orientée ONO-ESE), au nord de qui se développe la Dépression Prédobrogéenne~~.~~ (aujourd'hui cachée sous les dépôts tertiaires et quaternaires). **(3) Vers l'ouest**, l'OND (ainsi que la toute Dobrogea) est limité par le Danube, qui, selon nous (données inédites) a une vallée contrôlée par la « **Fracture du Danube (FrDa)**, au moins jusqu'à le méridien de Turnu Măgurele. Le segment septentrional de la cette fracture affecte aussi la Dépression Prédobrogéenne, la partie occidentale de la celle-ci étant déplacée vers le nord (données de forages de la région Bârlad). Le long de FrDa, le versant droit du Danube est toujours élevé tectoniquement, ainsi que dans ce versant affleurent les plus anciennes formations de la Dobrogea et, en amont de celle-ci (dans la Bulgarie), les dépôts des Crétacé supérieur, Paléogène et Miocène. Nous apprécions que le saut de la FrDa se chiffre à quelques centaines de mètres. **(4) Vers l'est**, l'OND (ainsi que l'ensemble de la Dobrogea) est affecté par la Fracture péri-bassin de la Mer Noire, le long de qui le fond sous-marin est baissé.(Mureşan, données inédites) en moyen avec 50-100 m..

Nous mentionnons que dans les conceptions antérieures (synthétisées par Săndulescu, 1984), l'OND représente un orogène alpin intra - cratonique assez étroit serré entre la Plate-forme Moésienne et la Plate-forme Est-Européenne. Aujourd'hui, puisque le Charriage Istrien représente en réalité le chevauchement (du type charriage) de la Plate-forme Moésienne sur l'OND, l'extension de l'OND sous celle-ci est sûrement réel. Selon notre nouveau modèle tectonique, l'OND est probablement étendu beaucoup vers le Sud sous la Plate-forme Moésienne, y compris sous les unités tectoniques moésiennes logées dans la Dobrogea méridionale. D'autre part, l'OND s'étendait initialement beaucoup vers le Nord (plus au nord par rapport à l'emplacement actuel de la Faille Sfântu Gheorghe), comme une grande nappe de charriage (de cisaillement) au-dessus des formations mésozoïques et paléozoïques de la Dépression Pré-Dobrogéenne. Nous supposons que ces relations de charriage entre les deux unités se prolongent en profondeur dans le compartiment méridional de la Faille Peceneaga-Camena. Ainsi, à notre avis, l'Orogène Nord-Dobrogéen a une extension considérable, qui initialement a dépassé au moins 100-150 km.

3. L'Orogène Nord-Dobrogéen

L'OND englobe les nappes de charriage, formées pendant les mouvements cimmériens nouveaux, qui représentent la dernière et la plus importante tectogenèse alpine déroulée dans l'OND. Les nappes de l'OND sont partiellement couvertes transgressiv par les dépôts post-tectoniques du Crétacé supérieur (Vraconien, Cénomanien, Turonien, Coniacien) du Bassin Babadag. Les nappes principales connues de l'OND (les premières quatrièmes ont été mises en évidence par O. Mirăuță (fide Patrulius et al. 1973, 1974) la cinquième et la sixième sont décrites par nous dans cet article et elles sont (de haut en bas) les suivantes: **Nappe de Măcin (NMa)**, **Nappe de Consul (NCo)**, **Nappe de Niculițel (NNi)**, **Nappe de Tulcea (NTu)**, **Nappe de Denis Tepe (NDT)**, **Nappe Souségissiéenne (NSEg)**. La NCo, la NNi, la NTu et la NDT sont unités de couverture étant constituées tant par de depôts sédimentaires triasiques et jurassiques que par des roches magmatogènnes (ophiolites et rhyiolites triasiques.). Nous les avons dénommées en ensemble (Mureşan 2005, 2006) **les Nappes égissiennes** (selon Aegissus, l'ancien nom antique de la ville Tulcea).

(A) <u>La Nappe de Măcin (NMa)</u> représente l'unité tectonique majeure la plus interne de l'Orogène Nord-Dobrogéen; elle est constituée principalement par des mésométamorphites du Protérozoïque moyen (parmi ceux-ci les mésométamorphites des Groupes Megina et Orliga et, au sud de FPC, ceux du Groupe Altîn Tepe), ainsi que des formations sédimentaires paléozoïques (parfois faiblement métamorphisées) et des granitoïdes (varisques et anté - varisques). Nous mentionnons que des dépôts du Trias moyen et du Jurassique ainsi que des rhyolites jurassiques se développent dans la partie méridionale de la Nappe de Măcin (très près de la Faille Peceneaga-Camena), dans la région de Cârjelari-Camena (aujourd'hui connue en détail par les études de Grădinaru, 1981, 1988). Cette région renferme une autre unité de l'Orogène Nord-Dobrogéen, selon nous inférieure vis-à-vis de Nappe de Măcin (l'appartenance tectonique de l'Unité de Cârjelari-Camena sera discutée dans le paragrpahe B dedié aux Nappes égissienes). Il en résulte que la Nappe de Măcin est dépourvue de formations mésozoïques. Nous soulignons l'importance des écailles (ou nappes?) pour la structure de la cette grande unité, parmi lesquelles: ceux de Balabancea-Bugeac, Megina, Orliga, (Seghedi, dans Krautner et al. 1988; Seghedi, 19988; Săndulescu 1984). La Nappe de Măcin est charriée sur la pile des Nappes égissiennes, le long de charriage cimmérien nouveau Luncavița-Consul-Babadag. Vers le SE, la NMa est cisaillée par la Faille Peceneaga-Camena, qui laisse dans son flanc méridional une partie de la NMa représentée, à jour, par la pile mésométamorphique du Groupe Altîn Tepe (Protérozoïque moyen).

(B) <u>Les Nappes égissiennes (NEg)</u> Les études stratigraphiques détaillées récentes des dépôts mésozoïques de ces nappes (Grădinaru, 1981, 1984, 1988; Baltreş, 1982, 1992; Baltreş & E. Mirăuță, 1995; Baltreş et al., 1992; Seghedi et al. (1990), Ionesi, 1994; Cătuneanu & Maftei, dans Ionesi, 1994) ont montré qu'il y a des différences lithofaciales notables entre la plupart des entités sédimentaires mésozoïques isochrones. Cette situation nous démontre que ces unités sont véritables nappes de charriage, ayant à leurs bases des plans de charriages importants.

(1) <u>Nappe de Consul (NCo),</u> orientée NNO-SSE, supporte vers SO le charriage cimmérien de la NMa, le long de la Ligne Luncavița-Consul-Babadag. Vers NO et vers SE, la NCo est dépassée par la NMa. La NCo renferme, principalement, des dépôts de l'intervalle Werfénien supérieur - Anisien, et des apparitions de basaltes et de rhyolites triasiques qui montre le caractère bimodal du ce volcanisme triasique pendant cette étape de développement. Vlad (1978) a expliqué cette situation rappelant que dans le stade initial des « bassins initiales ensialiques » (préconisés par Mitchell & Garson – 1976) se développe un volcanisme du tel type. Pour Vlad, il en résulte que dans le Triasique de la Dobrogea de nord. il y a le vestiges des manifestations volcaniques du type bimodal. Nous sommes d'accord avec cette affirmation. Les relations entre les roches magmatogènes et celles sédimentaires ont été présentées par Seghedi et al. (1990). Nous remarquons que, sous les premières formations triasiques fossilifères du Werfénien supérieur se développe **la Formation épiclastique de Bogza – FEB** (Baltres, 1982), non-fossilifère, typiquement développée près de Mihai Bravu. La FEB est constituée par des brèches polymictiques; dans une matrice sableuse, il y a des gallets assez fréquemment arrondis, représentés par des granits, des schistes cristallins, des roches paléozoïques (grès quartzitiques, siltites). Ayant les mêmes traits principaux, la FEB se retrouve tant dans la Nappe de Niculițel que dans la Nappe de Tulcea Selon nous, cet ensemble représente des roches triturées (donc, un faciès tectonique), du type mélange, formé entre les deux machoires de la zone de subduction. La rondeur des gallets nous l'expliquons par le roulement tectonique. Puisque cette entité représente un faciès tectonique, elle ne peu pas être une formation épiclastique; par conséquent nous la rénommons: **le Mélange de Bogza (MeBo)**. **(2) <u>Nappe de Niculițel (NNi)</u>** englobe les dépôts de l'intervalle Werfénien supérieur-Norien et le plus grand volume des roches magmatogènes basiques triasiques, connu dans l'Orogène Nord-Dobrogéen. Ces roches, caractérisées comme des ophiolites par Savu et al. (1980), sont représentées par: des basaltes (qui présentent des pilow - lava – Savu et al., 1980; Savu, 1986; des dolérites et des gabbros (Savu et al., 1980). Nous soutenons que dans la Nappe de Niculițel il y a les vestiges d'une suture (cicatrice) ophiolitique cimmérienne. Parce que les ophiolites, présentes dans la NNi ne sont pas associées avec des rhyolites, nous pouvons affirmer que ces roches ont pris naissance dans un stade plus récent que du celui-ci des volcanites bimodales existantes dans la Nappe de Consul (voir les discutions présentées dans le paragraphe antérieur). C'est-à-dire comme une conclusion des discussion concernant les roches magmatogènes acides et basiques (points 1 et 2), le rift (dans notre cas le Rift Niculițel a eu une évolution qui a commencée avec le magmatisme bimodal et s'a continuée avec le magmatisme ophiolitique proprement dit.

Comme dans le cas de la NCo, sous la Formation de Somova (Baltreş, 1982, 1992) du Werfénien supérieur), est logé **le Mélange de Bogza** (à les mêmes traits comme dans le cas de la NCo). Á Trestinic **(**dans les collines Coasta lui Nicu et Caracuş**)**, sous la Formation de Cataloi (Ladinien supérieur-Carnien) se développe (dans une position tectonique) une séquence formée par une matrice argileuse, dans laquelle sont logés des blocs (parfois de grandes dimensions) faites en calcaires (carniens ou noriens), silicolithes et basaltes, ensemble considéré par Mutihac (1964) comme un wildflysch de nature sédimentaire. Par contre, pour nous cette séquence représente un mélange du type franciscain **– le Mélange de Trestinic (MeTr).** Les roches dévoniennes, connues à l'ouest d'Isaccea, sont logées, peut-être (cf. Săndulescu, 1984), dans une fenêtre tectonique où représente un lambeau de charriage de la NMa. **(3) <u>Nappe de Tulcea (NTu)</u>**, qui supporte la NNi, englobe des roches basiques (basaltes et dolérites) et acides (rhyolites et pyroclastites), mises en place pendant le Werfénien supérieur-Anisien inférieur – Elena Mirăuță, 1982; Savu et al., 1985; Savu, 1986) ainsi qu'un important volume de dépôts triasiques et jurassiques, y compris ceux du Malm (Grădinaru, 1974; 1984; Ionesi, 1994). Vers la partie orientale de la NTu, en profondeur (données de forages) de la zone du shelf de la Mer Noire, Cătuneanu & Maftei (dans Ionesi, 1994) ont décrit également des dépôts triasiques et du Jurassique (y compris du Malm) et des roches magmatogènes basiques (basaltes et andésites basaltoïdes) du Jurassique supérieur (données d'âge K–A). Cette situation nous montre que dans la NTu il y a des preuves pour la continuation de l'activité du Rift Niculițel jusqu'à la fin du Jurassique supérieur. Dans la NTu, il est très intéressant de noter la présence du **Mélange de Bogza (MeBo)**, qui constitue de nombreuses petites apparitions, les plus connues étant celles développées dans les environs de la ville de Tulcea (Dealul Monumentului; Dealul Bogza; Tulcea Veche). Le MeBo supporte le Werfénien supérieur à fossiles (la Formation de Tulcea Veche) Dans l'aire de développement de la NTu, il y a quelques apparitions de roches anté-mésozoïques (mésométamorphites, épimétamorphites) et paléozoïques (parfois faiblement métamorphisées) et des granitoïdes, toutes ces entités englobées par tous les autres chercheurs dans la Nappe de Tulcea. Au contraire, nous avons avancé l'hypotèse (2005, 2006) que la Nappe de Tulcea est dépourvue d'entités antémésozoïques, étant charriée sur les roches anté-mésozoïques du soubassement, que nous les englobons et les dénommons la **la Nappe Souségissiènne (NSEg)**. Selon nous, les apparitions des roches anté-mésozoïques ont percé (comme d'habitude le long des failles) le corp de la NTu.

4. Situation des minéralisations triasiques barytinifères et de sulfures logées dans la Nappe de Tulcea Découvertes et explorées pendant les années '50 du siècle passé, ces minéralisations ont été considérées épigénétiques (hydrothermales) par tous les chercheurs (parmi les autres: Ianovici et al., 1957, 1977, Popescu, 1977), à l'exception de Vlad (1978) qui a élaboré une hypothèse génétique complexe, basée sur ses études concernant la minéralogie, les roches encaissantes, le contexte géologique et géotectonique des concentrations de barytine et de sulfures. Les occurrences principales, toutes logées dans l'Unité de Tulcea, sont (de l'ouest vers l'est) les suivantes: Movila Săpată, Ormanu cu Pari, Dealul Văcăriei, Somova (Dealul Cortelu), Dealul Trifan, Dealul Dobrişani, Dealul Bechir, Dealul Carierei, Marca, Malcoci et, plus au nord de celle-ci, à Bogza. Vlad (1978) a distingué **deux types génétiques** principales des minéralisations en question: **(a) syndiagénétiques**, les plus anciennes, représentées par les « corps syn - concordantes » de barytine (Somova–Dealul Cortelu, Dealul Bechir, Dealul Carierei), logés exclusivement dans les calcaires à intercalations dolomitiques du Ladinien; **(b) épigénétiques (hydrothermales)**, plus récentes que les premières, qui sont représentées par la barytine et par des sulfures métalliques (galène, blende, plus rarement chalcopyrite). La minéralisation polimétallique (Zn, Pb, Cu), accompagnée par la fluorine, plus une nouvelle génération de barytine constituent et des filons, imprégnations et des corps tabulaires (par exemple, à Somova-Cortelu), tant dans les roches carbonatées ladiniennes que dans le rhyolites triasiques. Vlad (1978) a encadré toutes les minéralisations discutées dans le type Mississippi Valley – Alpin, formées pendant l'existence du Rift triasique du l'Orogène Nord-Dobrogéen. **Nos discussions**. **(1)** En lieu de nom « corp concordant » (Vlad, 1978), nous proposons le nom de « couche lentilliforme concordante » ou même de « lentille concordante », les deux termes exprimant mieux les formes des gisement de la barytine syngénétique (par exemple Somova-Cortelu – voir les coupes géologiques faites par Ianovici et al., 1957). **(2)** Le même auteur a englobé tant les minéralisations syngénétiques que celles épigénétiques (hydrothermales) dans le type Mississippi Valley Alpin, pour souligner leur consang~~v~~uinité. Nous croyons que c'est mieux d'utiliser le terms « du type Mississippi Valley seulement pour la barytine syngénétique et pour l'ensemble des deux types génétiques « des minéralisations du type Mississippi Valley sensu lato ». **(3)** Les minéralisations syngénétiques de barytine, concordantes par raport avec les roches carbonatées ladiniennes, dans lesquelles sont logées, appartiennent de la lithostratigraphie du Ladinien. Ainsi, la colonne du Ladinien a une double nature: sédimentaire et hydrothemal-sédimentaire (puisque les processus de dépositions concordantes des minéralisations du type Mississippi Valley sont de nature hydrothermal. Ainsi, dans la Nappe de Tulcea, on peut parler d'un faciès barytinifer du Ladinien. **4) Nappe de Denis Tepe (NDT)**. L'important coude de la Vallée Teliţa (jalonné par les localités Poaşta, Cataloi, Mihail Kogălniceanu) limite une région constituée seulement par des dépôts du Jurassique inférieur (Lias), développés à l'Est de localité Nalbant. Ces entités sont représentées principalement par de grés argileux à intercalations d'argiles. Le monticule Denis Tepe est fait en dépôts flyschoïdes (grés à intercalations argileuses) et des grés. L'aire discutée coïncide avec uine anomalie gravimétrique que nous l'interprétons comme un effet d'une fenêtre tectonique où affleurent les formations du Lias. Nous considérons qu'il s'agit d'une nappe égissienne à une position tectonique inférieure vis-à-vis de la Nappe de Tulcea..

Unité de Cârjelari-Camena (UCC) se développe plus au sud de charriage Luncaviţa-Consul-Babadag, dans l'aire de développement de la Nappe de Măcin. Par sa constitution lithostratigraphique (des formations triasiques et jurassiques) s'approche clairement de Nappes égissiennes, surtout de Nappe de Denis Tepe,.les deux ayant des formations jurassiques. C'est très intéressant que Grădinaru (1981) a mis en évidence dans l'UCC des rhyolites jurassiques (oxfordiennes) – le Rhyolite de Camena – une nouveauté dans la littérature concernant l'OND. Aussi, cet auteur a décrite une brèche polymictique: dans une matrice gréseuse il y a des blocs (0,30-1,50 m) de grés quarzeuses, dolérites, basaltes, des marbles. Cette entité, qui affleure dans l'embouchure du ruisseau Bichit avec la Vallée Başpunar, a été interprétée par Grădinaru comme une olistostrome cisaillée ou comme un mélange; dans les deux cas, l'auteur suppose que cette entité a pris naissance sous l'influence tectonique (pendant l'Oxfordien) de la Faille Peceneaga-Camena. Pour nous cette brèche représente un mélange (**Mélange de Bichit - MeBi**), formé dans la zone de subduction liée par les mouvements cimmériens nouveaux, qui ont engendré l'OND. Étant associé seulement avec les formations ladiniennes de la formation d'Uspenia, nous considérons q'il est possible une âge anté-jurassique (triasique) pour ce mélange. Selon nous, l'apparition de l'UCC s'est produit le long de Faille Cârjelari-Camena, que nous la traçons par le sud de localité Cârjelari, puis par la localité Camena et d'ici le long de contact entre les apparitions de la Formations de Carapelit (Carbonifère inférieur ? – développé seulement dans la Nappe de Măcin).et la Formation d'Uspenia (Ladinien), les deux entité mises en évidence par Grădinaru (1981).

5. Nappe Souségissiéenne (NSEg)

Dans notre conception, la NSEg représente une unité de socle, qui, selon nous, est charriée directement sur les formations de la Dépression Prédobrogéenne (DPD). Selon nous, les apparitions des roches anté-mésozoïques, qui percent le corps de la nappe de Tulcea (comme d'habitude le long des failles) sont les apparitions à jour de la NSEg. Selon nous, cette unité représente la partie inférieure de l'Orogène Nord-Dobrogéene (OND). Notre hypothèse (Mureşan, 1971) concernant l'allochtonie du l'OND vis-à-vis de DPD a été confirmée par les résultats obtenus par les méthodes d'induction électromagnétique (Stănică & Stănică, 1989; Stanică, dans Visarion et al., 1990) qui montrent l'existence, en profondeur (environ de 4000 m), d'un plan tectonique de chevauchement à la base de l'OND vis-à-vis de la Dépression Prédobrogéenne. Cisaillant en profondeur les structures de l'OND, il s'agit d'un plan de charriage, produit à la fin de la tectogenèse cimmérienne qui a engendré finalement l'Orogène Nord-Dobrogéen. Le plan du charriage de l'OND sur la DPD a été ultérieurement fortement soulevé dans l'aile septentrionale de la Faille Sfântu Gheorghe (faille normale, inclinée vers le sud et orientée NO-SE.).

6. Conclusions

Selon nous (Mureşan, 2005, 2006), les nappes égissiennes ont pris naissance par obduction, pendant la fermeture fini-jurassique de l'océan, formé en liaison avec l'évolution du Rift Niculițel. L'existence du ce rift a été mise en discussion pour la première fois par Vlad (1978), qui l'a considéré actif seulement pendant le Triasique (opinion adopté ultérieurement parmi les autres par: Savu et al., 1980; Savu, 1986; Saccani et al., 2004; Săndulescu, 1984, Balintoni, 1997). Vlad a caractérisé cet élément géotectonique comme un rift du type alaucogène, formé intra - plaque (une opinion soutenue par Savu et.al., 1980, Savu, 1986). En revanche, nous avons montré que dans la Nappe de Tulcea, il y a des preuves pour argumenter la continuation de l'activité du Rift Niculițel jusqu'à vers la fin du Jurassique (voir II, B, 3).

Nous considérons que l'ensemble des nappes égissiennes représente un prisme d'accrétion (expulsé pendant la fermeture fini - jurassique de la zone de subduction). Notre argument principal est la présence, dans les toutes les nappes égissiennes, du faciès tectonique (trituré) du type Mélange de Bogza et la présence du mélange du type Trestinic dans la Nappe de Niculițel. Le magmatisme bimodal (ses roches sont présentes dans la Nappe de Consul) a pris naissance pendant l'étape de la formation du Rift Niculițel. Les ophiolites des Nappe de Niculițel se sont formées plus tard, marquand la période de maturité du ce rift. À notre avis, la croûte océanique, créée (dans l'intervalle Triasique-Jurassique) à la suite de la riftogenèse, était bordée à l'ouest par un continent constitué principalement par des formations anté-mésozoïques englobées dans l'actuelle Nappe de Măcin.:Au début des mouvements cimmériens nouveaux, la croûte océanique a subi un processus de subduction sous la plaque continentale occidentale du type Măcin. Il est possible que l'actuel plan de charriage de la Nappe de Măcin (la Ligne Luncavița-Consul-Babadag) représente le vestige déformé du paléo plan de la cette plaque.

Bibliographie

Balintoni I., 1997. Geotectonics of the metamorphic terranes from Romania (in Romanian). Edit. Carpatica, 176 pp., Cluj-Napoca.

Baltres A., 1982. Sedimentologic study of the Spathian banded limestones spathiene fromthe Mineri-Movila Săpată perimeter (North Dobrogea). Archive of the Geological Institute of Romania, Bucharest.

Baltres A., 1992. Somova Formation (North Dobrogea). Sedimentologic study (in Romanian). Ph.D. Thesis. Archives of the University of Bucharest.

Baltres A., Mirăuță E., 1995. Stratigraphy of the Triassic and lower Jurassic formations from North Dobrogea (in Romanian). Archive of the Geological Institute of Romania, Bucharest.

Baltres A., Seghedi A., Mirăuță E., Stanciu L., 1992. Complex Study of the Paleozoic and Mesozoic formations from Tulcea zone (in Romanian). Archive of the Geological Institute of Romania, Bucharest.

Gradinaru E., 1981. Sedimentary rocks, acid and basic volcanics of the upper Jurassic from Camena zone (North Dobrogea) (in Romanian). Analele Universității București, 30, 90-110, Bucharest.

Grădinaru E., 1984. Jurassic rocks of North Dobrogea. A depositional-tectonic aproach. Acad. R.S.R., Rev. Roum. Géol. Géophys, Géogr., Série Géol., 33, 61-72, Bucharest.

Grădinaru E., 1988. Jurassic sedimentary rocks and bimodal volcanics of the Carjelari-Camena outcrop. Studii şi Cercetări de Geologie, Geofizică, Geografie, Seria Geologie, 33, 97-121, Bucharest.

Ianovici V., Bacalu V., Giuşcă D., Stiopol V., 1957. Study of the mineralisation from the barite and base metal sulfides from Somova region (in Romanian). Analele Universității Parhon, 15, 149-159, Bucharest.

Ianovici V., Stiopol V., Măldărescu I., Popescu G.C., 1977. The Cimmerian metallogenesis in North Dobrogea (in Romanian). Academia Republicii Socialiste România. Studii şi Cercetări de Geologie, Geofizică, Geografie, Seria Geologie, 22, 11-17, Bucharest.

Ionesi L., 1994. Geology of the platform units and of the North-Dobrogea Orogen (in Romanian). Editura Tehnică, 280 pp., Bucharest.
Kräutner H. G., Mureşan M., Seghedi A., 1988. Precambrian of Dobrogea. In Zoubek V. (edit.): Precambrian in younger fold belt. 361-379, J. Wiley, London.
Mirăuță E., 1982. Biostratigraphy of the Triassic deposits in the Somova-Sarica Hill zone (North Dobrogea) with special regard of the eruption age. Dări de seamă ale şedințelor Institutului de Geologie şi Geofizică, 64/4, 63-78, Bucharest.
Mirăuță O., 1969. Tectonics of the upper Proterozoic from Central Dobrogea (in Romanian). Anuarul Institutului Geologic, 37, 8-36, Bucharest.
Mitchell A.H.G., Garson M.S., 1976. Mineralisation at plate boundaries. Minerals Science Engineering, 8, 129-169.
Mureşan M., 1971. On the presence of a tectonic window in the Greenschist Zone of the Central Dobrogea (Altîn Tepe Region) (in Romanian). Dări de seamă ale şedințelor Institutului Geologic, 57/5, 127-154, Bucharest.
Mureşan M., 1975. General view on the sequence of formation of the Paleozoic synorogenic and subsequent magmatic rocks (s.l.) from North Dobrogea (in Romanian). Dări de seamă ale şedințelor Institutului de Geologie şi Geofizică, 61/5, 113-133, Bucharest.
Mureşan M., 2005. L'allotochnonie tectonique alpine des unités de la Dobrogea et leur structure interne.
Symposium GEO 2005, Abstracts Volume, 67-77, Roşia Montană, Romania.
Mureşan M., 2006. Unités alpines, charriages et failles dans la Dobrogea. Anuarul Institutului Geologic. 74. 153, Bucharest.
Mutihac V., 1964. Tulcea zone and its position in the structural framework of Dobrogea (in Romanian). Anuarul Institutului Geologic, 148-153, Bucharest.
Patrulius D., Mirăuță E., Mureşan M., Iordan M., 1973. Stratigraphic and structural syntesis of North Dobrogea. I. Paleozoic formations (in Romanian). Archive of the Geological Institute of Romania, Bucharest.
Patrulius D., Mirăuță E., Iordan M., Baltreş A., Țicleanu N., 1974. Stratigraphic and structural syntesis of North Dobrogea. II. Mesozoic formations (in Romanian). Archive of the Geological Institute of Romania, Bucharest.
Popescu C. Gh., 1977. Metallogenetic similarities between the North Dobrogea and the Eastern Carpathians in the view of the global tectonics (in Romanian). Studii şi Cercetări de Geologie, Geofizică, Geografie, Seria Geologie, 22, 19-25 Bucirueşti.
Saccani E., Seghedi A., Nicolae I., 2004. Evidence of Rift magmatism from preliminary petrological data on Lower Triassic mafic rocks from the North Dobrogea Orogen. Ofioliti, 29, 231-241.
Savu H., 1986. Triassic, continental intra-plate volcanic in North Dobrogea. Revue Roumaine de Géologie, Géophysique, Géographie (série Géologie), Academia Republicii Socialiste România, 30, 21-29, Bucharest.
Savu H., Udrescu C., Neacşu V., 1980. Structural, petrological and genetic study of the ophiolites from the Niculițel Zone (North Dobrogea). Dări de seamă ale şedințelor Institutului de Geologie şi Geofizică, 65/1, 41-64, Bucharest.
Săndulescu M., 1980. Geotectonic analysis of the Alpine mountain belts around the western Black Sea (in Romanian). Anuarul Institutului Geologic, 56, 5-55, Bucharest..
Săndulescu M. (1984). Geotectonics of Romania (in Romanian), Editura Tehnică, 334 pp., Bucharest.
Seghedi A., 1998. Petrologic study of the magmatic and metamorphic study from the Megina-Mircea Voda zone (Dobrogea) (in Romanian). Ph.D. Thesis. Archives of the University of Bucharest.
Seghedi A., Szakács A., Baltreş A., 1990. Relationships between sedimentary deposits and eruptive rocks in the Consul Unit (North Dobrogea). Implications on tectonic interpretations. Dări de seamă ale şedințelor Institutului de Geologie şi Geofizică, 74, 5, 125—136, Bucharest.
Stănică D., Stănică M., 1989. The investigation on the deep structure of the Moesian Platform (Romania) by means of electromagnetic induction methods. Gerlands Beitrage zur Geophysik 155-163, Leipzig.
Visarion M., Săndulescu M., Roşca Vl., Stănică D., Atanasiu L., 1990. La Dobrogea dans le cadre de l'avant pays carpathique. Rev. Roum. Géophys., 34, 55-65, Bucharest.
Vlad Ş., 1978. Triassic metallogenesis from Tulcea zone (North Dobrogea) (in Romanian). Studii şi Cercetări de Geologie, Geofizică, Geografie, Seria Geologie, 23/2, 249-258, Bucharest.

MEDICAL GEOLOGY AND LIFE CYCLE ASSESSMENT – THE MISSING LINK

Grigore BUIA[1], Monica RĂDULESCU[2]*
[1] University of Petrosani, Strada Universitatii 20, Jud. Hunedoara, Petrosani, Romania; E-mail: *grigbuia@yahoo.com*
[2] Conestoga-Rovers & Associates, 1880 Assumption Street, Unit 200, Windsor, Ontario, N8Y1C4, ph:1-519.966.9886 ext. 2267, fax:1-519.966.3894, e-mail: *mradulescu@craworld.com*

Abstract Life Cycle Assessment (LCA) is a technique that assesses environmental impacts associated with all the stages of a product/process' life from-cradle-to-grave. LCA is used to provide an enhanced outlook on environmental concerns of particular interest in a defined spatial/temporal space. In the recent years, complex Life Cycle Impact Assessment (LCIA) methodologies have been developed and refined, covering a wide range of environmental effects, harmonized from a midpoint approach (climate change, terrestrial and aquatic toxicity, eutrophication etc) towards integrated endpoint environmental effects such as ecosystem damage, human health quality, resource depletion etc. The wide range of environmental media in LCA encompasses geology as well, through the complex relations between soil-water and air. However, LCA, by its own definition, deals only with anthropic processes. Medical Geology (MG) as an emerging science deals with the relationships between geological factors and health problems in humans, animals, plants and generally, ecosystems. Is there any way of establishing a working link between the findings of the two disciplines, LCA and MG - can the effects of the anthropic processes emphasized by LCA be linked to short-term geologic effects reflected in health, as explored by MG? The current essay is a first attempt of response to this question.

Keywords: Life Cycle Assessment, Medical Geology, link, environment, impacts.

1. Introduction

Life Cycle Assessment (LCA) is a technique that assesses environmental impacts associated with all the stages of a product/process' life from-cradle-to-grave, including the upstream and downstream activities in its entire life, from extraction of raw materials, through materials processing, manufacturing, distribution to the consumer, use, repair, maintenance, to end of life as disposal or recycling. LCA provides an enhanced outlook on environmental concerns of particular interest associated with the assessed product/process, in a defined spatial/temporal boundary. A selected range of environmental impacts is evaluated, in order to provide an enhanced comprehension of the environmental implications associated with the life of the product/process. LCA is mostly used to support business strategy (18%), research and development (R&D) (18%), as input to product or process design (15%), in education (13%) and for labeling or product declarations (11%) (Cooper and Fava, 2006).

In the meantime, Medical Geology (MG) is a new interdisciplinary scientific field, which explores the relationships between natural geological factors and their effects on human, animal and ecosystems health (Finkelman et al., 2001). Medical Geology investigates these subtle relationships through identification of overexposure or deficiency of trace elements, minerals and harmful chemical compounds in the human or animal body. The connecting pathways between these elements and the body occur through a variety of processes, including inhalation of naturally occurring and/or anthropogenic mineral dusts and volcanic emissions, transportation, modification and concentration of organic compounds, exposure to radionuclides, microbes and pathogens etc. (Finkelman, et al., 2001).

While the elementary flows quantified by LCA include inputs of water, energy, and raw materials, and releases to air, land, and water, defined by a variety of chemical compounds, with concentrations within a wide range of magnitudes, the MG deals essentially with the subtle pathways, at low concentrations, of trace elements, minerals and harmful chemical compounds (as results of natural and anthropic processes) between the geological environment and human/animal body. Usually, such subtle variations are difficult to identify and quantify and, furthermore, any potential relationship between these elements and human/animal/ecosystem health has to be scientifically documented and proven.

Is it possible to identify within the life cycle of a product/process sensitive hot-spots for the human/animal/ecosystem health, and use these findings as a starting point to further explore through MG the potential connection between environmental flows of elements in the geological environment and health?

No dedicated attempt has been made so far to investigate a potential connection between the different outcomes of LCA and MG. The current paper is a short essay that addresses the viability of such potential connection.

2. Life Cycle Assessment and environmental flows

As defined by the ISO 14000 series of environmental management standards, 14040:2006 and 14044:2006 (ISO 14040, 2006), LCA consists of four main phases:

- Definition of goal and scope: defining the technical details that guide the entire LCA process, including identification of the entire system of the product/process, with corresponding geographical and temporal boundaries and definition of a relevant functional unit
- Life Cycle Inventory (LCI): inventory of flows from and to nature within the boundaries of the product/process system, including inputs of water, energy, and raw materials, and releases to air, land, and water
- Life Cycle Impact Assessment (LCIA): evaluating the significance of potential environmental impacts based on the LCI results
- Interpretation of results: identify, quantify, check, and evaluate information from the findings of the LCIA.

Once the goal and scope of the study have been defined, the system boundaries and functional unit within the system identified and the LCI performed, LCIA comes as a next step of particular importance within the broader context of a potential connection between LCA-MG. While the aim of the LCI is to identify to the widest extent possible the environmental releases of chemical compounds to air, land, and water within the defined system, the outcome of this phase constitutes just a summary of emissions, with no direct link to any potential environmental impacts related to their existence. Such environmental link is established through LCIA, which evaluates the significance of potential environmental impacts based on the LCI through:

- Selection of significant environmental impact categories related to the life cycle of the assessed product/process
- Selection of category indicators and characterization models
- *Classification* of the LCI, where the inventory emissions are sorted and assigned to specific impact categories; and
- Impact quantification through *characterization*, where the LCI flows previously classified within a specific environmental impact category are characterized into common equivalence units and quantified into a defined environmental impact
- Comparison of the quantified impact to a certain reference value through *normalization*, for example the average environmental impact of a citizen in a given geographical area in one year.

For each environmental flow represented by the chemical compounds identified and summarized during the LCI, a schematic cause response pathway is developed to describe the environmental mechanism of the substance emitted and to quantify an environmental effect. Along this environmental mechanism, an impact category indicator result can be chosen either at the midpoint or endpoint level (LCA Methodology, 2012). Some methods used for LCIA convert the emissions of chemical compounds and extractions of natural resources into impact category indicators at the midpoint level, while others employ impact category indicators at the endpoint level.

The midpoint impact category, also known as problem-oriented approach, quantifies impacts into environmental categories such as climate change, ozone depletion, terrestrial acidification, freshwater eutrophication, marine eutrophication, human toxicity, photochemical oxidant formation, particulate matter formation, terrestrial ecotoxicity, freshwater ecotoxicity, marine ecotoxicity, ionising radiation, land occupation, natural land transformation, water depletion, mineral resource depletion, fossil fuel depletion, etc.

Endpoint impact category, or the damage-oriented approach, takes a step further and converts the midpoint environmental impacts into issues of concern. Impact categories at the endpoint level correspond to areas of protection that form the basis of decisions in policy and sustainable development. For the environmental domain, these areas of protection are human health, ecosystem quality, resource availability, and, occasionally, man-made environment (ReCiPe, 2008). While easier to understand by the public and decision makers, endpoint quantification has a higher level of uncertainty compared to midpoint (LCA Methodology, 2012).

Within the context of the potential connections between LCA-MG, of particular relevance are two environmental impact categories defined at endpoint, respectively damage to human health and damage to ecosystem diversity. These endpoint categories rely on toxicity impacts at midpoint, that describe and quantify the impacts on human health and on ecosystems linked to the use and emissions of chemical substances in the environment.

3. Trace elements and human health in Medical Geology

Medical Geology examines the relationships between geologic materials and processes and human/animal/ecosystem health (Human Health/Medical Geology, 2012). Identification and characterization of natural and anthropogenic sources of chemical compounds as harmful materials in the environment is performed, followed by prediction of the movement and alteration of chemical, infectious, and other disease-causing agents over time and space. The goal of Medical Geology is to understand how people are exposed to harmful materials and what can be done to minimize or prevent such exposure.

However, demonstrating unequivocally the relationship between the presence of chemical compounds (natural or anthropogenic) in the geological environment and state of human health it is a challenging task. The correlation between assimilation of such compounds in the body and health state relies on identifying the origin of compounds, the migration pathways of the compounds from the geological environment, followed by understating of the interaction mechanisms between the identified chemical compounds and health.

4. Potential connections between LCA-MG – a hypothetical example

Extended research has been dedicated through MG to the source characterization and identification of natural and anthropogenic harmful compounds, with direct repercussion on health of humans/animals/ecosystems (Kolker et. al., 2009, Orem et. al, 2009b).

A special emphasis on the environmental and human health affected by the exploitation of resources such as coal, oil and natural gas was addressed by recent research work (Orem et. al, 2009a). Exploitation of these resources has side effects that triggered public concerns, as people become more aware of the concept of global warming or the increasing incidence of diseases like cancer or asthma (USGS, 2012). In the classic example of MG application, special cases such as the Balkan Endemic Nephropathy (BEN), panendemic nephropathy, environmental contamination related to mountain top mining, were approached as follows:

- Documenting the incidence of a certain health condition in an investigation area
- Finding evidence of the environmental (geologic) conditions potentially responsible for such condition and
- Identifying the communication pathways of harmful chemical compounds between the geologic environment and human/animal/ecosystem health.

However, this approach addresses documented cases of prevalent health conditions in a geographical region where the effects of an anthropic activity on health are already recognized. In other words, at this point, it is mostly a matter of dealing with the effects of a negative impact rather than preventing the occurrence of such negative impact.

To date, extensive LCA work has been dedicated to different loops of the overall life cycle of coal, natural gas and oil (cradle to grave, cradle to gate, gate to gate), from exploitation, to coal/natural gas fired power production, and diversified uses of these resources (Spath et. al, 1999). Several environmental impact categories were quantified, generally at midpoint, including global warming/climate change, eutrophication, acidification, ecotoxicity of soil and water, with direct repercussion on endpoint effects such as human health and ecosystem biodiversity. Triggering attention on sensitive environmental areas through LCA and connecting the occurrence of disturbed environmental conditions with MG documented cases of specific illnesses could establish a productive link between LCA and MG. The MG research could be oriented earlier towards assumptions based on previous research of similar conditions, followed by identification of characteristic health conditions – if any – in the investigated areas, research of environmental mechanisms and possibly mitigation of the harmful sources.

References

Cooper J.S., Fava J., 2006. Life Cycle Assessment Practitioner Survey: Summary of Results. Journal of Industrial Ecology

Finkelman R.B., Skinner H. C. W., Plumlee G. S., Bunnell J. E., 2001. Medical Geology. Geotimes. *http://www.agiweb.org/geotimes/nov01/feature_medgeo.html*

Human Health/Medical Geology, retrieved April 2012. *http://energy.usgs.gov/HealthEnvironment/EcosystemsHumanHealth/ MedicalGeology.aspx*

ISO 14040, 2006. Environmental management – Life cycle assessment – Principles and framework, International Organisation for Standardisation (ISO), Geneve

Kolker A., Engle M., Stracher G., Hower J., Prakash A., Radke L., Schure A., Heffern E., 2009. Emissions from coal fires and their impact on the environment: U.S. Geological Survey Fact Sheet 2009-3084. (*http://www.nrel.gov/docs/fy99osti/25119.pdf)*

LCA Methodology, retrieved April 2012. *http://www.pre-sustainability.com/content/lca-methodology#Impact assessment*

Orem W.H., Bunnell J.E. Tatu C.A., Pavlovic N., 2009a.Toxicological pathways of relevance to medical geology. In: Encyclopedia of Environmental Health (Nriagu J., editor), Elsevier Science 2011.

Orem W., Tatu C., Pavlovic N., Bunnell J., Kolker A., Engle M., Stout B., 2009b. Health Effects of Energy Resources. U.S. Geological Survey Fact Sheet 2009-3096

ReCiPe, 2008. A life cycle impact assessment method which comprises harmonised category indicators at the midpoint and the endpoint level First edition, Report I: Characterisation. (*http://www.lcia-recipe.net/)*

Spath P., Mann M., Kerr D., 1999. Life Cycle Assessment of Coal-fired Power Production. USGS retrieved 2012. Source Characterization and Identification of Natural and Anthropogenic Harmful Materials. (*http://energy.usgs.gov/HealthEnvironment/EcosystemsHumanHealth/MedicalGeology.aspx)*

IMPACT OF HEAVY METALS IN SEWAGE SLUDGE ON SOIL AND PLANTS (COLZA and WHEAT)

Najla LASSOUED[1], Essaid BILAL[2*], Mohamed Nejib REJEB[1], Saloua REJEB[1],

[1] Laboratoire de recherche Gestion des Risques Environnementaux en Agriculture Irriguée à l'Institut National de Recherche en Génie Rural Eaux et Forêts (INRGREF), Soukra, Tunis. lassoued_najla@yahoo.fr, rejeb.nejib@iresa.agrinet.tn, rejeb.saloua@iresa.agrinet.tn

[2*] Département Géosciences et Environnement, Ecole Nationale Supérieure des Mines de Saint Etienne, France. bilal@emse.fr

Abstract We are testing the impact of heavy metals in sludge from urban and industrial wastewater treatment plants. We try to understand their influence on plant growth and their bioaccumulation. We chose two plants: the wheat and rapeseed to their specific characteristics; wheat is a herbaceous low accumulator of heavy metals, however rape (colza) is a plant of the family Brassica napus, is an excellent bio-accumulator of heavy metals.

The mean levels found in the soil are organized in the following order: Fe >> Mn> Zn> Pb> Cu> Ni> Co> Cd The contents of heavy metals in the sludge is made very high and exceed European values allowed for that type of use but remain in the standard NT106 Tunisia.

The effects of the contribution of sludge are manifested by a significant increase in the weight gains of the whole plant, these results in a variation of the ratio between the aerial part and roots of the plant; this ratio tends to increase with dose of mud brought in soil increase. The roots of both plants show high levels of Zn even on the ground untreated control. The contents of Ni, Pb and Zn compared to Cu and Co are higher in the roots of rape than wheat.

Keywords: Mud, urban, industrial, heavy metals, rape, colza, wheat, bio accumulator, wastewater treatment plant, Tunis, Nabeul.

1. Introduction

The main objective of this study is to evaluate the wheat and canola the effect of two types of sludge (urban sludge / industrial sludge) containing heavy metals especially lead and chromium. These mud is made at different doses (5, 25, 50 and 100 t / ha). We are therefore interested in the growth and absorption of heavy metals by plants (Durum wheat and rapeseed Colza) and follow the fate of the latter in the ground to prevent pollution events and toxicity.

2. Materials and methods

The experimental protocol was installed in the field to the Agricultural Experiment Station of Oued Souhil - Nabeul, situated about 60 kilometers from Tunis (Fig. 1) and belonging to the National Institute for Research in Rural Engineering Water and Forest.

The urban mud used in this study is taken from the wastewater treatment plant in Korba with a treatment system at low load activated sludge followed by maturation. Sludge from this station underwent a stabilization in aerobic followed by drying on beds. The dry sludge is removed from the drying bed.

The mud is from the industrial wastewater treatment plant Bou Argoub which hosts two industrial zones, companies in the Refrigeration and Brasserie Company of Tunis (SFBT) specialized in the food industry, and Assad specialized in the electrical industry. Sludge from this station underwent a stabilization in aerobic followed by drying on beds. This sludge is loaded with heavy metals especially lead and chromium.

The plant material used in this experiment is the Wheat, herbaceous, monocot genus Triticum of the grass family and rapeseed (Brassica napus) is an annual plant with yellow flowers of the family Brassicaceae. These two species were chosen for their ability to levy metals. Wheat is a small accumulator of heavy metals while rape is an accumulator of these elements.

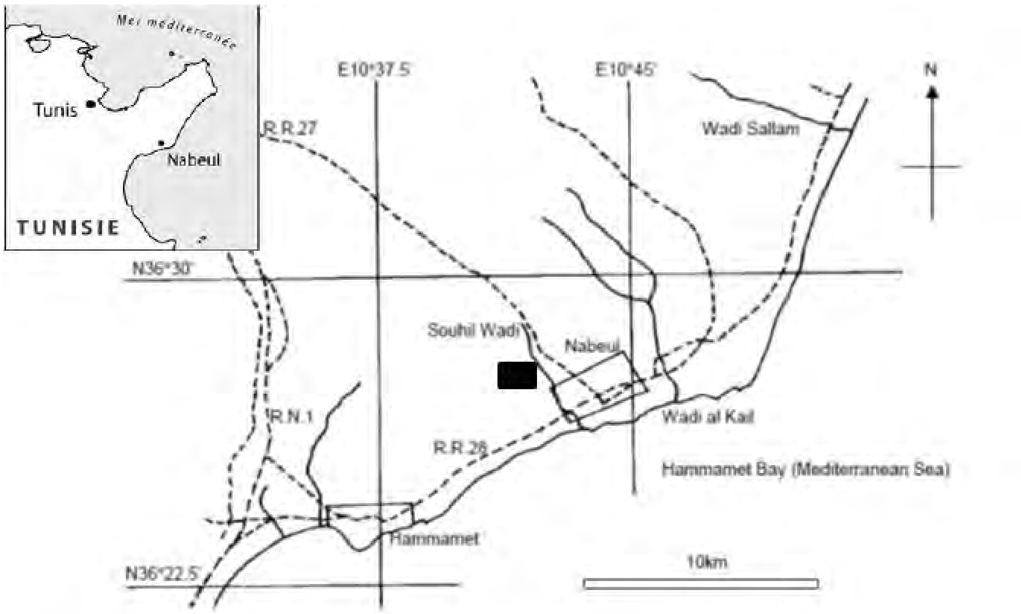

Fig. 1. Location map of Oued Souhil – Nabeul Agricultural Experiment Station (the black rectangle).

The test device is installed on two juxtaposed plots reserved for each crop (wheat or rapeseed). For each type of sludge, four doses (5, 25, 50 and 100 t / ha) were brought into play and compared to control soil without any addition.

Field work began in September 2010 with the spreading of sludge realized September 20, 2010. They were manually dug into the ground. Before application, the sludge was analyzed.
The soil was sampled twice, first before the application of sludge and the second time after harvest. The samples were taken between the lines by auger at four depths (0-10, 10-20, 20-40 and 40-60 cm).

In the laboratory, soil samples were dried in open air and sieved to 2mm or 0.2mm depending on the type of analysis required. Soil testing is in progress. The main parameters are determined particle size, total calcium, conductivity, carbon, organic matter, total nitrogen and determination of heavy metals.

For the particle size we used the method of the International pipette Robinson, it is primarily the destruction of soil organic matter using H_2O_2 and dispersion of clays by sodium hexametaphosphate. Clays and silts are measured in the suspension of land following the decay time that depends on particle diameter (NF X 31-107). The settling velocities of particles can be calculated by the formula of Stokes.

For plants, we performed the semi rapeseed (50 seeds / m²) December 29, 2010 and semi wheat (350 seeds / m²) January 5, 2011. The rapeseed harvest was performed after the formation of siliques May 25, 2011. The aerial part and the root have been weighed. The same work was done with wheat June 9, 2011. The samples were subsequently dried and crushed ore to determine the mix of metals in different parts of the plant.

3. Results

Sand is the most representative size fraction in this soil, which is a sandy loam soil texture. The analytical results show that the soil of the plot used is characterized by an alkaline pH, conductivity ranging from 1.06 to 1.52 mmho/cm resulting low salinity, soil saturation is between 30.4 and 31.8ml/100g. Limestone is a total of inherited components of soil, light and possibly modified by repeated and massive supply of amendments basic. The analysis of the limestone is needed to refine the characterization of soil constituents. Inspection of Table 1 shows the percentages of limestone in the different horizons are less than 5% so it is a non-calcareous soil, with organic matter content very low.

Contents of total nitrogen are relatively low. The C/N ratio is widely used to characterize and classify types of organic matter in soil. This ratio C/N is about 7 at the first horizon (0-10cm) indicates that organic matter will be quickly mineralized.

Concerning trace elements, iron is the most representative. The mean levels found in the soil are organized in the following order: Fe >> Mn> Zn> Pb> Cu> Ni> Co> Cd mean concentrations of heavy metals introduced by the sludge are shown in Table 1.

With the addition of sludge, there is a parallel increase in the number of ears and an increased number of grains per m². The ears and grains also increase with increasing dose of mud, whatever the type of sludge made. The increase in the number of grains with the addition of mud has the consequence of decrease in PMG this can be explained by the decrease in weight and grain quality response to stress. The numbers of feet of wheat increases dice the contribution of 5t/ha sludge, this increase is more pronounced with the addition of urban sludge.

Table 1. Chemical composition of different horizons of the soil profile and sludge:

	Soil Profile					**Sludge**		
	0-10	**10-20**	**20-40**	**40-60**	**NF U 44-041**	**BU**	**BI**	**NT 106**
Limestone	1	2,2	1,8	2,4		n.d.	n.d.	
pH	8,36	8,4	8,38	8,5		6,9	6,33	
MO %	0,64	0,24	0,24	0,14		52,6	60	
C%	0,34	0,12	0,14	0,06		30,58	34,88	
N %	0,0453	0,0561	0,0475	0,0515		4,9	6,1	
C/N	7,511	2,138	2,948	1,166		6,24	5,71	
Cd	1,6	1,6	1,4	1,8	2	3	11	20
Co	11,6	10,8	12,2	14,8		28	18	
Cu	23,4	13,8	11,8	11,2	100	158	68	1000
Fe	8628	8800	10328	11675		10700	8300	
Mn	128	118	119	131		152	81	
Ni	19	26	26	22	50	78	49	200
Pb	39	39	35	31	100	63	577	800
Zn	55	39	43	38	300	440	360	2000
Cr	n.d.	n.d.	n.d.	n.d.	150	155	8030	

NFU 44-041: French norm of heavy metals in sol.
NT 106: Tunisian norm of heavy metals in sludge
BU: Urban sludge and BI Industrial sludge
n.d.: no determined

One can see that the leaf area increases with the contribution of sludge as well as for urban or industrial sludge's. The leaf surface of this crop varies between 15.77cm^2 of the oldest leaf to 3.78 cm^2 for the youngest leaf in the control soil.

The leaf surface increases by 10cm² for 5BI and 11cm² 5BU. We noted that the young leaf appears to 5BI and 25BI, but it is not yet developed with input from 50t/ha to 100t/ha. This developmental delay may be due to toxicity effect more pronounced with industrial sludge.

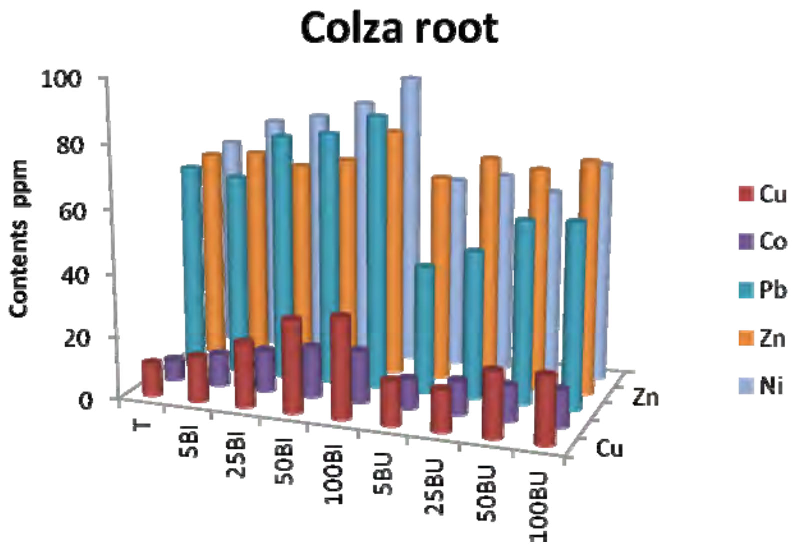

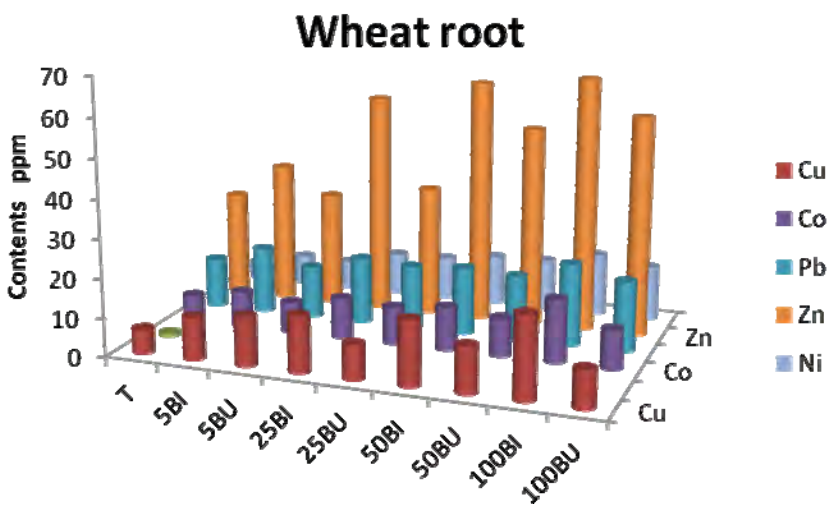

Fig. 2. Distribution of heavy metals in the roots of colza and of wheat in soils with addition (5, 25, 50 and 100t/ha) of urban (BU) and industrial (BI) sludge and control soil (T).

4. Conclusions

The effects of the contribution of sludge are manifested by a significant increase in the weight gains of the whole plant, these results in a variation of the ratio of the aerial part and root (PA / R) which tends to increase with the increase the dose sludge made. In all cases, the increase in leaf weight gain following a contribution of mud is still perceptible from the low inputs applied with a more significant effect with the provision of urban sludge. The important contribution of sludge rich in heavy metals causes stress in plants. We found a high content of Ni, Pb and Zn in these plants (Fig. 2).

PHOSPHORIC ACID EXTRACTION AND RARE EARTH RECOVERY FROM APATITES OF THE BRAZILIAN PHOSPHATIC ORES

Fernando **PEREIRA**, Essaid **BILAL**
Ecole Nationale Supérieure des Mines de Saint-Etienne (France)
fernando-pereira@bbox.fr ; bilal@emse.fr

Abstract Various experiments led in laboratory on the concentrate of Angico dos Dias phosphate allowed us to define the following steps in the process of hydrochloric treatment: 1 – Acidification of the concentrate by HCl at 20% during two hours at ambient temperature (solid/liquid ratio of 40%, agitation speed of 200 rpm). In these conditions, the solubilisation rates of CaO and P_2O_5 are commonly superior to 95% (around 80% for $(REE)_2O_3$) ; 2 – Precipitation, at ambient temperature, of Na_2SiF_6 after the addition of a sodium salt to the chlorophosphate solution. The precipitate gotten reveal that more than 80% of the fluorides, initially present in the phosphate rock, can be recovered as sodium fluorosilicates ; 3 – Liquid-liquid extraction of the phosphoric acid by the tributylphosphate. The aqueous phase obtained is treated by ammonia so as to precipitate the rare earth elements as a phosphate concentrate. The application of the process practically does not allow the formation of residues or liquids. The (REE) recovery rate of 80% constitutes a valorization source of the proposed process.

Keywords: phosphoric acid production, fertilizer industry, rare earth elements recovery, phosphate rock, hydrochloric acid route.

1. Introduction

The sulphuric acid route for phosphate rock (intended to the fertilizers industry) presents many inconveniences: impossibility to recover high commercial value by-products such as the rare earth elements, existence of severe restrictions imposed by the legislation on environmental protection, 250 millions of tons of impure and radioactive phosphogypsum annually produced, environmental problems bound to the phosphogypsum storage (pollution of the ground and surface waters etc). This technology of phosphate rock treatment of is by far the most widespread (essentially, because of the economic imperatives). Nowadays, it is the only one used in Brazil. For this country, which does not have any economic deposits of sulfur, the choice of another process imposes itself, on the one hand to reduce sulfur imports and, on the other hand, to reduce the environmental nuisances generated at the time of the phosphogypsum formation. On this purpose, it is necessary to study alternative routes and methodologies so as to make a choice for the one that offers the most ecological, economic and technical advantages.

The hydrochloric acid route can be presented as an interesting alternative to the traditional sulfuric acid route thanks mainly to the recovery of commercially valuable by-products, as for example, the rare earth elements. This article refers to the rare earths recovery in the context of the phosphoric acid production (fertilizer industry) from the phosphatic ore Angico dos Dias (Brazil) using the hydrochloric acid as leaching agent. There are several methods for purifying the phosphoric acid. The most widely used involves the liquid-liquid extraction. The main components of the leachate, which include the crude phosphoric acid, have the following qualitative behavior in relation to the organic extractant:

- easily extracted : H_3PO_4, H_3AsO_3 ;
- extracted with more or less difficulty (considering the nature of the solvent used): H_2SO_4, HF, H_2SiF_6;
- extracted very poorly : Al^{3+}, Fe^{3+}, Ca^{2+}, Mg^{2+}, UO_2^{2+}, …
- in the industrial process of purification by extraction, there are two classes of molecular solvents depending on their solubility in water:
- the solvents relatively soluble in water: light alcohols such as butanol, isobutanol and isopropanol ;
- the solvents, whose solubility in water is very low, for example the tributylphosphate TBP $(C_4H_9O)_3PO$, which was used in the process.

For this study, the first optimized were the parameters related with the chlorine leaching (hydrochloric acid concentration of 20%, solid/liquid ratio of 40%, stirring speed of 200 rpm and reaction time of 2h). The chemical composition of the leachate obtained (as major constituents Ca, P and F) is shown in Table 1.

2. Removal of fluorine

In order to avoid any contamination problems of the fertilizers, due to the fluorinated acids (in particular, H_2SiF_6), it is necessary to eliminate such acids before extraction. On this purpose, the precipitation in the form of H_2SiF_6 after addition to the leachate of a sodium salt NaCl was chosen. Ten series of tests were carried out from on liter of leachate: 100 ml of leachate were added to various amounts of NaCl at ambient temperature with stirring during 30 minutes. The reactive mixtures were filtered and the precipitates dried and milled before being analyzed by X-ray diffraction. The solutions were analyzed by ion chromatography, especially for the fluoride ions.

The hydrochloric acid route for the production of phosphoric acid can be shown by reaction (1):

$$Ca_{10}(PO_4)_6F_2 + 20\ HCl \rightarrow 6H_3PO_4 + 10CaCl_2 + 2HF \qquad (1)$$

The addition of NaCl reveals to be efficient in the precipitation of Na_2SiF_6 according to reaction (2):

$$2NaCl + SiF_6^{2-} \rightarrow Na_2SiF_6 + 2Cl^- \qquad (2)$$

Fig. 1 shows the evolution of the percentage of removal of fluorine from the leachate as a function of the amount of sodium salt added.

Table 1. Chemical composition of the leachate resulting from the hydrochloric attack of the concentrate from Angico dos Dias (Brazil).

Components (g/l)	Composition (g/l)
P_2O_5	116
CaO	151,5
$(REE)_2O_3$	2,95
F	8,8

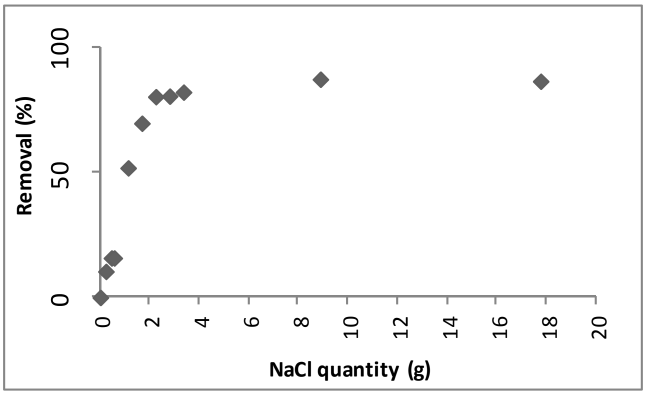

Fig. 1. Removal of fluorine in the leachate obtained by Na_2SiF_6 precipitation after the addition of a sodium salt (analyses by ion chromatography).

The precipitation of Na_2SiF_6 is more effective at room temperature using twice the stoichiometric amount of NaCl required (according to reaction (2)). In a typical test, 3.36g of NaCl (twice the stoichiometric amount necessary) were added to 100 ml of leachate (fluoride content = 8.74g/l) and subjected to stirring for half an hour. The precipitate obtained, analyzed by X-ray diffraction, showed that more than 80% of the fluorides initially present in the rock can be recovered after hydrochloric acid leaching as Na_2SiF_6.

3. Separation $CaCl_2$ – H_3PO_4

As it is impossible to crystallize the calcium chloride from the leachate, *e.g.*, as in the case of the nitric acid route where $Ca(NO_3)_2{\cdot}4H_2O$ can be precipitated by simple cooling, we used the tributylphosphate to separate the calcium chloride from the phosphoric acid. The extraction tests were carried out in continuous mode using a laboratory mixer/settler of 4 stages (organic phase/ aqueous phase ratio = 1).

A single-stage mixer/settler successively performed the following operations: (i) bringing into contact in the mixer the multi-components A phase to be purified and the B phase of extraction (insoluble in the previous) which selectively extract one or several elements (solutes) from A phase ; (ii) separation into two phases, by gravity, of the emulsion formed in a settler associated with each mixer. The two phases are then in countercurrent to the contiguous stages. The successive mixing/separation operations allow the transfer of the solute from A to B thereby creating an A’ phase, impoverished (or refined), and an enriched B solvent (or extract). At each stage, a motor unit, interchangeable and adjustable in height, drags one mixture and pumping turbine station. This aspires the phases from the settlers of the adjacent stages, puts them in contact and takes in the settler the emulsion thus created in the mixer, the transfers from one stage to another are made through distributors above the overflow.

It has been demonstrated (Pereira, 2003) that three successive extractions with an organic phase/aqueous phase ratio of 1 are sufficient to extract the entire amount of phosphate initially present in the leachate. This ratio was selected on mainly economical, since the use of solvent is reduced. The results are shown in Table 2.

The liquid-liquid extraction carried out on three of the four-stages mixer/settler allowed the recovery of almost 96% of phosphate initially present in the leachate without any fluoride. Calcium ions, account also for 9% in the organic extract. The latter may subsequently be eliminated during the treatment of the organic phase. The rare earth elements largely remain in the aqueous phase. The chloride ions are more than 60% concentrated in the refined. Significant amounts of iron are retained in the organic extract.

Table 2. Liquid-liquid extraction of the hydrochloric leachate by the tributylphosphate (extraction on three stages with an O/A of 1).

	Leachate (V = 500ml)		Refined (V = 324.67ml)		Extract
	Concentration (g/l)	Weight (g)	Concentration (g/l)	Distribution (%)	Distribution (%)
P_2O_5	116	58	8.45	4.73	95.27
CaO	151.5	75.75	212.38	91.03	8.97
Cl^-	275.2	137.6	266.45	62.87	37.13
$(REE)_2O_3$	2.95	1.475	4.5	98.97	1.03
Fe	2.7	1.35	0.18	4.3	95.7
Al	1.9	0.95	2.85	97.3	2.7

4. Rare earth elements recovery

Not too much attention has been given to the economically viable recovery of the rare earth elements as by-products of the phosphoric acid production, when the phosphate rock/concentrate is done following the nitric or hydrochloric acid route. The rare earths have good commercial value, numerous applications and, according to Chinese researchers, are excellent micronutrients in agriculture, improving from 8 to 10% the productivity of various cultivars (CRE, 2005; Zhou, 1993). In carbonatites without specific mineral occurrences of rare earths-bearing fluorine and strontium ore, the bastnasite and monazite are the minerals from the apatite group that usually contain most of these elements, together with its most common variety, the fluorapatite, whose unitary cell is composed of $Ca_{10}P_6O_{24}F_2$.

The rare earths are present in apatites as accessory elements, ranging from some tenths percent to about 20% (Dutra and Formoso, 1995). Dutra and Formoso (1995) studied 22 samples of apatites and phosphate rocks and concluded that:

- all the carbonatite apatites have REE (Rare Earth Elements) contents exceeding 1000 ppm ;
- in Brazil, the highest values were found in rocks of the carbonatitic complex of Angico dos Dias-Bahia (7483ppm), Araxa-Minas Gerais (6347ppm) and Catalao-Goias (5585ppm).

It was observed that most part of the rare earth elements (over 90%) remained in the aqueous phase after the liquid-liquid extraction by the tributylphosphate. Considering the study by Abashi and Awadalla (1986), we opted for a precipitation of the REE. After extraction by the tributylphosphate on three stages, 20 ml of refined were then added to various amounts of ammonia and of oxalic acid in different conditions but always under stirring for 30 minutes. The precipitates were dried, crushed and calcined (1000° C) before being analyzed by Inductively Coupled Plasma Atomic Emission Spectroscopy (ICP/AES). To do this, we proceeded to stripping in its excess hydrochloric acid. The pH of the aqueous-ammonia mixture remained constant throughout the reaction. In Fig. 2, we represent the variation of the pH of the reactive mixture as a function of the volume of ammonia added.

The Fig. 3 and 4 show the recovery of the solid phase CaO, P_2O_5 and $(REE)_2O_3$ by ammonia only or by ammonia and oxalic acid.

The rare earth elements recovery is excellent regardless of the treatment which has been subjected to the aqueous refined. After treatment with ammonia only, its recovery was very close to 100% using an additional volume of 5ml. In parallel, the rare earth concentrate present some phosphate impurities. Somewhat, less than 90% of phosphates from the aqueous refined (low phosphate content, since the great majority is present in the organic phase after extraction by the tributylphosphate) is in the residue obtained. The content of this residue remains very low. After treatment with oxalic acid and ammonia, the (REE) recovery is total whatever the amount of ammonia added.

The main drawback of this aqueous refined treatment lies in the presence in the residue of large amounts of CaO (more than 90% of the CaO from the aqueous refined very rich in this oxide). Furthermore, for reasons of cost (removal of one process step), it is preferred the processing of the aqueous refined by ammonia only to recover the rare earth elements.

With this method, a recovery rate of approximately 80% of the REE initially present in the phosphate rock (in the form of a rare earth phosphate concentrate) is achieved.

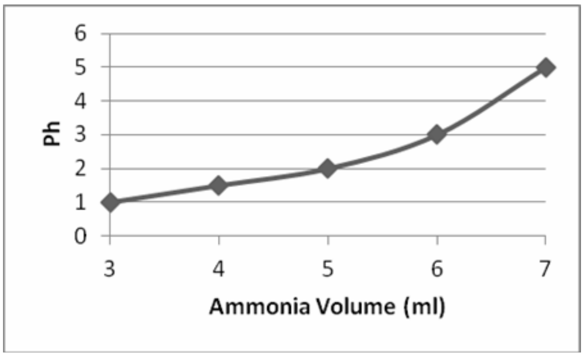

Fig. 2. Variation of the pH of the reactive mixture in function of the volume of ammonia added.

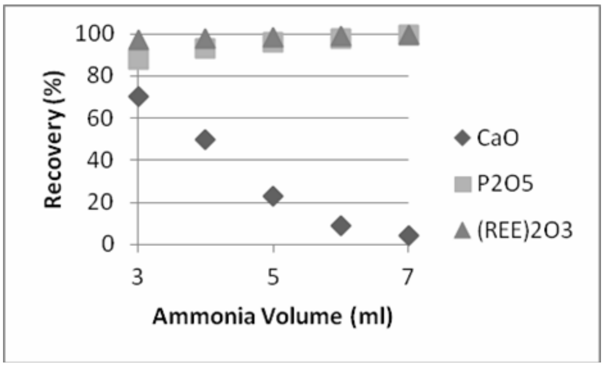

Fig. 3. CaO, P_2O_5 and $(REE)_2O_3$ recovery in solid phase (calcined residue) versus the volume of ammonia added – aqueous refined treated by ammonia (ICP/AES analyses).

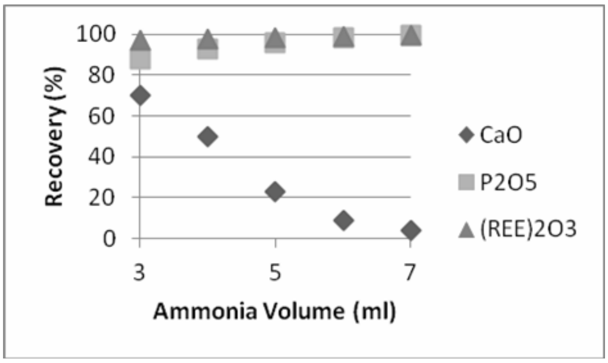

Fig. 4. CaO, P_2O_5 e $(REE)_2O_3$ recovery in solid phase (calcined residue) versus the volume of ammonia added – aqueous refined treated by ammonia and oxalic acid (ICP/AES analyses).

5. Conclusions

Various laboratory experiments carried out on the concentrate of Angico dos Dias allowed us to define the following process of hydrochloric treatment:

1 – Acidification of the concentrate by HCl at 20% during two hours at ambient temperature (solid/liquid ratio of 40%, agitation speed of 200rpm). In these conditions, the solubilisation rates of CaO and P_2O_5 are superior to 95% (around 80% for $(REE)_2O_3$);

2 – Precipitation, at ambient temperature, of Na_2SiF_6 after addition to the chlorophosphate solution of a sodium salt. The precipitate obtained reveals that more than 80% of the fluorides, initially present in the phosphate rock, can be recovered as sodium fluorosilicates;

3 – Liquid-liquid extraction of the phosphoric acid by the tributylphosphate. The aqueous phase obtained is treated by ammonia to precipitate the rare earth elements as a phosphate concentrate.

The process used does not allow the formation of residues or liquids. The REE recovery at the rate of 80% constitutes a valorization source of the proposed process.

References

CRE (2006) – China Rare Earth information (www.cre.net/english).

Dutra C.V. and Formoso M.L.L., 1995. Consideraçoes sobre os elementos terras raras em apatitas. Geochimica Brasiliensis, 9 (2), pp. 185-199.

Habashi F. and Awadalla F.T., 1986. The recovery of uranium during the purification of phosphoric acid by organic solvents. Separation Science and technology, 21(4), pp. 327-37.

Pereira F., 2003. Production d'acide phosphorique par attaque chlorhydrique de minerais phosphatés /…/ et récupération des terres rares. EMSE/SPIN, Saint-Etienne, France.

Zhou C., 1993. Rare earth industry of China. Journal of alloys and compounds.

CORRELATION BETWEEN ROCK CHEMISTRY AND F-CONCENTRATION IN GROUNDWATER FROM SÃO FRANCISCO COUNTY, MINAS GERAIS, BRAZIL

Claydson Ferreira FARIA[1*], Adolf Heinrich HORN[2], Joel Jean Gabriel QUEMENEUR[3]

1 - Instituto de Geociências / Universidade Federal de Minas Gerais, Belo Horizonte, Minas Gerais, Av. Antônio Carlos, 6627, Tel.: +55313409 4446, Fax: +553134095420, claydsonf@gmail.com,

2 - Geological Institute, Federal University of Minas Gerais, Belo Horizonte, Av. Antônio Carlos, 6627, Minas Gerais, Brazil, hahorn@ufmg.br,

3 - Retired

Abstract In the investigated region, fluorosis occurs within habitants. This work shows that the F^- comes from the argillites-pelitic rocks of the Bambuí Group (São Francisco Supergroup) and not from its carbonate rocks, how it was supposed. The carbonate rocks of the region trapped the F^-, liberated by pumping from groundwater in fluorite. This process can be used to help people to avoid F^- ingestion and reduce the disease occurrence.

Keywords: anomalies, fluorides, fluorine, geochemistry of rocks, groundwater, São Francisco

1. Introduction

The municipality of São Francisco, was determined as one of the Brazilian regions with high F-anomaly in water and soil. The population shows effects like dental fluorosis and deformation of skeletal structure.

These problems can be correlated with the concentration of F^- in the drinking water from wells in the rocks of Bambuí Group. There are argillites, arenites and carbonates with F^- in the mineral structures, in fluorite and in the intergranular space.

1.1. Location

The studied area corresponds to the southern portion of the municipal district of San Francisco town. It is located in the northern area of Minas Gerais state, in the middle hydrographic basin of the San Francisco River and limited by the parallels 45° 15' and 44° 25' the meridians 15° 33' and 16° 10'.

The distance from the capital of Belo Horizonte is of approximately 578km. The access is possible by using first the highway BR-040 and then the BR-135 until the city of Mirabela. From there you have to pass the city of Brasília of Minas by the highway MG-202 and then the highway MG-402, until the town of San Francisco (Fig. 1).

1.2. Climate

The climate of the area is classified as semi-humid tropical type (NIMER 1979), with annual temperature average of 24ºC and a maximum of 32,3ºC and minimum of 17,7 ºC.

The medium precipitation is of 1133mm/ year with the rain period from December to March, and a dry period from April to December (driest between September and December).

1.3. Surface

The altitudes oscillate from 455m, in the valley of river Sucurana, and up to 815m in the southern mountain part of the area.

Flat and dissected areas dominate the region, being developed preferentially on the metasediments of Bambuí Group, with upper plane parts, hills, elevation with shallow slope convex hillsides, together with alluvial plains. There can be also observed karstic features like sinkholes, lapiez, caves, dolines and drains in the limestone and dolomites.

In the highest parts, mainly in the southern portion of the district, there exist large planes built over Cretaceous sandstones.

Colluvial ramps formed by diffuse and torrential surface drainage and composed by areno-pebbly and areno-silty sediments with big blocks alternates with sandy and loamy layers of the alluvial plains. The largest expression, in area and thickness, of this unit can be observed in the northwestern part and accompanies the right margin of the river São Francisco.

1.4. Vegetation

The regional vegetation cover is composed of typical biomes: Cerrado and Caatinga (SEMAD 2003). The Cerrado (Savannah) is quite diversified and presents very open rural forms, as the “Campos Limpos” and a wide variation in tree-density from open to closed, dense areas. The Caatinga (Savannah

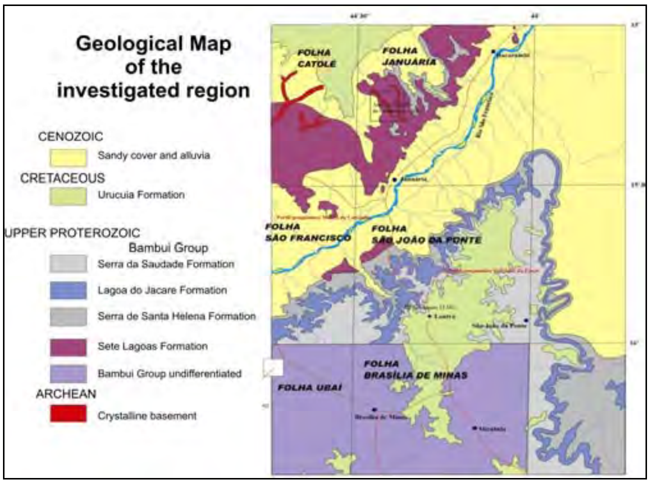

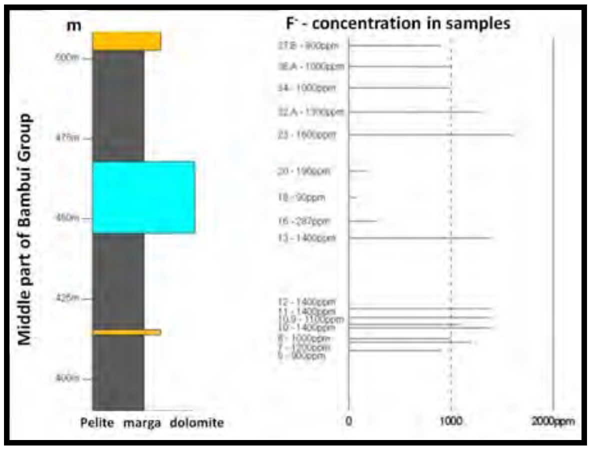

Fig. 1. The map shows the location and geology of the working area and the way of access.

Fig. 2. Concentration of F in the rocks (Horn et al. 2004; Claydson 2011, in press). Profile from Bambuí Group near the town of São Francisco. Blue: marls; grey: argillites, pelites; orange: carbonate rocks.

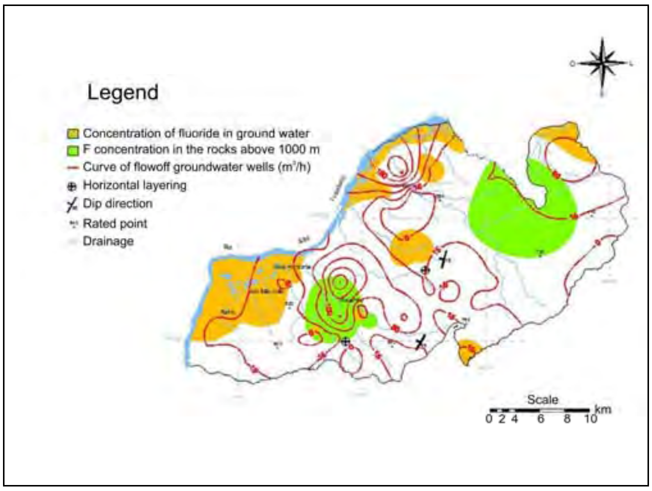

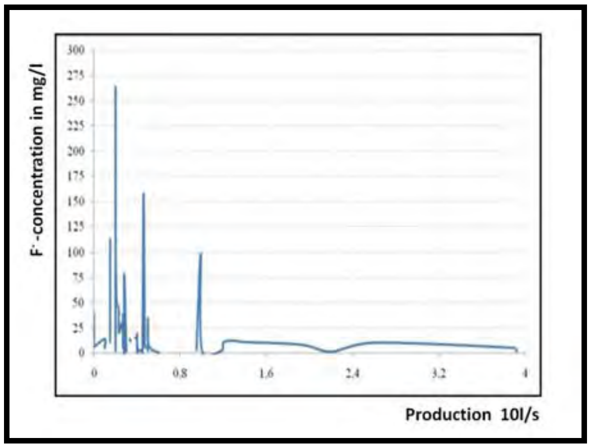

Fig. 3. Map with isolines of F and other selected elements, well location and F- concentration in the drinking water.

Fig. 4. Correlation of F- concentration in water and medium well production.

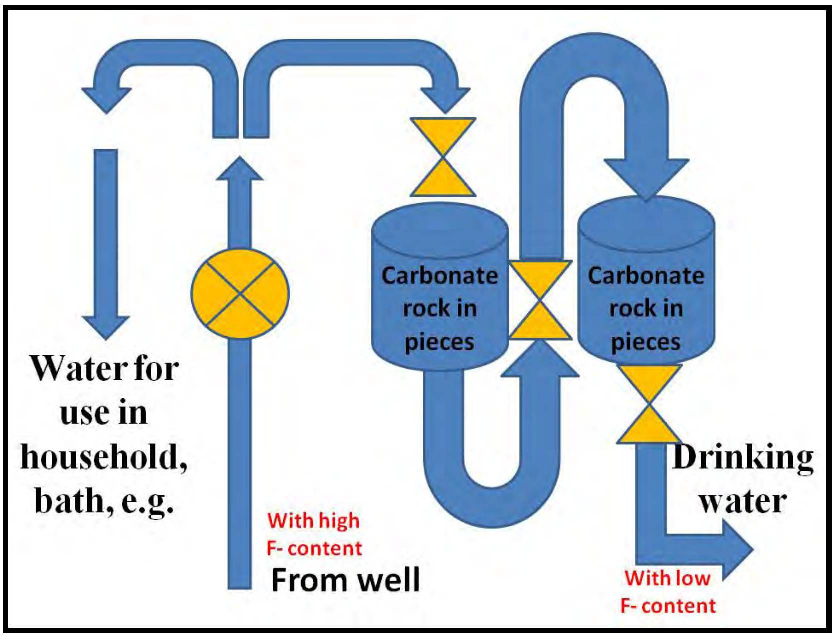

Fig. 5. System that may be used by the local population (after Souza et al. 2003, modified).

dry) is represented by small thorny arboreal species associated with bromeliaceous. In the humid places (Várzeas) humid low type vegetation occurs, which is represented by grass, cyperaceous and juncaceous.

1.5. Hydrographic situation

The San Francisco River cut the county territory approximately in the middle and in a SW - NE direction. The drainage presents dendrite and rectangular patterns, conditioned by the system of substratum fractures. In the northern portion the drainage presents an oscillating main direction of N45º-55ºW, and secondary of N30º-45ºE and N15º-20ºW, and in the southern part (area of this study) the main directions are N35º-50ºW and N40º-50ºE.

1.6. Occupation and population impact

The local population is formed principally by farmers and fishermen who live from their products. The overall situation for the major part of population is near poverty.

1.7. Geological Situation

Almost the entire area is formed by the units of Bambuí Group. The main mineralization types described in this group are of lead, zinc, silver, barium and fluor.

The latter consist of a series of small occurrences of fluorite in the argilitic-carbonate sediments along the São Francisco river valley, especially in the surroundings of the municipalities of São Francisco, Januária, Itacarambi, Montalvânia and at the Saw of Ramalho.

2. Fieldwork

2.1. Sampling

The water samples were taken from the existent wells. The sample volume was 1l. The samples were filtered, cooled down and prepared for analysis.

From the sediments were collected samples of 1-2Kg. After drying and crushing, the smaller fraction was leached and analyzed using normal procedure and cooled down.

2.2. Other field data

Other relevant data taken in the field geological mapping and in the rock composition (minerals and chemistry).

2.3. Laboratory work

The solutions were analyzed for metals using an ICP-OES equipment. F^- was determined by colorimetric test, using normal procedure (See Fig. 2).

3. Results

In São Francisco, Minas Gerais anomalous values of fluoride (>0.8 mg/l) occur in groundwater, and these values are very harmful to human health.

Microscopic studies done in the limestone and pelites do not confirm the presence of disseminated fluorite crystals. Those crystals are only found in veins of recrystallized calcite, located in sub parallel fractures of the carbonate rocks.

Chemically the limestone shows anomalous values of As (25ppm), Cl (733ppm) and F (293ppm). The pelites also display high values of As (28ppm), Cl (424ppm) and F (800ppm).

There is no correlation between the location of the wells pumping, fluoride concentration in groundwater and the location of rocks with anomalous values of F (See Fig. 3).

An indirect correlation between wells pump rates (<15m^3/h), and fluoride values were confirmed (See Fig. 4).

The amounts of fluoride in groundwater are a product of leaching pelites (See Fig. 2). The chemical profile of the area of Mocambo presented concentrations of F close to or above 1000ppm for the pelites and the limestone presented concentrations below 300ppm.

Three principal carbonate types were defined (CQ, CSQ and MQ), determined based on Ca-Mg, granulometry and chemical composition, but without important disseminated F concentrations.

Some samples present anomalies of As, Cl and F and the average values for trace elements were: 25ppm (As), 733ppm (Cl) and 293ppm (F), confirming the data from Horn et al. (2004) from São João da Ponte near Januária.

Cl and F are correlated, indicating a probable sedimentation under dry atmosphere in hot evaporític environment probably also valuable for the fluorite. No correlation was detected between this chemical rock data of F and the data from underground waters presented in Menegasse et al. (2003).

4. Conclusions

The F content is principally concentrated in the argilitic sediments. After liberation of F from these rocks due to tectonic space opening (fractures) it enters the Ca-Mg rocks were it precipitates in the form of fluorite due to the physical-chemical conditions.

The opening of wells permits the liberation of F from both sources with low extraction velocity. By higher exploitation the water passed the rocks with lower leaching effect.

To solve the health problems of the habitants from the study region, it is possible to:

- Use of surface water (São Francisco; lakes) with the problem of tropical diseases
- Split the water for drinking and washing. Use of different materials for cleaning the drinking water. This is possible but depends on the costs.

Due to the bad economic situation the use of sophisticated cleaner without governmental support is not possible and here are suggested different cheaper possibilities by using limestone s.l., argilitic material, calcined bones, etc. Figure 5 shows a simple flux diagram for the process that may be used at the farmhouses (See Fig. 5).

Acknowledgements

We thank NGqA-IGC-UFMG for logistic and the FAPEMIG for financial support.

References

Horn, A.H., Dupont, H., Souza, F.De B. &, Menegasse, L. 2004. Distribuição de Flúor em dois perfis estratigráficos do Grupo Bambuí, situados nos mapas de São Francisco e São João da Ponte, MG. In Anais XII. Simpósio de Minas Gerais Ouro Preto 2004 Ouro Preto: UFOP

Faria, C.F., Horn, A.H. & Quéméneur, J.J.G. 2011. Fluid inclusions in fluorite from São Francisco District, Minas Gerais State, Brazil. Classification and results of micro thermometric analyzes. In Memorias 14th Latin American Geological Congress/ 13th Colombian Geological Congress Medellin 2011 1 335-336 Bogota: Sociedad Colombiana de Geologia.

Menegasse, L.N., Fantinel, L.M., Knauer, L.G., Horn, A.H., Dupont, H.S.B., Castro, R.E.L., Freire, A.P.S. 2002. Flúor na Água Subterrânea e fluorose dental no Município de São Francisco, Minas Gerais. In: XLI. Cong. Bras. Geol., 2002, João Pessoa. Anais. João Pessoa, SBG-NN, 1, 554.

Menegasse, L.N. (Coord). 2003. Origem do Flúor na Água Subterrânea e sua Relação com os casos de fluorose dental no município de São Francisco, Minas Gerais. Relatório de Pesquisa Fapemig. Belo Horizonte, 138 p.

Souza, F., Horn, A. H., Dupont, H.S.B. 2003. Desenvolvimento de filtros para a retirada do flúor da água potável proveniente de poços no Município de São Francisco, MG. Sem. Inic. Científ., UFMG Belo Horizonte, Anais, 158.

HYDROGEOCHEMICAL STUDY ON THE RARE EARTH CONCENTRATION IN GROUNDWATER

Adriano FIORUCCI*, Barbara MOITRE

Politecnico di Torino, DIATI, C.so Duca degli Abruzzi 24, 10129 Torino, Italy
*****Corresponding author: adriano.fiorucci@polito.it, +39-0110907713

Abstract The purpose of this research is to investigate the possibility to characterize, from a geochemical point of view, the groundwater of some springs in different geological contexts using the rare earth elements contents. Groundwater have been sampled from aquifer hosted in several lithologic complexes and the analysis results show a close correlation between the contents of rare earth elements in groundwater and aquifer lithology in which they flow.

Keywords: Groudwater, Italy, Post-Archean Australian Shale, Rare earth elements

1. Introduction

The purpose of this research is to investigate the possibility to characterize, from a geochemical point of view, the groundwater of some spring in different geological contexts. The main elements of this characterization are rare earth elements (REE). Rare earths elements, in hydrogeochemistry, can be used to study the water-rock interaction and the traceability of the water. In fact, REE have a distribution in the different types of water extremely varied, depending specifically on the different rocks through which groundwater have flowed.

2. Regional setting and geology of the study area

Groundwater have been sampled from aquifer hosted in carbonate complexes, flysch complex, arenaceous marly complex, granitic detrital complex, metamorphic complexes (located in Piedmont) and volcanic complexes (located in Latium). REE were determined in 17 springs and in 10 thermal springs (located in 3 thermal places) collected in Piedmont, under low and high flow condition, and in 10 springs collected in Latium under low flow condition (Table 1 and 2).

3. Materials and methods

The study involves the measurement, in situ, of the characteristic parameters (temperature, pH, specific electrical conductivity and redox potential) and the chemical analysis of the samples to determine the main parameters (sodium, potassium, calcium, magnesium, hydrogencarbonates, sulfates, nitrates, chlorides), accessory parameters (nitrites, bromides, bromates, phosphates, chlorides and ammonium ion), some metals (lithium, aluminum, vanadium, chromium total, hexavalent chromium, manganese, iron, cobalt, nickel, copper, zinc, arsenic, selenium, rubidium, strontium, cadmium, cesium, barium, lead and uranium) and REE (Lanthanum, Cerium, Praseodymium, Neodymium, Promethium, Samarium, Europium, Gadolinium, Terbium, Dysprosium, Holmium, Erbium, Thulium, Ytterbium, Lutetium). Rare earth elements were determined by Inductively Coupled Plasma Mass Spectrometry (ICP-MS).

The concentration of each REE in groundwater samples was normalized to the corresponding concentration of a common rock standard, the Post-Archean Australian Shale (PAAS), so as to identify the aquifer type.

4. Results and discussion

Figures from 1 to 14 show the concentration of the rare earth elements in groundwater normalized to the corresponding concentration in the PASS, under low (*name of the sample – I*) and high flow condition (*name of the sample – II*).

REE patterns of waters in carbonate complexes show a marked negative Ce anomaly and a marked positive Eu anomaly. The effect of the morainic overburden is noted in Rio Martino spring, especially under low flow condition (Figs. 1 and 2). Also in groundwater from flysch and arenaceous marly complex (Fig. 3) the positive Eu anomaly has been observed, but in this case the negative Ce anomaly is absent. Groundwaters circulating in granitic detrital complex (Fig. 4) were characterized by a negative Ce anomaly and an increasing abundance of REE contents from Pr to Lu. The PAAS-normalized REE patterns of the basic metamorphic complexes are very different among them. The trends of San Meinerio,

Table 1. Geographic coordinates (Gauss Boaga–Roma 40) and lithology of the springs

Groundwater samples	X	Y	Lithology
Spring Baiso	1347370	4939071	Basic metamorphic complex
Spring Borello superiore	1406890	4897057	Carbonate complex
Spring Dragonera	1376610	4902472	Carbonate complex
Spring Fontanacce	1444293	5068543	Granitic detrital complex
Spring Fuse	1400170	4889398	Carbonate complex
Spring Grandi Boschi	1360525	5023143	Basic metamorphic complex
Spring La Purissima	1512192	4952151	Flysch complex
Spring Maira	1335766	4926290	Carbonate complex
Spring Montellina	1406677	5045496	Basic metamorphic complex
Spring Pian della Mussa	1357692	5018194	Basic metamorphic complex
Spring Pian della Valle	1420042	4928154	Arenaceus marly complex
Spring Regina	1361884	4896249	Metamorphic complex (Gneiss)
Spring Rio Martino	1353135	4951189	Carbonate complex with a morainic overburden
Spring Rio Secco	1442421	5125715	Basic metamorphic complex
Spring San Meinerio	1365487	5033715	Basic metamorphic complex
Spring Santa Maria	1343635	5007115	Basic metamorphic complex
Spring Tenda	1385726	4891643	Carbonate Complex
Spring Le Vene 1	1738278	4728806	Vulsino and Vicano Volcanic District
Spring Le Vene 2	1738177	4728780	Vulsino and Vicano Volcanic District
Spring Montecalvello	2290414	4714288	Vulsino and Vicano Volcanic District
Spring Caprarola	2294932	4685922	Vulsino and Vicano Volcanic District
Santa Maria delle Mole	2319894	4627045	Colli Albani Volcanic District
Fonte Egeria	2315033	4636615	Colli Albani Volcanic District
Fonte Appia	2318896	4631448	Colli Albani Volcanic District
CA1	2327066	4626958	Colli Albani Volcanic District
CA2	2328135	4627943	Colli Albani Volcanic District
CA3	2327325	4628207	Colli Albani Volcanic District

Table 2. Geographic coordinates (Gauss Boaga–Roma 40) of the thermal springs

Groundwater samples	X	Y
La Bollente	1458064	4947072
I – 2 (Vinadio)	1346680	4905854
I – 2b (Vinadio)	1346677	4905838
I – 1a (Vinadio)	1346829	4905814
I – 1b (Vinadio)	1346811	4905809
I – 1d (Vinadio)	1346814	4905822
Spring Santa Lucia (Valdieri)	1361959	4896306
Polla (Valdieri)	1361888	4896377
II – 2 (Valdieri)	1361915	4896375
II – 4 (Valdieri)	1361927	4896386

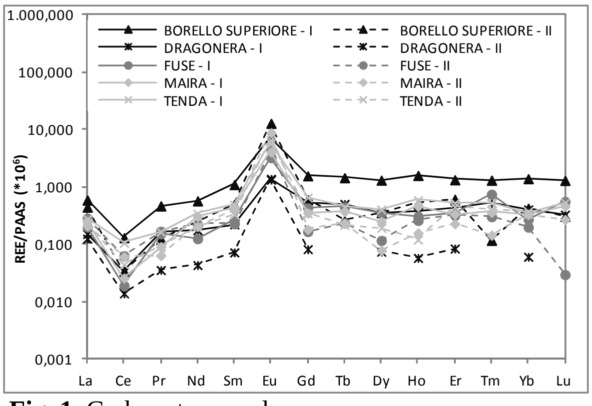

Fig. 1. Carbonate complex

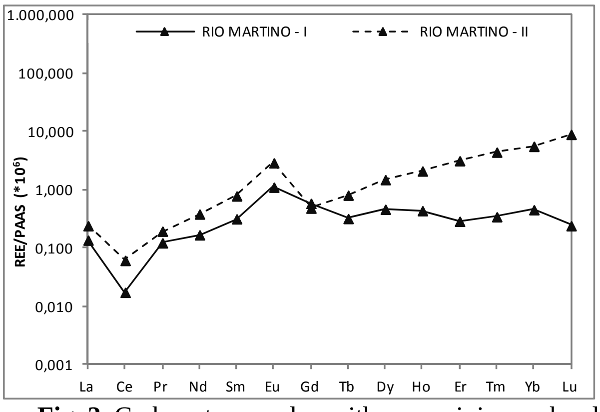

Fig. 2. Carbonate complex with a morainic overburden

Grandi Boschi and Baiso springs are relatively smooth and show only a negative Ce anomaly, but San Meinerio spring (Fig. 5) has higher values than the others (Fig. 6). Fig. 7 shows the pattern of Montellina, Pian della Mussa and Rio Secco springs, also in these cases the negative Ce anomaly is present, but exists a fluctuating shape from Pr to Lu. In Fig. 8, the PAAS-normalized plots are characterized by a positive anomaly from Nd to Tb. REE patterns of water of Regina spring (Fig. 9) are relatively smooth, but a Ce anomaly is present in low flow condition.

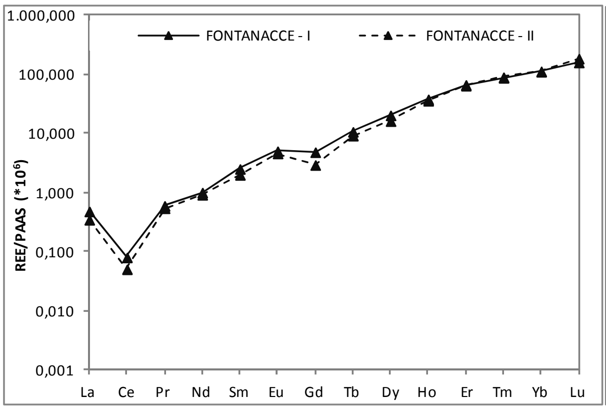

Fig. 3. Granitic detrital complex

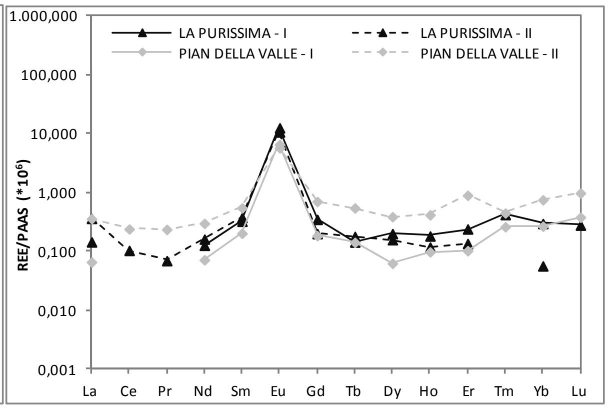

Fig. 4. Flysch and arenaceous marly complex

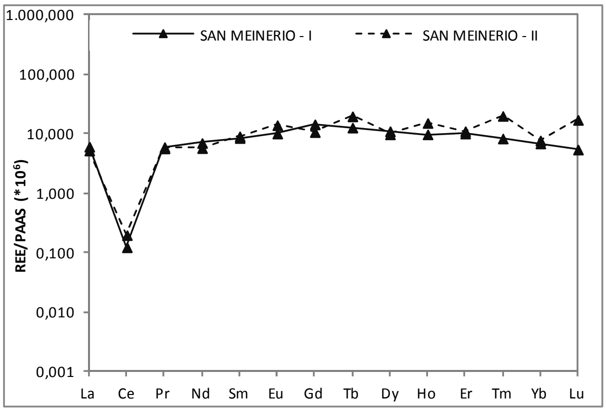

Fig. 5. Basic metamorphic complex

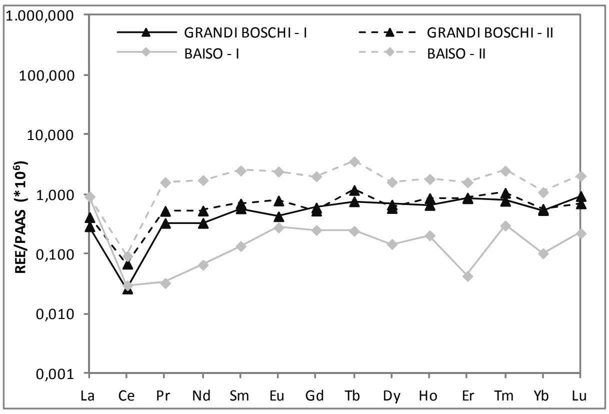

Fig. 6. Basic metamorphic complex

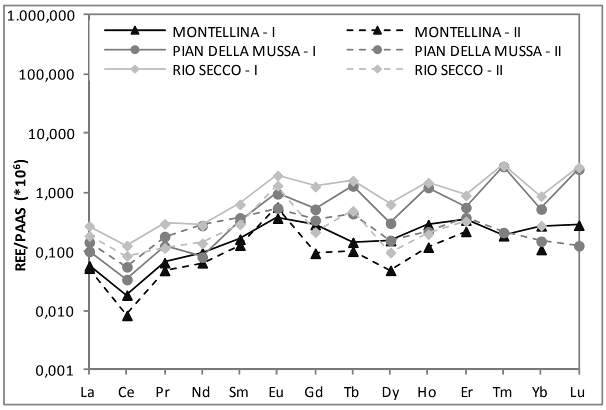

Fig. 7. Basic metamorphic complex

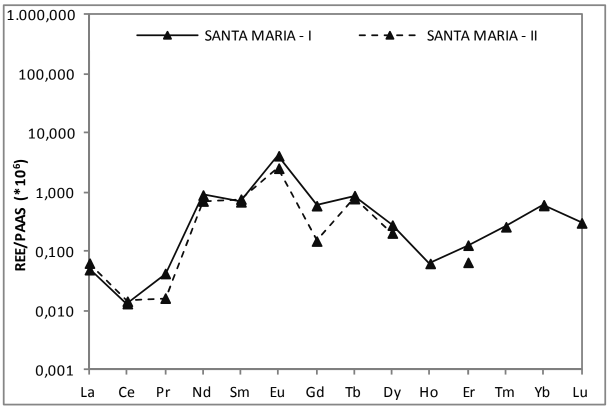

Fig. 8. Basic metamorphic complex

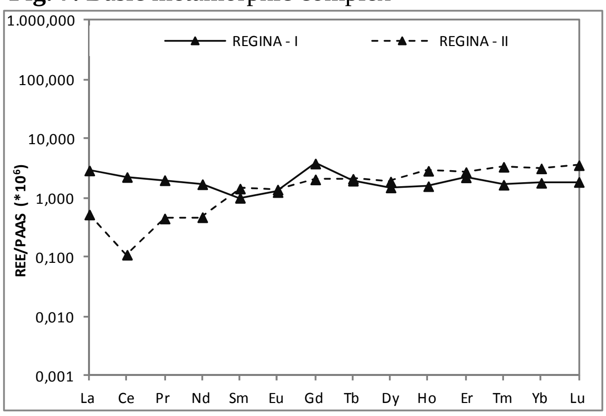

Fig. 9. Metamorphic Complex (Gneiss)

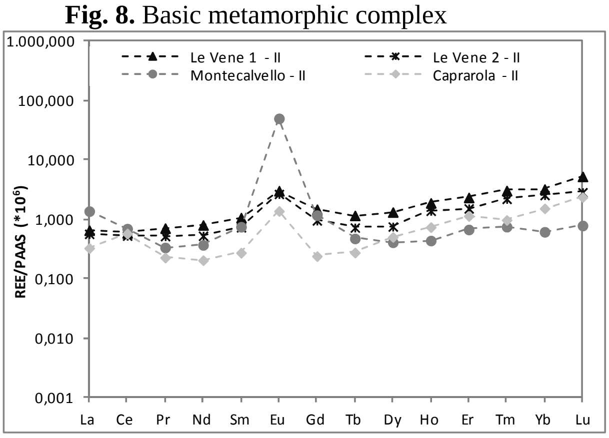

Fig. 10. Vulsino and Vicano Volcanic District

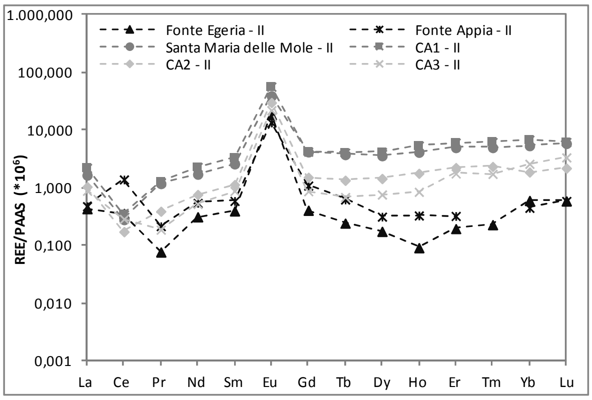

Fig. 11. Colli Albani Volcanic District

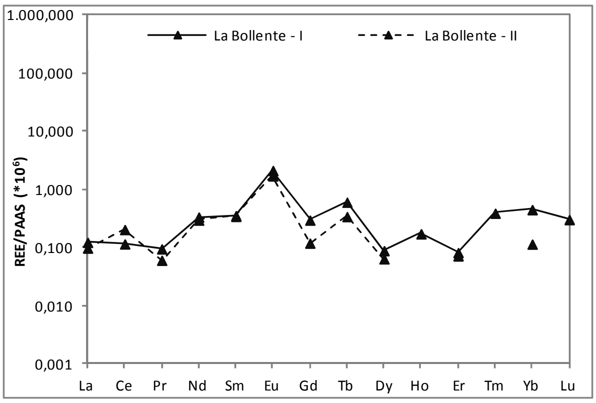

Fig. 12. Acqui Terme hydrothermal groundwater

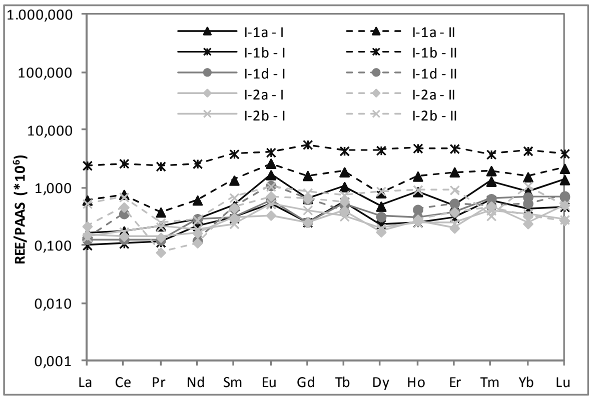

Fig. 13. Vinadio hydrothermal groundwater

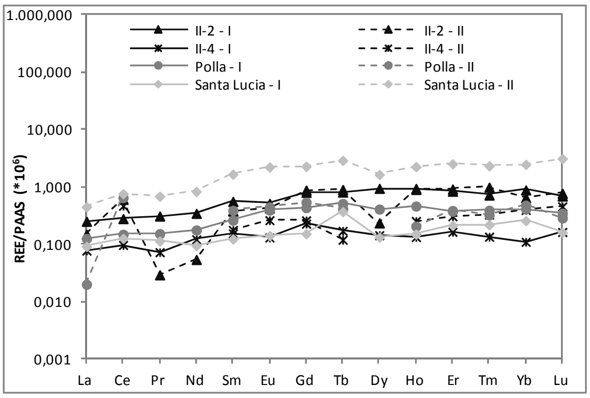

Fig. 14. Valdieri hydrothermal groundwater

The springs of volcanic complexes show a positive Eu anomaly. Springs of Vulsino and Vicano Volcanic District (Fig. 10) are similar in shape, while in the Colli Albani springs (Fig. 11) exists a difference in the content rather than in the shape.

The PAAS-normalized REE patterns of the thermal springs of Vinadio e Valdieri (Fig. 13 and 14) are similar, while La Bollente (Fig. 12) is different, especially in the shape.

5. Conclusion

The results obtained in this study show a close correlation between the contents of REE in groundwater and aquifer lithology in which they flow. As already highlighted by Biddau et al. (2009 and 2002), Johannesson et al. (1997) and Janssen and Verweij (2003). The many trend observed in basic metamorphic complex were correlated with the great variety of these types of rocks found in Piedmont. For other complexes, there are considerable similarities within the same complex. For example, the trends of the thermal waters prove to be quite similar in the cases of Vinadio and Valdieri that are located both in the Crystalline Massif of Argentera.

References

Biddau R., Bensimon M., Cidu R., Parriaux A., 2009. Rare earth elements in groundwaters from different Alpine aquifers, Chemie der Erde Geochemistry 69, pp. 327-339

Biddau R., Cidu R., Frau F., 2002. Rare earth elements in waters from the albite-bearing granodiorites of Central Sardinia, Italy, Chemical Geology 182, pp. 1-14

Johannesson K. H., Stetzenbach K. J., Hodge V. F., 1997. Rare earth elements as geochemical tracers of regional groundwater mixing, Geochimica and Cosmochimica Acta, Vol. 61, N. 17, pp 3605-3618

René P.T. Janssen, Wilko Verweij, 2003. Geochemistry of some rare earth elements in groundwater, Vierlingsbeek, The Netherlands, Water Research 37, pp. 1320–1350

MINE TAILING OF DEALUL NEGRU – FUNDU MOLDOVEI (SUCEAVA COUNTY, ROMANIA). PRELIMINARY ASSESSMENT OF THE ENVIRONMENTAL RISK

Dan STUMBEA
University "Al. I. Cuza" of Iaşi, 20A, Carol I Bvd., 700505, Iaşi, Romania; E-mail: dan.stumbea@uaic.ro; Tel.: +40 232 201 464; Fax: +40 232 201 462

Abstract The study reports on the main specific features of the impoundments from the unconfined mine tailing of Dealul Negru (appearance and color, grain size, mineralogy, acidity, amounts of the heavy metals and potentially toxic elements) in order to make a preliminary assessment regarding the environmental risk. The sludge mainly displays a yellow-ochre to brown color and a clayey appearance (fine and very fine sand+silt+clay fractions are up to 88%). In terms of mineralogy, the impoundments consists of primary (chlorite, quartz, sericite, plagioclase, biotite, and pyrite) and highly water-soluble secondary minerals (jarosite and basaluminite/ coquimbite), the latter being produced by the acid mine drainage; the amounts of Pb, Cd, As, Ba, Fe, Zn, Cu, Cr and the acidity values (pH=2.3-4.7) are rather high. The main environmental risk factors identified so far appear to be: the erosion by water during the heavy rainfall events, the highly acidic leachates and their amount of heavy metals and toxic elements; the effects of the acid mine drainage seem to decrease by the development of hardpans onto the flanks of the mine tailing and by an alleged lack of air-born transportation of the sludge.

Keywords: mine tailing, mineralogy, acid mine drainage, toxic metals, pH, XRD, XRF.

1. Introduction

The unconfined mine tailing of Dealul Negru is located on the southern bank of Moldova River, at a distance of about 15km west from the town of Câmpulung Moldovenesc (Suceava County, Romania). It contains the waste material (sludge) from the former milling and preparation plant of the sulfide mineralizations from the area; starting with late 1990^s, both mining of sulfide ore deposits and ore processing activities ceased. The waste deposit is about 30m high, occupies a surface of 5 hectares and is built up as 9-10 superposed steps (Fig. 1) and seems to develop a high risk for environment contamination through the acid mine drainage processes.

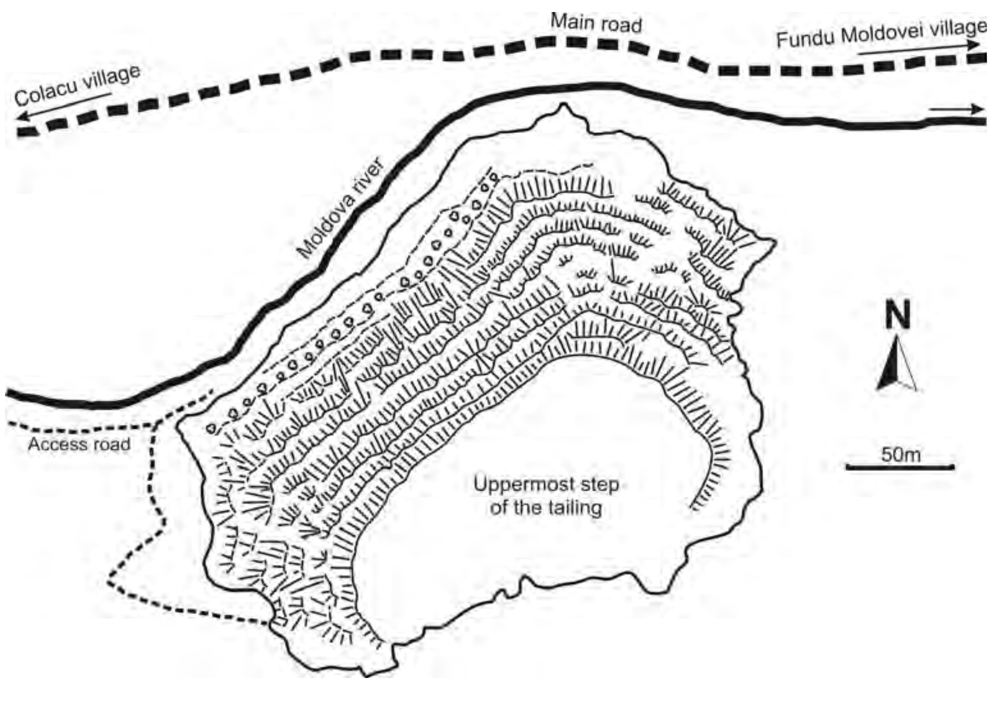

Figure 1. Sketch of the mine tailing from Dealul Negru (47°32'08.01" N; 25°22'45.42" E)

2. Geology of the perimeter

The preparation plant use to process the sulfide mineralizations of stratoid volcano-sedimentary type related to and hosted by the low-grade metamorphic rocks of Tulgheş Group (quartz-, chlorite-, sericite- schists); the Tulgheş Group forms the Variscan nappe of Putna that represents the deepest part of the Bucovinian tectonic unit and is developed after a NNW-SSE direction, along the Eastern Carpathians. The mineral constituents of the schists are generally quartz, chlorite, sericite, feldspars; ankerite, barite, and tourmaline appear only accidentally. The main component of the sulfides is pyrite (generally cupriferous), associated with chalcopyrite and subordinate galena and sphalerite; some scattered occurrences show a larger abundance of the last two minerals.

3. Material and methods

The mineralogy of the sludge samples was identified using both microscopy (Meiji 9400 ML microscope) and X-ray diffraction (Cu K ; Philips PW 1739 X-ray diffractometer) followed by a Rietveld computational refinement of the X-ray patterns. The chemical analyses for metals and trace elements with toxicity (Pb, Cd, As, Ba, Fe, Zn, Cu, and Cr) were carried out using an ED-XRF Epsylon 5 spectrometer equipped with 15 secondary targets. Measurements of both sludge and surface-water pH and Eh were made with a MeterLab PHM 250 Ion Analyzer – Corning 555.

4. Results and discussion

The sludge of the mine tailing displays a yellow-ochre to brown color, but in some sectors it shows a grey-greenish tint. It has a sandy to clayey appearance and the grain size measurements revealed an extremely large variation of the sand fraction amount (15-82%); however, in some samples the silt + clay fraction can reach up to 85%. The grain size data regarding the finest fractions show that the sum of fine sand + very fine sand + silt + clay fractions is higher than 88%; lower values (50-55%) were identified in samples from the deeper horizons of the tailing steps. Onto the surface of the sludge from the lowest steps of the tailing, brown-reddish to black cemented layer (crusts) occur.

Microscope observations show that the material is formed mainly of quartz, chlorite, sericite, and biotite; accidentally, altered feldspars, galena and sphalerite were recorded. Along with these minerals, much smaller, generally needle-like (rarely tabular), whitish-translucent crystals were observed.

XRD patterns confirm the mineralogy identified through the microscope analysis; in addition, they show that the mass of the translucent minerals is mainly formed of jarosite, fibroferrite and an Al-sulfate, possibly basaluminite or coquimbite. The Rietveld refinement revealed that the sludge consists mainly of primary minerals (Table 1) – over 85% of the mineralogical composition, and only less than 15% of secondary minerals (mostly jarosite, less fibroferrite and basaluminite/coquimbite).

The laboratory tests carried out to determine the susceptibility of the solid wastes to dissolution revealed a soluble fraction of less than 3.5%; the leachates obtained this way have pH values ranging between 2.3 and 4.7. An obvious increasing of pH data from the top (average pH of 2.6) to the bottom of the waste pile (average of 4.1) has been recorded.

The XRF analyses of the Dealul Negru sludge samples (Table 2) show high concentrations of toxic metals and trace elements with toxicity. The average of contents determined for both crust and regular sludge samples show an increase of Pb, Ba, Zn, Cu and Cr amounts in the samples unaffected by crustification, compared to crusts (Figure 2). The exceptions to this alleged general behavior are As (whose content varies inversely), as well as Fe (not showed in Figure 2) and Cd, which display constant contents.

Table 1. Mineralogical composition (%) of the sludge (based on Rietveld refinement of the XRD patterns)

	Variation	Mean
Quartz	24 – 46	24
Chlorite	12 – 31	32
Sericite	5 – 19	12
Plagioclase	3 – 9	6
Biotite	0 – 4	2
Pyrite	0 – 31	10
Jarosite	11 – 15	13
Fibroferrite	0 – 4	2
Al-sulfate	0 – 2	1

Table 2. Toxic metals and trace elements with toxicity (mg·l^{-1}) from solid milling wastes

	Toxic metals				Trace elements with toxicity			
	Pb	Cd	As	Ba	Fe (wt%)	Zn	Cu	Cr
Min.	37	0	63	297	3	40	34	0
Max.	900	3	294	1577	12	623	943	239
Average	345	1	135	908	8	153	199	112

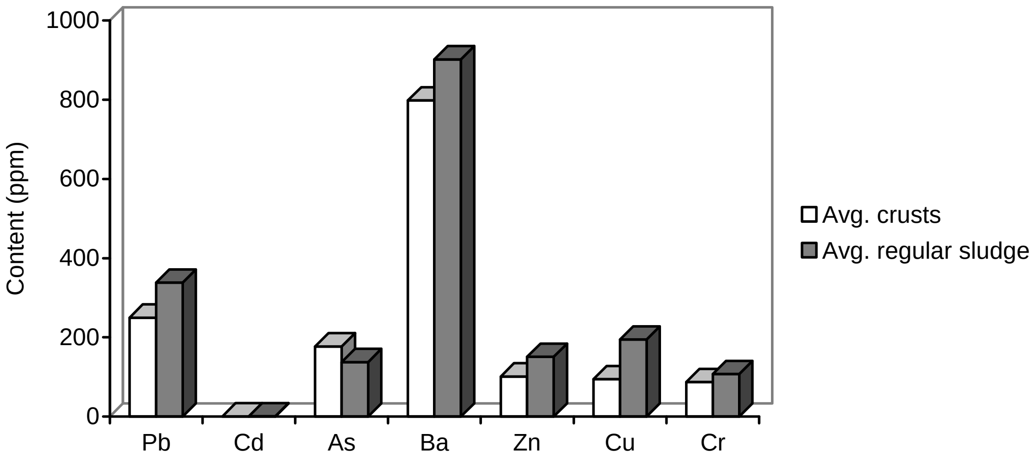

Figure 2. Average contents of some toxic metals and trace elements in both crusts and the regular sludge

The southern bank of Moldova River that flows at about 4-5m from the bottom of the sludge deposit, displays a 30-40m long area of a brown-reddish color; the pH of the waters in the area of the mine tailing ranges between 6.4 and 8.7. TDS data of the waters displays an interval of 137-616mg·l^{-1} and show a high negative correlation with the pH data (r^2 = 0.93). Chemical analyses of the water samples are to be foreseen.

5. Conclusions

The preliminary data acquired so far lead to the assumption that the impoundments of the unconfined mine tailing of Dealul Negru represents a serious threat to the environment. The primary source of contamination seems to be the surface water flows and the infiltration caused by the heavy rainfall events, as the torrent ditches developed onto the flanks of waste deposit suggest. The heavy runoffs are eroding the sludge from the tailing steps and transport the material downstream Moldova River; beside the mechanical transport of the solid waste, heavy rains are likely to induce large inputs of acidic and toxic metal-rich leachates into the environment, as former studies carried out on similar waste deposits have emphasized (e.g. Concas et al., 2006; Andrés and Francisco, 2008). Moreover, the presence of highly water-soluble efflorescent sulfates increases the risk of acidic and heavy-metals discharges into the environment (Bea et al., 2010).

However, as was observed during each of the field stage carried out in the perimeter, the sludge remains wet most of the time (even the uppermost flat surface of the tailing impoundments). In addition, especially onto the lower steps of the waste tailing, cemented layers (crusts) were observed; the crusts display lower contents of Pb, Ba, Zn, Cu and Cr compared to the regular sludge of the upper impoundments, leading to the presumption that the bottom of the tailing plays a less important role in the contamination of the environment. Also, although the area is rather heavily exposed to wind and the fine fraction of the sludge prevails over the larger fractions, the moisture retained by the impoundments and the development of hardpans prevents the wind-driven erosion (e.g. Graupner et al., 2007). Finally, the Moldova River does not seem affected by the acidic inputs as expected, due to a neutralizing process generated by an upstream quarrying activity for limestone.

Acknowledgements

The author gratefully thanks to prof. Jean-Hugues Thomassin from the High School of Engineering (ESIP), University of Poitiers, France, for his help regarding the XRD analyses and the Rietveld refinement of the XRD patterns.

References

Andrés N.F., Francisco M.S., 2008. Effects of sewage sludge application on heavy metal leaching from mine tailings impoundments, Bioresource Technology, 99, 7521–7530.

Bea S.A., Ayora C., Carrera J., Saaltink M.W., Dold B., 2010. Geochemical and environmental controls on the genesis of soluble efflorescent salts in Coastal Mine Tailings Deposits: A discussion based on reactive transport modeling, Journal of Contaminant Hydrology, 111, 65–82.

Concas A., Ardau C., Cristini A., Zuddas P., Cao G., 2006. Mobility of heavy metals from tailings to stream waters in a mining activity contaminated site, Chemosphere, 63, 244–253.

Graupner T., Kassahun A., Rammlmair D., Meima J.A., Kock D., Furche M., Fiege A., Schippers A., Melcher F., 2007. Formation of sequences of cemented layers and hardpans within sulfide-bearing mine tailings (mine district Freiberg, Germany), Applied Geochemistry, 22, 2486–2508.

CLOSING AND REHABILITATION WORKS OF TIBLES-TOMNATEC MINING AREA REGARDING THE MANAGEMENT OF MINING WATER AND DUMP SITES

Ioan DENUT*, Ioan BUD, Dorel GUSAT

Technical University of Cluj Napoca, North University Centre of Baia Mare, Dr. Victor Babes Street, No. 62/A, 430083 Baia Mare, Romania, Tel. +40 0362-401266, Fax: +40262-276153, E-Mail: ioandenut@ubm.ro

Abstract The closure activities of Tibles-Tomnatec mining area in Maramures County, Romania have been analyzed with respect to water management and dump sites, the weaknesses and the gaps procedures of the closure works can be observed in the analyses of the mine water. The paper will present a part of the results of a project carried out in North University Centre of Baia Mare.

Keywords: mine closure, water management, dump sites, rehabilitation works

1. Introduction

The Tibleş-Tomnatec mining area is located in Maramures County, in NW of Romania (Fig. 1). An evaluation of the Tibles-Tomnatec mining area regarding the landscape, the research works performed here according to water quality management and mine closure and rehabilitation works designed, have been compared to how their performance and solutions have changed the environment in these area.

Based on the first studies made by A. Koch between years 1881-1886, Gh. Panto in 1942 and E. Stoicovici in 1948 and 1949, the systematic geological research has started in Tibleş-Tomnatec Mining Area in year 1952, by the S.M.E. Bucureşti. The first complex studies about Țibles geology and ore deposit mineralogy and geochemistry, have been published by Pavelescu (1956) and Stiopol (1962).

The systematic research has been rerun by I.P.E.G. Maramureş between 1970 and 1988, with the 4,400 ha of total area. Several papers have been published about the massif petrology, mineralogy, and the characteristics of ore deposit mineral associations and genesis, by many specialists (Edelstein O., Petrulian N., Udubaşa G., Kalmar J., Pop N. and many others) between 1973-1983 (ICPM, 2002, unpubl.). Edelstein et al. (1973, 1974, 1981), Petrulian et al. (1975, 1976), Udubaşa et al. (1976, 1977, 1978, 1979), Kalmar and Pop (1977), Pop et al. (1980, 1981, 1983) (ICPM, 2002, unpubl.).

The Tibleş polymetallic ore deposit is located in the igneous-andesitic rocks – especially, and sedimentary and contact-metamorphic rocks - subordinated. With six principal veins (Tomnatec, Tomnatec Ramura 3, Ramură, Preluci, Preluci Ramură 2, and the Vein 18) the total length of the veins reaches is 1,500 m and the thickness is up to 2 m. The mineralogical associations contain primary minerals (pyrite, pyrrhotite, chalcopyrite, galena, sphalerite) and secondary minerals (marcasite, melanterite, limonite, malachite, bornite, covelite, chalcocite).

A surface of 10,766 m^2 has been affected by the exploration and prospecting works. As a result of these works, a surface of about 10,644 m^2 is occupied by the waste dumps (Table 1).

Fig. 1. Localization of Tibles Tomnatec Mining Area.

Table 1. Waste dumps summary in the Tibles Tomnatec Mining Area.

No.	Waste dump	Level above sea (a.s.l.)	Bench inclination (degree)	Dump volume (m^3)	Occupied surface (m^2)
1.	Căliman Adit	+884	35.6	20,300	4,110
2.	Tomnatec Adit	+930	37.0	20,700	6,534
3.	Izvorul Rău Adit	+964	-	-	-
		TOTAL		41,000	10,644

The total length of the excavated galleries at the level 1 (+884m a.s.l.) reaches 2,705 m, and at the research level 2 (+930 m a.s.l.) 2,755 meters. A total of more than 5,000 m of galleries have been excavated.

Due to these prospective works, after the closure of the mining area, it can be concluded that the results of these excavations are only the waste rock, because of the high level of minerals oxidation. Therefore, at the end of the exploration works the Tibleş-Tomnatec ore deposit could not be proposed for exploitation.

2. Closure and rehabilitation works

The mine closure activities were done according by the Law no. 85/2003, modified by the Law 284/2005 and Govern Emergency Ordinance no. 101/2007.

The closure activities have been done after the recommendation included in the "Mine Closure Manual" of the Ministry of Economy and Trade, Romania. However, these closure and rehabilitation works should take into account two sides of this mining area – the underground (the galleries) and the surface (the waste dumps). The concept was proposed by the S.C. Institutul de Cercetări şi Proiectări Miniere S.A. Baia Mare in 1999 (ICPM, 2002, unpubl.). Fig. 2 shows the "closure concept" of the underground levels.

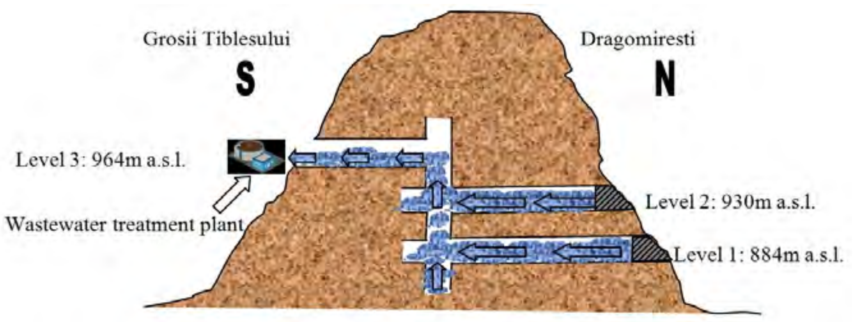

Fig. 2. Closure concept of the underground levels and the "ideal" underground water path.

The underground water management consists of collection of more than 51,700 m³ of water from underground mining works (Fig. 3). The estimated water flow for treatment in the water treatment plant was 60 to 80 l/s. To capture the water, there was planned to construct three underground retaining dams on each level − 1st, 2nd and 3rd. The retention dams are designed to allow flooding those three levels in order to control the level mine to the water treatment plant on level 3. Because these dams would bear the pressure of accumulated water column, they were designed according to the requirements of hydraulic construction to ensure a good behavior in time and prevent infiltration at the dams.

Choosing the location of the dam was made so that the surrounding rock will provide good physical and mechanical characteristics with a minimum of micro-fractures. After analyzing the mapping data available from the Caliman Adit, the most favorable location for retention dam is about 100 m from the mouth of the gallery, a section that is the least tectonized.

The Fig. 4 shows the waste dump of Izvorul Rău Adit after its "rehabilitation".

Fig. 3. Wastewater – from the Tomnatec I Adit (left) to the treatment plant (built but never used).

Fig. 4. Waste dump of Izvorul Rău Adit (in 2007 on the left side and in 2009 on the right side) after its "rehabilitation".

3. Critical observations

The rehabilitation works of the waste dumps have been designed to stabilize the dump on the one hand and on the other one to control the pollution of the surface water with heavy metals.

Based on our field observations made on the stability of waste dumps, we want to make the following statements:

- the waste dumps are located at the mouth of the lateral galleries, their constituent material being deposited gravitationally;
- resulting stability is the limit, giving them a stability coefficient of about 1;
- due to high slope angle of the waste dump, vegetation was not able to grow on the dump's surface and will affect the overall stability of the dumps;
- the waste dumps located on the north side, due to a difficult access, were not executed correctly with respect to rehabilitation and correction of the slope angle.

This poor slope stability affects the surface water quality, especially during periods of precipitation. To remedy this situation is to require rehabilitation and ensuring the slopes stability.

Regarding the underground water situation, to show the "results" of these underground closure works, different water analyses have been done. The pH for the 6 samples ranged from acidic to slightly acidic (3.30 to 6.25).

Results exceeding the MCA (Maximum Admissible Concentration) occurred mainly in samples taken from the Dragomireşti side (2x suspension over MCA on sample T2 –Tomnatec II Adit; 3x Fe content over MCA for sample T3- Pietrosul Creek, dump and with 6x over MCA for sample T3- Pietrosul Creek, dump; also for sample T3- Pietrosul Creek, dump we found a 4x Pb content over MCA and for Zn 23x over MCA on sample T1- Căliman Adit) and for the Țibleş side on Izvorul Rău the sample T4- Izvorul Rău I Adit exceeds for parameter Zn the MCA).

It can be concluded by now, that the closure method did not work on its full capacity, on one side because the underground water has found another flow path outwards (due to inhomogeneous rock) and the other side because the wastewater treatment plant has been never used. In different publication (Bud and Duma, 2010; Gusat and Drebenstedt, 2010) there were presented and discussed already the effects regarding the slope stability. One can observe that the design and construction of the waste dumps in this mining area have many weaknesses. After the rehabilitation works of the waste dumps (see Fig. 4), the

We can conclude at this point, that the initial involved costs of underground mine works (7 billion ROL respectively more than 210,000 US$ in the year 2003) have reached 39.9 billion ROL (Romanian old lei respectively 1.2 million US$) without reaching the final proposed aim of the closure activities. Due to the advanced oxidation of the ore, it has been not eligible to enter the operational phase, as negative effect it was prepared the closing mining area.

4. Conclusions and proposed solution for remediation of the current situation

In all cases, these "closure activities" have been done after the recommendation included in the "Mine Closure Manual" of the Ministry of Economy and Trade. But this "Manual" does not include steps and rules which have to be done for any kind of mining areas (waste dumps, tailing dumps, underground mining works, surface perimeter), in respect with the hydrology, geology or geotechnical parameters of rocks.

The Mine Closure activities in Romania have created serious deficiencies both at the design, which were reflected in the design phase and in the execution, with a lack of a national strategy for closure of mining perimeters (Denut et al., 2007). Generally, the mine closure works were not enough prepared because of:

- lack of specialists training;
- design of closure, security and rehabilitation of mining works including the hazard analysis not completely finished;
- weak execution of rehabilitation works;
- lack of planning of the cash flow;
- lack of a good manual of mine closure works;
- monitoring the execution works with specialists not planned.

In this case of Tibles-Tomnatec Mining Area, for the treatment of the underground polluted water the applicability of a calcareous bed method in a surface channel could be studied.

Acknowledgments

Many thanks to the Ministry of Economy and Trade, Romania, Sponsor of the project "Identificare soluții tehnice de reducere a impactului de poluare a componentelor de mediu (sol, apă) generat de apele de mină/deşeuri cu conținut de metale grele" [Identification of technical solutions to reduce the impact of environmental components (soil, water) pollution generated by the mine water / waste containing heavy metals] with the number 41/22.08.2007.

References

Bud I., and Duma S.S., 2010. Închiderea minelor în Romania. Amenajarea haldelor de steril. Revista minelor nr. 3/2010, 23-28.

Denuț I., Baciu D., Bud I., Cozmuța-Mihaly A., Duma S., Cozmuța-Mihaly L., Ciaca L., Hotea L., 2007. Identificare soluții tehnice de reducere a impactului de poluare a componentelor de mediu (sol, apă) generat de apele de mină/deşeuri cu conținut de metale grele". Unpubl. Report, Project number 41/22.08.2007.

Denuț I., Bud I., Duma S.S., Baciu D., Mihaly-Cozmuța A., Mihaly-Cozmuța L., 2008. Mining water management in the eastern part of Baia Mare mining area. Proceedings of International Symposium „Mineral Resources and Environmental Engineering" 24-25 October 2008, Baia Mare, Romania .

Guşat D. and Drebenstedt C., 2010. Geomechanische Modellierungen der Bodenbewegungen - angewendet auf Kohlebrände in China. In: 11. Geokinematischer Tag. 6.-7. Mai 2010, Freiberg, Germany, 363-372.

Pavelescu L., 1956. Studiul geologic şi petrografic al masivului Țibleş. An. Com. Geol., vol. XXVI.

Stiopol V., 1962. Studiu mineralogic şi geochimic al complexului filonian din Munții Țibleşului. Ed. Academiei R.P.R.

ICPM (2002) - SC. Institulul de Cercetări şi Proiectări Miniere S.A - Proiect tehnic pentru închiderea perimetrului Țibleş. Unpubl. Technical Project.

THE USE OF MINE WASTE IN AGRICULTURE. EXAMPLE OF AN EMERALD-BEARING BIOTITE-AMPHIBOLE-QUARTZ-SCHIST OF GARIMPO, MINAS GERAIS, BRAZIL.

Heinrich Adolf HORN[1*], Amando AGUIAR[2], Vieira da Alexandre Sylvio COSTA[3]

1- Geological Institute, Federal University of Minas Gerais, Belo Horizonte, Av. Antônio Carlos, 6627, Minas Gerais, Brazil, hahorn@ufmg.br, Tel.: +55313409 4446, Fax: +553134095420
2- Postgraduate Course in Geology, Federal University of Minas Gerais, Belo Horizonte, Av. Antônio Carlos, 6627, Minas Gerais, Brazil, apaagro@yahoo, com.br
3- Agriculture Institute, State University of Rio Doce, Governador Valadares, Minas Gerais, Brazil, asylvio@univale.br

Abstract In this work it is shown how the use of minewaste can avoid environmental impacts around the mining areas, better the productivity of agriculture and lower the costs of importations. The emerald-bearing schist is rich in P, Ca, Zn and other elements important for plants and permits the support in poor laterite tropical soils.

Keywords: Emerald mining, mining waste, soil corrective, environmental impact, laterite soils, tropical climate

1. Introduction

The growing world population induces a significant increase in the quantity of mining and industrial processes to guarantee the wellfare of people. A consequence of this intensification is an extensive use of natural resources and the generation of a huge amount of residues.

The mining groups which try to supply the world demand of raw materials are one of the major producer of waste tailings, causing optical and phyisico-chemical impacts providing environmental interferences with dangerous consequences to the maintenance of the life on the Earth.

The formation of these tailings created an economical-environmental problem, being cosiderated as an environmental passive of high cost and complex dealing for the involved bussiness groups from the present into future (Machado 1994).

On the other hand, due to the increase of the number of inhabitants of the planet, a larger production of foods and consumption goods will be necessary and also a more efficient and maintainable exploration of the natural resources (soils and minerals), as well as the necessity to determine an appropriate destination of those mining wastes, to reduce the impact to the environment and the danger to the creatures.

A lot of those mining wastes are composed of primary and secondary minerals which are able to liberate from their composistion chemical elements demanded by plants in their physiologic development and for food production (Aguiar et al. 2011).

To obtain a good production rate and a recovery of the used substrates (soils), it is necessary to do fertilization and correction to prepare soils for planting, especially in tropical region were high erosion and deep weathering results in acid and poor laterite type soils (Fernandes 1996).

To secure a production for use and exportation, in Brazil this demands a very high consumption of mineral input (fertilizers, correctives) and the high percentage of importation of these materials is changing negatively the importation-exportation balance of the country. In this way, using tailing material alone or together with industrial products, can reduce environmental impacts on the mining sites and industrial plants together with a reduction of the cost for agricultural production. Here are shown experiments for the use of waste material from tailings from an emerald digging and mining region in Minas Gerais for blending with lateritic soils to reduce the cost and better the production for small farmers and to reduce the waste piles and tailings (Fig. 1).

The biotite-, biotite-phlogopite-schists and amphibolites derived from metamorphosed rocks of the Archean ultramafic units, contain in their constitution chemical elements such as Mg, Ca, P and K and trace elements like Zn, Fe, Cu, Co that are necessary in physiological processes of plant development.

Brazil has three principal emerald provinces (Nova Era - Minas Gerais; Campo Formoso - Bahia; Santa Terezinha - Goiás) that can supply significant amounts of waste in the fertilizer industry.

The waste generated by the mining of emeralds in Brazil exceeds 45,000 tons in 2010, as informed by Belmont Company, allowing the use on >4,500 ha planted area/year.

In this way the import of lime and fertilizer inputs for agriculture can be reduced considerably, jobs can be generated by involving the workers in logistics, processing and distribution of the prepared material, which may increase the profits of industry and farmers.

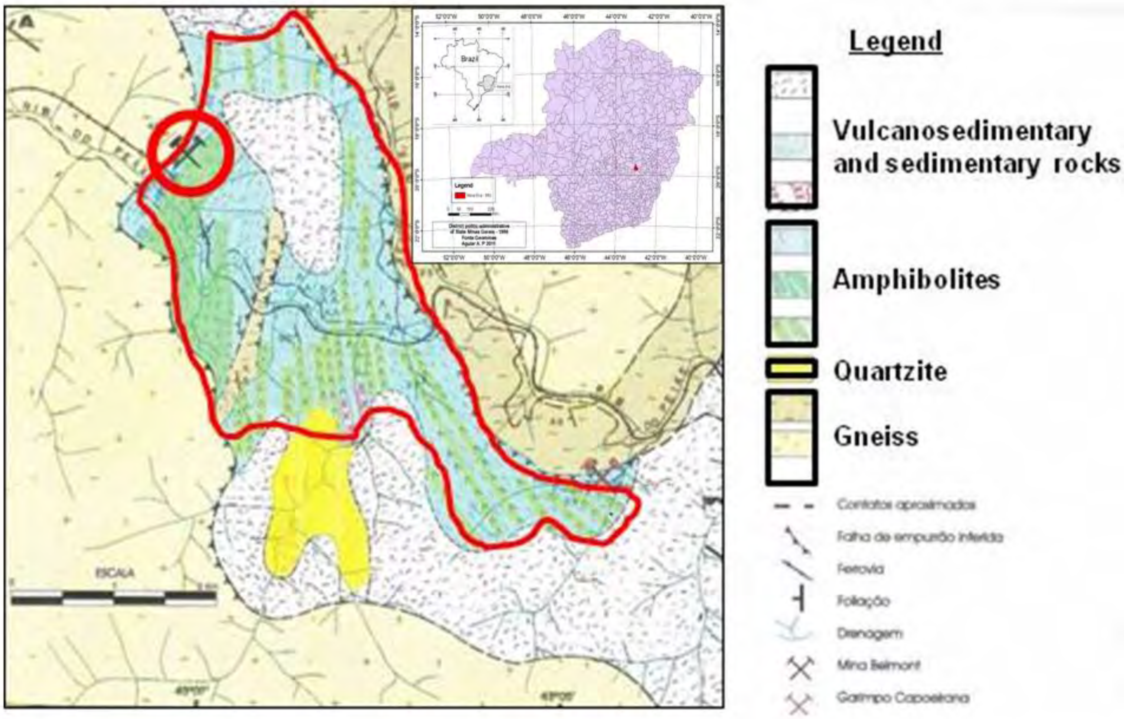

Fig. 1. This figure show the location and geology of the emerald mining district near Nova Era. The red line marks the area with exploited rocks. The red circle represents the principal mining locality.

Fig. 2. Example of waste material used in the experiments. The material is composed by different schists, amphibolite and quartz veins.

2. Activities

2.1. Sampling

In this work was used waste material from different tailings of emeralds mining region in the Nova Era County-MG (Fig. 2; Table 1) and agricultural soil collected at the experimental area of the agronomic department of the State University of Rio Doce Valley (UNIVALLE) in Goverandor Valadares, Minas Gerais State (Table 2).

The soil used in the experiments is a medium-sandy soil and in the agriculture related analysis were determined relevant parametres (DeFelipo and Ribeiro 1997) and are presented in Table 2. The samples were collected in the 0-20 cm depth interval in normal conditions 25-30^{o}C (Picture 3).

The soil was collected from the upper layer (0-20cm), dried under normal conditions (25-30^{o}C; shadow), crushed down and homogeniezed by sieving (<5,0mm) to a uniform soil substrate.

The mining residue was crushed and reduced to a granulometry <0,560 mm and mixed with the soils in different relations (Table 2).

Table 1: Composition of the mining waste used in this work.

	Al_2O_3	CaO	Fe_2O_3	K_2O	MgO	MnO	P_2O_5	SiO_2	Cr_2O_3	Pb	Cd	Cu	Ni	Ti	Zn	LOI
Sample	92,7	43,7	97,9	31,4	19,15	1,6	0,2	502,5	3,0	5,15	<0,1	4,4	166,8	5,1	107	2,46

Table 2: Agriculture-related parametres of the used soils such as pH, soluble match (P), potassium (K), calcium (Ca), magnesium (Mg), aluminum (Al), potential acidity (H+Al), Sum of bases (S), total CTC (T), CTC executes (t), Saturation of Bases (V) and saturation of Aluminum (m) Determination after Defelipo and Ribeiro (1997).
This table also shows the parameters for the used soil-minewaste mixtures.

	pH	P	K	Ca^{2+}	Mg^{2+}	Al^{3+}	H+Al	SB	T	t	V	m
		(mg/ dm^3)		(cmo-lc/ dm^3)				(cmolc/ dm^3)			(%)	
Areno-soil	5,40	4,10	110,40	1,10	0,10	0,55	2,60	1,48	4,08	2,18	36,27	32,11
Areno-soil (4t/ha)	5,33	4,50	142,64	0,90	0,68	0,53	2,68	1,94	4,62	2,47	42,12	21,12
Areno-soil (40t/ha)	5,40	5,40	206,81	1,00	1,30	0,40	2,68	2,83	5,51	3,23	51,50	9,94

2.2. Laboratory leaching tests

The waste and soil were mixed in the proportions 99.8:0.2 P/P, (99.8 g of soil: 0.2 g of waste); 98.0:2.0 P/P, (98.0g of soil; 2.0 g of waste), corresponding to the use of respectively 4 or 40 t/ha of the waste in field aplication, considering a soil density of 1.00g/cm^3.

After preparing always 100 g of sample, those were put in plastic beakers and irrigated until they reached 80% of the field capacity, with humidity control every other day, leaving them in incubation room for 60 days with controlled temperature varying between 27º and 33ºC. The beakers were covered with transparent plastic blanket to reduce the evapotranspiration of the sample and to maintain the humidity tenor.

The experiments were repeated four times for each waste dose used. After the incubation period, the soils were collected and put to dry under normal conditions (TFSA: air temperature; darkness), and afterwards submitted to the preparation for routine chemical analyses according with the method described by De Felipo and Ribeiro 1997.

2.3. Greenhouse tests

To analyze the disponibility of nutrients available for plants in the soil, a hybrid corn test in a greenhouse was organized.

The experimental design was completely randomized with five treatments and five repetitions. The following mixtures were used (0 t/ha, 5 t/ha, 10 t/ha, 20 t/ha, 40 t/ha).

The prepared materials (waste and soil) were placed in plastic containers with volume 63 dm^3 in the predetermined proportions and two corn plants were planted in every pot.

To determine the efficiency of the used waste as a nutrient source for plants, every month, the weight of dried roots, stems and fruit samples was determined.

Fig. 3. Soil samples from UNIVALE used in the work.

Fig. 4. Evolution of the plants from beginning untill after 3 month. The greenhouse tests were performed at the experimental area of UNIVALLE in Goverandor Valadares – MG.

2.4. Chemical analyses

The analyses were done in the ICP-OES laboratory of NGqA-IGC (leaching), in the DRX laboratory of CPMTC-IGC (mineral composition) and in the ICP-MS laboratory (bulk rock and soil chemistry) and in the soil laboratory of the University in Viçosa.

The greenhouse tests were performed at the experimental area of UNIVALLE and the freeland experiences at a farm north of Goverandor Valadares.

Were used three different specimens of plants to have information about soil depth and the variation with short-time (beans, maize, grass) and long-time cultures (trees).

3. Results

3.1. Leaching experiences

The results of leaching tests support the idea that in relation to the original soil (soil: 110,4mg/dm^{3}K) can be observed considerable changes in the K-values of the soil for the different used mixtures with a variation about 29 to 87% for the treatments with 4 and 40 ton/ha, respectively.

In relation to Al-saturation, the significant reduction was shown in the order of 70% (soil: 32,11% mixture: 9,94% for waste application of 40 t/ha). These may be caused by two factors, the reduction of the free Al and the increase of the base-saturation (Mg and K), due to the waste composition (Table 1) and the disponibility of elements in soil. The leaching tests show considerable liberation of important elements from tailing material like K, Ca, Mg,Co, Cu, Cr, Fe, Zn an Mn and considerable retention of other PTE´s with Cd, Pb.

The material do not change significantly the pH of the original soils (acidity of the soil pH = 5.6; low acidity).

3.2. Greenhouse experiences

This series are still ongoing. We expect to obtain the first results at the end of 2012 and beginning of 2013

4. Conclusions

The waste material from the tailings of emerald mining can, according to its amount, structure, location, mineralogical and chemical composition, serve as complementary inputs for the fertilizer industry, reducing in this way the costs of food production and also mitigate the problems caused by the deposition of the mining waste.

The observed preliminary results confirm an increment in disponibility of some elements like magnesium and potassium together with a low correction of the pH in soils for agricultural production.

Field experiments with more plant groups (beans, corn, eucalyptus) are in execution.

It may be necessary to use also blending with industrial waste to obtain better pH-correction data.

Acknowledgements

To the institutes and universities (NGqA-IGC - UFMG, FAAG - UNIVALE and FAPEMIG) for support in logistics and financial support, and to Dr. J. M. Leal for the consultancies.

References

Aguiar A.P., Horn A.H., Costa A.S.V**.,** 2011. Agricultural use of emerald mining residue (biotite-quartz-schist and amphibolites) from the Nova Era region, Minas Gerais State - viability and effects. In *Memorias* 14th Latin American Geological Congress/ 13th Colombian Geological Congress Medellin, Bogota, Sociedad Colombiana de Geologia: p. 1230-1231.

Braz V.D., Ribeiro, A.C.**,** 1997. Análise química do solo. Boletim de Extensão 29, 2ª Ed. UFV, Minas Gerais, 26p.

Fernandes M.M., 1996. Viabilidade agronômica e uso do Rejeito de garimpo do distrito pegmatito de Araçuaí - MG.

Leal J.M., 1999. Estudo das Inclusões Fluidas em Esmeraldas e Quartzo Associados no Garimpo de Capoeirana Nova Era, MG.

Machado G.A.A., 1994. Geologia da região e aspectos genéticos das jazidas de esmeraldas de Capoeirana e Belmont, *Nova Era* - Itabira, *Minas Gerais*. 1994. Dissertação de Mestrado em Geociências (mineralogia e Petrologia) - Universidade de São Paulo, Conselho Nacional de Desenvolvimento Científico e Tecnológico.

AIR POLLUTION IN THE NEIGHBORHOOD OF SI AND SI-FE FOUNDRIES NEAR PIRAPORA AND VÁRZEA DA PALMA, MINAS GERAIS, BRAZIL. IMPACTS OVER WATER, SOIL AND PLANTS.

Heinrich Adolf HORN[1*], Veloso Elizêne RIBEIRO[2], Magalhaes Wallace TRINDADE[3], Hernando BAGGIO[4], Essaïd BILAL[5]

1 - Geological Institute, Federal University of Minas Gerais, Belo Horizonte, Av. Antônio Carlos, 6627, Minas Gerais, Brazil, hahorn@ufmg.br, Tel.: +55313409 4446, Fax: +553134095420
2 - Geological Institute, Federal University of Minas Gerais, Belo Horizonte, Av. Antônio Carlos, 6627, Minas Gerais, Brazil,, elizenev@yahoo.com.br
3 - Geological Institute, Federal University of Minas Gerais, Belo Horizonte, Av. Antônio Carlos, 6627, Minas Gerais, Brazil,, wallacegeografo@yahoo.com.br
4 - Federal University of Jequitinhonha e Mucuri Valleys , Diamantina, Campus, Minas Gerais, Brazil, hernandobaggio@yahoo.com.br
5. Ecole des Mines de St. Etienne, St. Etienne, France, bilalessaid@gmail.com

Abstract In the middle São Francisco Basin, five Si- and Si-Fe-foundries are localized. This foundries cause notable environmental impact due to the emission of a smoke very rich in particles, organic compounds and PDE Please, write PDE in unabbreviated form, because it was not explained.Also, explain this abbreviation at the first use in the text. The effects over air, soil, water, plants and its gravity are shown in this paper. The results of ICP-OES and ICP-MS show PDE, C and P enrichment. Microprobe investigations give information about the wide variety of the Si (amorphous and crystalline), Fe (magnetite) and C-based particles.
Investigation about the impacts in livinig beings are still ongoing.

Keywords: industrial dust, melting processes, Fe-Si industry, metal sources, contamination, human activities

1. Introduction

Industrial activities that use high temperature furnace processes in the production of metallic Si and Si-Fe alloys, starting from diversified raw materials, are causing, among other problems, the liberation of fine dusts particles which are built up by parts of these compounds and their cracked products (Santos et al., 2011, Horn et al.2006, Horn et al. 2009).

Due to the high degree of distribution (smoke, dust), the surface-volume relation and the chemical activity given by the particle size and its composition, they may have adverse impacts on health of plants, animals and people, the quality and quantity of agricultural products in the surrounding areas and drastic changes in the aquatic and irrigation systems. This influence can happen following two different ways:

- Direct deposition on plants and animals is causing a direct chemical interaction;
- Through the deposition on soil and water surfaces with the indirect input into the bio-cycles.

Dust and soil samples studied in this work come from the neighborhood of foundries located in the Pirapora - Várzea da Palma region in Central to Northern Minas Gerais State, Brazil (Fig. 1).

The raw materials used in these processes are barite, crushed vein quartz, argillite, charcoal and wood for the Si production together with scrap materials (Fig. 2).

Particulate matter in smoke display spherical C-compounds (μm), chromium-spinel balls (μm), irregular amorphous and crystalline SiO_2-agglomerates and rare crystallized magnetite, SiO_2 and Si crystals. The particle shapes are irregular to spherical. Grain size varies from tenths of a micrometer to <1 millimetre.

Together with the natural air dust (argillites, oxides and quartz may occur by secondary reactions. The smoke plumes show transport distances of up to 50 km with changing flux conditions due to temperature (inversion) and wind direction changes. The preferential transport directions are: NE to SSW 50%, NW - SW 15% and N - S 35% (Fig. 1).

The samples were investigated by various methods: grain-size measurements, XRD, optical microscopy, environmental SEM and microprobe. ICP-OES and ICP-MS analyses of the primary dust composition, to obtain information about mineralogical, granulometric and chemical characteristics (total composition; leaching tests).

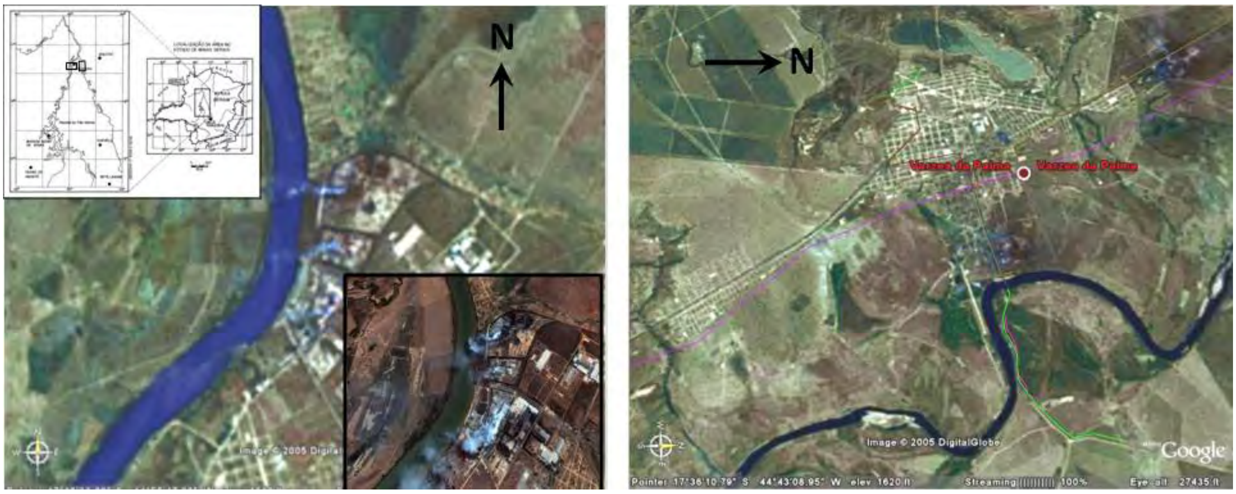

Fig. 1: Location of the Si and Si-Fe foundries. The regional location of the investigated regions is indicated in the small upper maps. The smaller satelite fotograph shows a detailed view of Pirapora and Várzea da Palma Si-plant and the smoke evolution.

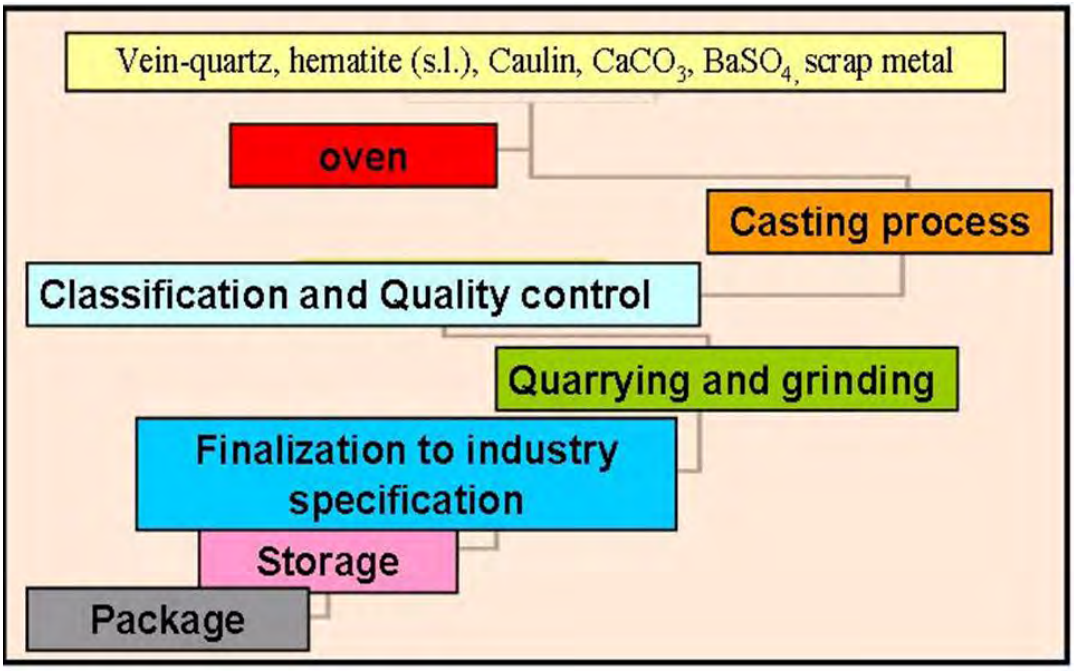

Fig. 2: Electrothermal process used at the foundries. The raw material (scrap; industrial metallic residual) explain the variety of PDE´s and dangerous particles. At all stages, liberation of contaminants occurs, especially in the oven step (smoke, ashes), casting processes and grinding processes (dust, contaminated water).

Fig. 3: This figure shows the used equipments for the measurement of dust distribution. Left: portable Laser equipment; Middle: Foil Dust collector; Right: Counting facility with a weak dust sample;

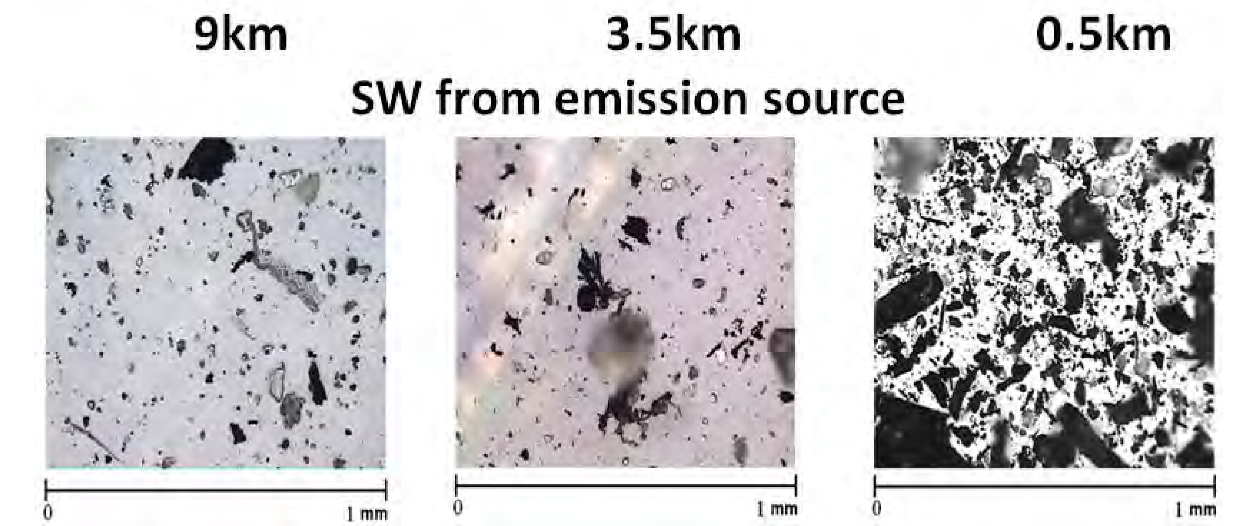

Fig. 4. This figure shows sample distribution correlated with distance from a source at Pirapora. From right to left a distribution in a E-E profile from industrial plant in Pirapora, crossing the São Francisco River.

Fig. 5. Examples of plant exposure to the smoke. The high density of particles inhibits the respiration of the plants. Also, unlimited growth can be observed (cancerigenous-like effects). In function of the distance from the source, plants show changes in the normal evolution, irregular colors and forms.

This shows the hazardous potential of the smoke and its danger for plants and soils in the concerned area. Investigation performed in the laboratory about the bio-leaching of the particulate matter in smoke and leaching tests point out direct and chronic dangers by direct plant-dust and dust-soil-plant contacts.

2. Activities

2.1. Field activities

Air dust sample collections were performed regularly over three years in various directions and distances from the sources (Fig. 1). The sampling substrates are collant foils which were exposed to pollution over a period of 1 to 4 weeks (Fig. 3 middle), in function of dust density and then sent to laboratry.

Collection of bigger dust samples was realized directly from chimney stocking filters.

In some special places were executed analyses with a portable Laser equipment to obtain information of the very small particles (PM5, 2.5 and smaller; figure 3 left).

2.2. Laboratory work

Different activities were executed with the collected samples:

- Granulometric evaluation with Laser Scattering Particle Size Distribution Analyzer LA-950 and counting facility using graphic programs (Fig. 3, left and right),
- Whole sample chemistry by ICP-MS,
- Microscopic identification of types, form and structure of dust grains by petrographic microscope, analyses in profiles over different dust grains with a CAMECA microprobe
- Statistical work with the obtained informations.

Table 1 Chemical composition of the two distinct dust types formed by specific processes (Si or Si-Fe) obtained directly from chimneys collected powder.

ppm	Ba	Co	Cs	Ga	Hf	Nb	Rb	Sn	Sr	Th	V	W	Zr	Y	La	Ce	Pr	Nd	Sm	Eu
LD	1	0.2	0.1	0.5	0.1	0.1	0.1	1	0.5	0.2	8	0.5	0.1	0.1	0.1	0.1	0.02	0.3	0.05	0.02
HI	3	0.6	0.2	2.6	<	0.2	3.6	<	14.2	<	49	<	2.1	<	0.3	0.6	0.04	<	<	<
IB1	2235	1.3	1.6	5.8	0.4	1.2	43.6	4	<	0.2	42	0.7	9.5	0.3	1.6	1.9	0.15	0.5	0.09	0.02
IB2	2981	1.8	1.7	8.7	0.4	0.9	44.3	12	<	0.2	36	0.6	15.2	0.7	2.5	4.1	0.33	0.7	0.12	0.02

ppm	Gd	Tb	Dy	Ho	Er	Tm	Yb	Lu	Mo	Cu	Pb	Zn	Ni	As	Cd	Sb	Bi	Ag	Au	Tl
LD	0.05	0.01	0.05	0.02	0.03	0.01	0.05	0.01	0.1	0.1	0.1	1	0.1	0.5	0.1	0.1	0.1	0.1	0.5	0.1
HI	<	<	<	<	0.06	<	<	<	0.2	2.8	3.1	391	1.0	<	<	0.2	<	<	<	<
IB1	0.06	0.01	0.14	0.02	0.07	0.01	0.12	0.01	9.4	18.2	17.0	103	5.9	5.4	0.2	1.2	0.5	<	<	0.1
IB2	0.17	0.02	0.14	0.03	0.10	0.02	0.33	0.02	4.1	40.3	22.6	96	4.6	7.1	0.2	1.3	0.6	0.1	2.7	0.2

3. Results

a. There are two distinct types of smoke (Table 1), one formed principally by amorphous (up to 90%) and crystalline SiO_2 (<15%) and another formed by crystalline magnetite, crystalline and amorphous SiO_2.

b. A wide range of granulometric distribution from µm down to nm, causing physical and chemical effects (Guthrie et al. 1993; EPA, 2012).

c. A clear correlation between distance from source and particle distribution in size, quantity and composition (relation between industrial- and surface-related particles) is visible (Fig. 4).

d. Distribution of PDE´s in soil surface is determined by industrial production peaks, rainfall quantity, sunshine intensity and by various wind directions (Braga 2007).

e. A wide variety of grain composition and textures can be seen. The granulometric and compositional variety permits a wide range of physical and chemical reactions from macroscopic to submicroscopic scale. An important factor is the high potential activityof the amorphous SiO_2, Al_2O_3 and Fe-oxides rich particles.

4. Conclusions

There is a very strong healthy and visual impact due to the high particle concentration in the air. A big part of the local community has longtime health problems (skin, lung, eyes) or allergic reactions in function of the smoke impact over the town- or countryside. Plant surface and soil are covered by a distinct quantity of particles (Fig. 5).

Acknowledgements

IGC-UFMG gave logistic and FUNDO FUNDEP financial support.

Analyses were executed at the NGqA of IGC-UFMG, laboratories of the Universities of Rouen and Marne-la-Vallée, both in France. The granulometric investigations were done by HORIBA, São Paulo, Brazil.

References

EPA 2011. http://www.epa.gov/. accessed 8.1.2012.

Guthrie, J.G.D.Jr., MossmannT, B. 1993. Health Effects of Mineral Dusts. Reviews in Mineralogy, 28, 584 p.

Horn H.A., Farias, B., Bilal, E., Karfunkel, J., Moraes, M.C. 2006. Atmospheric mineral pollution NE of Belo Horizonte, Minas Gerais, Brazil. A case study of Pedro Leopoldo cement industry. 20 LAK, Kiel Abstracts: 125.

Horn, A.H., Baggio, H., Trindade, W.M & Ribeiro, V.E. 2009. Environmental disequilibrium due to anthropogenic activities until today - An actual ¨pollution¨ example from the São Francisco River Basin between Três Marias and Pirapora, Minas Gerais, Brazil. In Freiberger Forschungshefte, V1: 58-62.

Braga, L.L. 2007. Avaliação do impacto ambiental da usina de beneficiamento Fe E Si, Várzea da Palma, MG, Brasil– Distribuição e transporte dos contaminantes. Federal University of Minas Gerais, Belo Horizonte, Master thesis: 120p.

Santos, J. O.De, Horn, A.H. & Trindade, W.M. 2011. Study on atmospheric pollution: Mineral and chemical composition of particulates surrounding industries in Pirapora, Minas Gerais, Brazil. In GAEA heidelbergensis 22th LAK Heidelberg 2011, 18: 157-157.

THE DISTRIBUTION OF POTENTIALLY DANGEROUS ELEMENTS (PDE´S) IN THE UPPER AND MIDDLE SÃO FRANCISCO RIVER BASIN, MINAS GERAIS, BRAZIL. AN EXAMPLE OF CHANGING, DISTRIBUTION, CONCENTRATIONS AND SOURCES

Heinrich Adolf HORN [1*], Veloso Elizêne RIBEIRO[2], Magalhães Wallace TRINDADE[2], Hernando Filho BAGGIO[4]

1- Geological Institute, Federal University of Minas Gerais, Belo Horizonte, Av. Antônio Carlos, 6627, Minas Gerais, Brazil, hahorn@ufmg.br, Tel.: +55313409 4446, Fax: +553134095420
2- Postgraduate student - Federal University of Minas Gerais, Belo Horizonte, Av. Antônio Carlos, 6627, Minas Gerais, Brazil, elizenev@yahoo.com.br, wallacegeografo@yahoo.com.br
3. Federal University of Jequitinhonha e Mucuri Valleys , Diamantina, Minas Gerais, Brazil, hernandobaggio@yahoo.com.br

Abstract. In this work is shown that water and sediment polution in river basins of Central Minas Gerais State is more and more dominated by agriculture-related sources and to a lesser extent by the heavy industry. This can be shown by the alteration in PDE-Spectra, type of distribution and chemical occurrence of the elements such as ions or colloid-argillite fixed compounds.

Keywords: metal concentration, metal sources, industry, agriculture, environmental impact, tropical climate conditions, human activities

1. Introduction
1.1. Region

From the beginning of the occupation of the medium to upper São Francisco River, this area was used intensively by the population. The installation of artificial lakes and the construction of hydroelectric power plants led to the increase of its attractiveness for the implantation of heavy industry and agriculture (IEF 2005).

With the beginning of the industrialization and its strong need of water and cheap energy, a lot of industry was installed in this area, counting with heavy industry along the rivers Paraobeba and São Francisco, a foundry of Zn in Três Marias, Si - Si/Fe smelters and other industries in Pirapora, Várzea da Palma and Bocaiúva. Also, several charcoal plants and ovens for bricks production were built. These activities are favored by the easy access to raw materials like clay and firewood found in the Cerrado.

With this intensive human influence and the lack of state and federal supervision, the situation escalated and an immense degradation of this region happened (CPRM 2003).

The increasing interest of the population and the progress in environmental sciences and investigation, medicine and biology alerted more and more people and organizations for the negative impacts caused by human influence. Actually, due to a more efficient legislation and stronger appropriate surveillance and control by public institutions, the industries were forced to rethink their behavior. This way of thinking introduced from the end of the 20th century lead to a significant reduction in the liberation of the harmful agents by the manufactures, reducing significantly the impact caused by their activity. Nevertheless, the contamination levels are actually beyond the permitted limits. (CETESB 1988, 2001).

The development of farming in the study area caused a second impact wave over the Cerrado-Biomes, in different way from the first, but with almost the same results. Great areas of the Cerrado were transformed in corn-, soybean- and coffee plantations and big projects of reforestation with eucalyptus and pinus, allowing the exposure of large soil surfaces to the atmosphere (rain, wind, etc.) for a long time.

The use of soil correctives, agrotoxics and other compounds, together with extensive mechanization, completes the scenery of interventions by agriculture in the study region.

Contrary to the pointedly pollution of industries, the agriculture activities cause a more diffuse contamination pattern for the whole area.

1.2. Localization

The investigated area is localized in the north-eastern part of Minas Gerais State, between the cities of Três Marias and Pirapora (Fig. 1).

In this region, in the middle part of one of the most important rivers of Brazil there are dams, varied industries, dense agriculture and a numerous population living from the products.

2. Activities

2.1. Fieldwork

Sampling of water and sediments was done beginning from the 1990 (Lundhamer 1991; Schilling 1991), near Três Marias, continued with Oliveira (2007) and finished with the works of Trindade (2010) and Ribeiro (2010) by detailed sampling between the Três Marias Lake and the das Velhas River confluence (Fig. 1b).

On sampling point other physical-chemical parameters like temperature, pH, conductivity, eH, water and sediment colors, turbidity and DOB were determined.

2.2. Transport

The samples (water 1 l, sediments 1-2 kg) were transported in plastic bags and bottles in cooling boxes to the laboratories in Belo Horizonte, where the preparation took place, then the samples were stored in freezer.

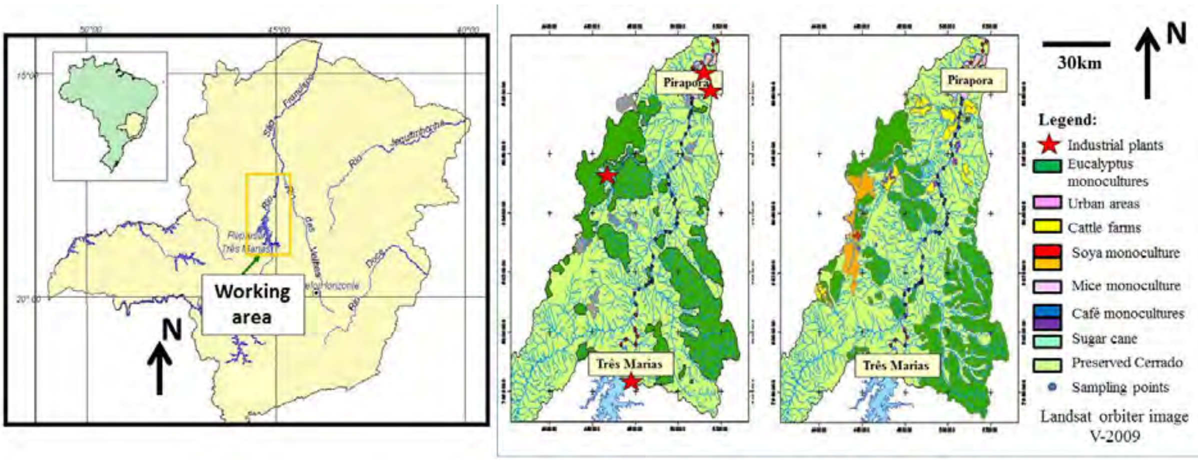

Fig. 1. Leftside (a); Location of the investigated region. Rightside (b): Location of samples and indication of regional activities (sources)

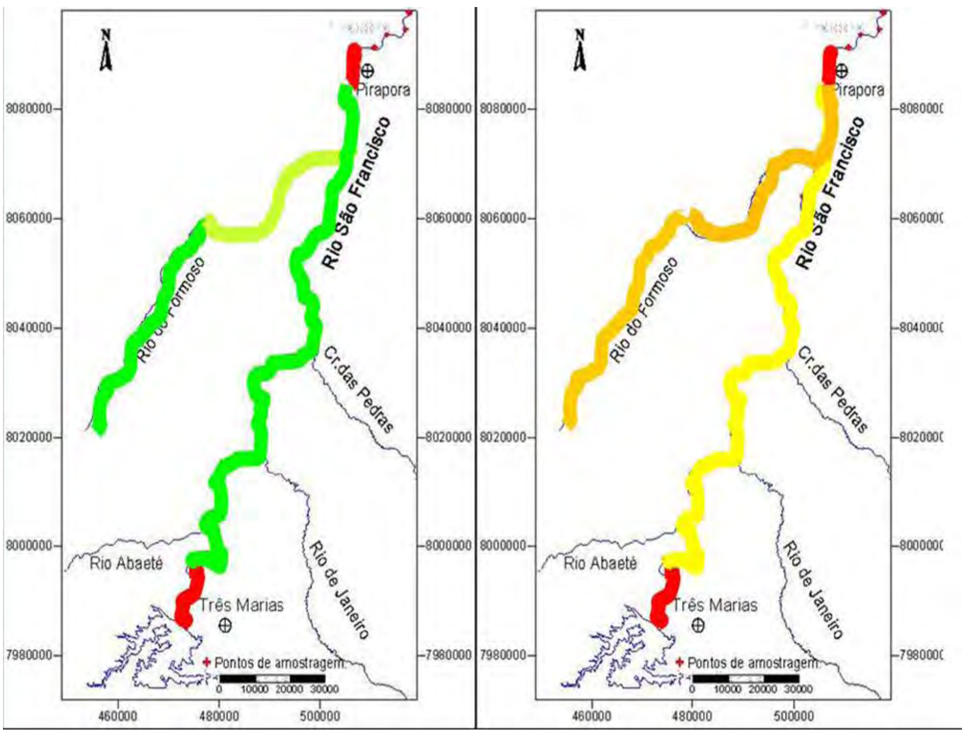

Fig. 2. The changes in element distribution of sediments with time. **Left:** 2008; **Right:** 2010. The colors indicate the degree of polution calculated by weighting all significant elements. **Green:** below base level, free of contamination (0%); **yellow:** slightly above base level, weak contamination (0-25%); **orange:** intermediate contamination (25-75%); **red:** above contamination limits (CONAMA resolution 344/04), very contaminated (75-100%).

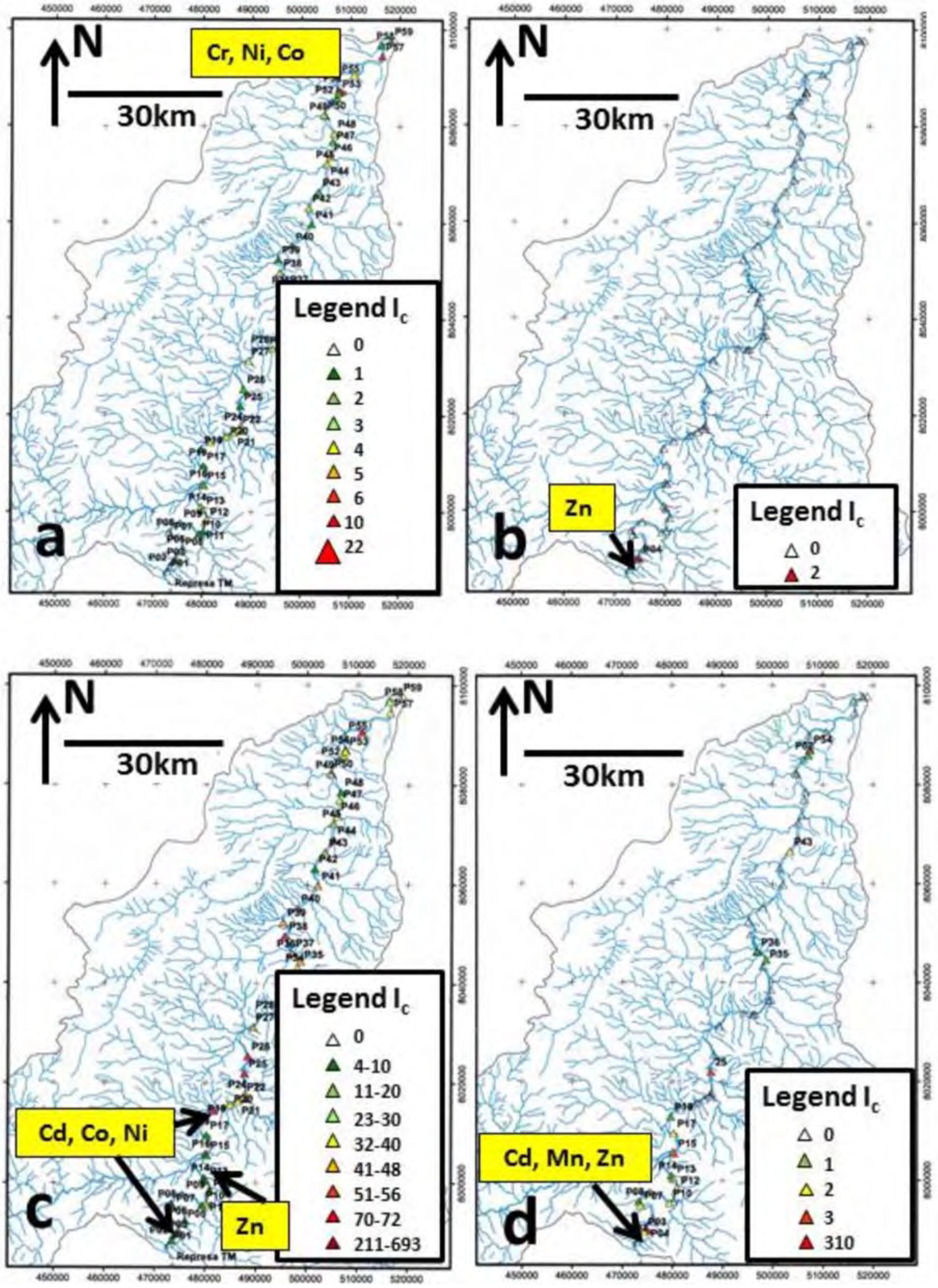

Fig. 3. Seasonal changes in the investigated area, showing the changes in total amount and colloidal transported amount calculated in contamination index (I_c). The changes between summer and winter show the significant influence of agriculture in 2009. **a and b:** Winter 2009; **c and d:** Summer 2009 The yellow boxes show highes concentration of important elements connected to industrial contamination (Zn; Cd, Mn, ionic) or agrotipic influence (Cd, Cr, Ni, Co; coloidal or adsorbed).

2.3. Preparation

The water samples were filtered and stabilized by acid to pH 1-2.

The sediment samples were dried, sieved and the fine fraction (<0.640 µm) was separated in two portions; one of them was leached with water and the other one with diluted HNO_3 (10%) in a microwave oven.

2.4. Laboratory

The water and leaching samples were analyzed for selected element by determination with ICP-OES spectroquant Arcos equipment using internal and international standards. The samples were analyzed in duplicates.

3. Results

3.1.Sediments

The anomalous element concentrations in sediment are clearly connected to human activities (Fig. 2). There is a change from high tenors of Zn, Cd, Pb, near the industrial plants and higher concentrations of Zn, Cu, Pb, Hg in agriculture-influenced regions.

There is a clear difference between the sediment quality from the regions influenced by industrial sources and those affected by agricultural activities. In general, a reduction of PDE´s overall concentrations in the sediments occurred.

3.2. Water

The elements in solution are higher near industry whereas the elements connected to argillite and colloidal components are higher in agricultural regions (Fig. 3).

The PDE´s contents are reduced in the industry- influenced regions and high in the agriculture-influenced regions.

4. Conclusions

The changes in the location and concentrations of PDE´s and its spectra indicate clearly a change in primary sources.

Together with climatic changes, such as stronger rains, winds and higher temperature alterations, this form of contamination increases continuously in intensity and reach.

The most important observations and conclusions are:

a. There occur significant changes in the shape of contamination areas (previously: points – nowadays: clouds);

b. Element concentrations near agriculture influence region and away from industry are increasing;

c. Element-spectra of found contamination have changed due to changes in contamination sources;

d. Heavy element concentration fixed in sediments from industry-influenced areas continues to be high and is showing slowly tenor reduction.

Acknowlwdgements

We thank NGqA-IGC-UFMG, UNIMONTES, Votorantim, Brazilian Navy for logistic and FAPEMIG, CNPq for financial support.

References

CETESB, 1988. Guia de Coleta e Preservação de amostras de água. São Paulo. 149p.

CETESB, 2001. Relatório de Estabelecimento de Valores Orientadores para Solos e Águas Subterrâneas no Estado de São Paulo. São Paulo. 73 p.

CPRM, 2003. Projeto São Francisco. 455p.

IEF, 2005. Mapeamento da Cobertura Vegetal e Uso do Solo do Estado de Minas Gerais.

Ribeira V.E., 2010. Avaliação da qualidade da água do Rio São Francisco no segmento entre Três Marias e Pirapora – MG: Metais pesados e atividades antropogênicas. M.Sc. Thesis, IGC-UFMG, B. Hte. 197p.

Trindade M. W., 2010. Análise da concentração e distribuição de Metais Pesados em sedimentos no rio São Francisco no segmento Três Marias/Pirapora: Fatores naturais e antropogênicos. M.Sc. Thesis, UFMG, B. Hte. 126p.

DETERMINATION OF URANIUM, THORIUM AND POTASSIUM CONTENTS IN ROCK SAMPLES FROM DITRĂU ALKALINE MASSIF USING GAMMA-RAY SPECTROMETRY

Adriana ION
Geological Institute of Romania, Bucharest, Romania, e-mail: adi75riana@yahoo.com

Abstract Uranium, thorium and potassium have been determined in rock samples from the Ditrău massif for each lithological unit by a non-destructive gamma spectrometry technique. The average concentrations of radioactive elements ^{238}U, ^{232}Th and ^{40}K were measured by gamma-ray spectrometry using a HPGe detector and found to be 2.2-13.7, 11.6-35.1 and 1.4-4.6, respectively, for the rock samples.

Keywords: natural decays, gamma-ray spectrometry, potassium, thorium, uranium

1. Introduction

This paper presents the results of uranium, thorium and potassium concentrations measured for the rock samples of Ditrău Alkaline Massif using laboratory gamma-ray spectrometry with HPGe detector. The natural radionuclides, which occur in typical rocks of the massif, are ^{238}U, ^{232}Th and their decay progeny, and the primordial radionuclide ^{40}K. The Ditrău Massif consists of a large variety of rocks (hornblendite, diorite, syenite, nepheline syenite, monzonite, monzodiorite, aplite, granodiorite). Radioactivity in the rocks of Ditrău Massif is given by the naturally-occurring radioactive elements in the minerals. The degree of radioactivity is dependent on the concentration and types of isotope present in the mineral. Thorium and uranium are constituents of the accessory minerals zircon, monazite, sphene, allanite, apatite, xenotime. ^{40}K is present in alkali-feldspathic syenite (alkali feldspar series, nepheline, biotite).

2. Geology of the study area

The alkaline massif of Ditrău is unique in Romania by size and petrographic variety (Fig. 1). It is an intrusive body with zonal structure, which was emplaced into the pre-Alpine metamorphic rocks from the basement of the Bucovinian nappe complex of the Eastern Carpathians, close to the Neogene – Quaternary Calimani-Gurghiu volcanic arc (Kräutner and Bindea, 1998). The massif is of intermediate size (about 800 km^2) and exhibits an eccentric ring structure in which the more basic rocks tend to lie to the west, with an arcuate zone of syenitic rocks, extending from the far north to the south-east, and a large area dominated by nepheline syenite on the eastern side (Constantinescu et al., 2010).

The center of the Ditrău massif was formed by nepheline syenite, which is surrounded by syenite and monazite. North–western and north–eastern marginal sectors are composed of hornblende gabbro/hornblendite, alkali diorite, monzodiorite, monzosyenite and alkali granite. Small discrete ultramafic bodies (kaersutite-bearing peridotite, olivine, pyroxenite and hornblendite) and alkali gabbros occur in the Jolotca area. The latter are also known from drill-cores in the Ditrău area. Hornblende gabbro/hornblendite and diorite represent the earliest intrusive phase, and are embedded within younger syenite and granite (Morogan et al., 2000). All this rocks are cut by late-stage dykes with a large variety of compositions including tinguaite, phonolite, nepheline syenite, microsyenite, and aplite. (Anastasiu and Constantinescu, 1979; Anastasiu et al., 1994). The age of the Ditrău Alkaline Massif is Ladinian (Mid Triassic), indicated by $^{40}Ar/^{39}Ar$ dating obtained on hornblende by Dallmeyer et al. (1997).

The rock samples were collected from outcrops created by the hydrographic network and roads cuts. Samples were collected throughout the massif area from all types of representative rocks. Because ^{238}U, ^{232}Th and ^{40}K are long life isotopes, rock samples have been analyzed in 2009 using new techniques of analysis. Rock samples were crushed to a grain size of 1 mm, and placed into sample containers. The containers were made of plastic and were sealed so that no radon can escape. All rock samples were kept in air-tight containers (Marinelli beakers-500 ml) for about 40 days to ensure that the radionuclides ^{227}Ra and ^{228}Th attained radioactive equilibrium with their daughter products. (IAEA-TECDOC-1363, 2003).

3. Materials and methods

The samples were analyzed non-destructively using gamma-ray spectrometry with high purity germanium (HPGe) detector. The detector has a relative efficiency of 27%, resolution of 1.90 keV and peak/Compton ratio of 56:1 at 1.33 MeV and it is coupled to conventional electronics connected to a multichannel analyzer card (MCA- DSPEC jr.2.0-ORTEC) installed in a PC computer. The use of advanced Multi-Channel Analyzer emulation software (MAESTRO-32) allows data acquisition, storage, display and online analysis of the acquired γ-spectra (Ion and Anastase, 2010).

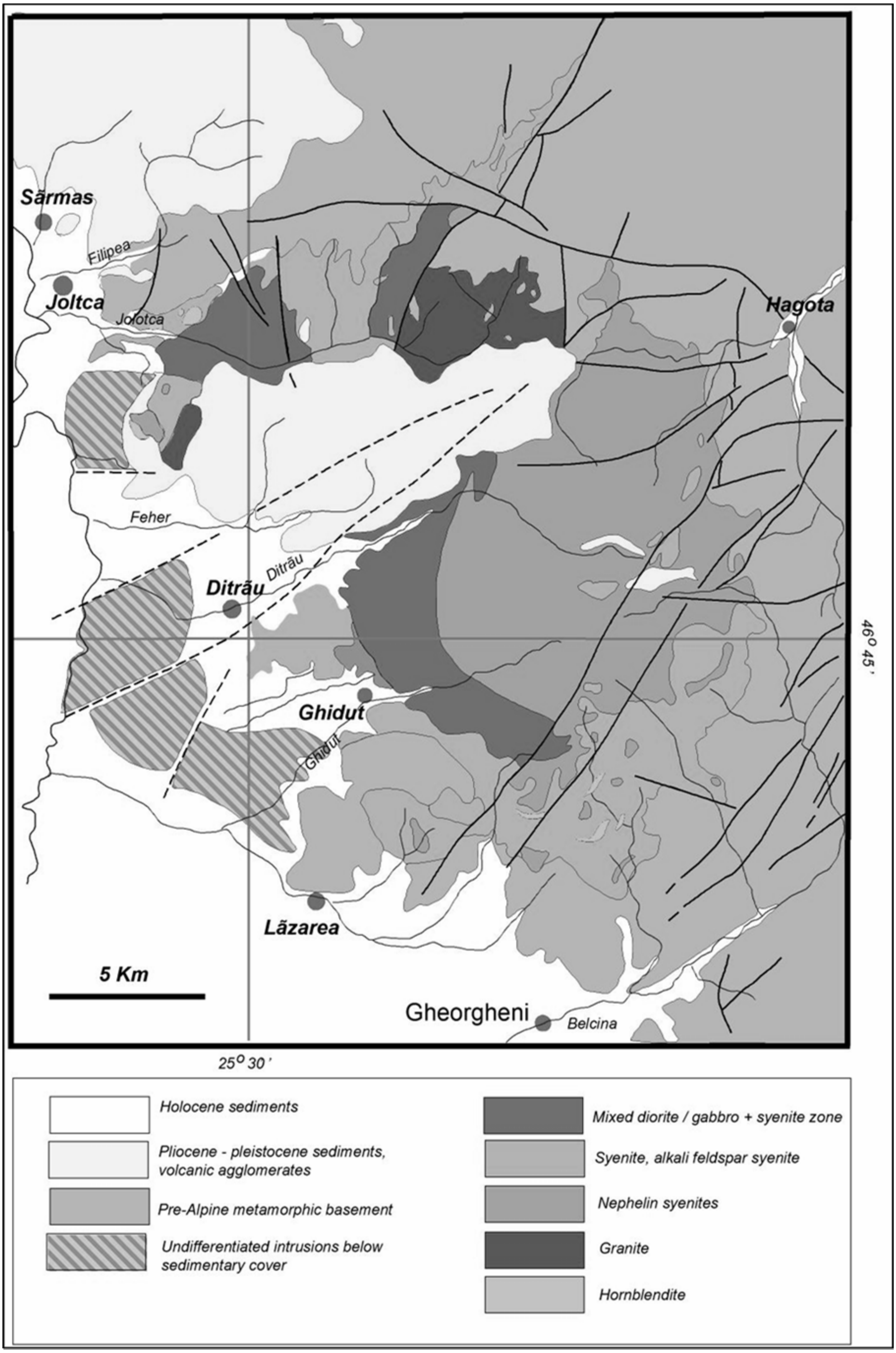

Fig. 1. Geological map of Ditrău Alkaline Intrusive Complex (after Kräutner and Bindea, 1998).

Table 1. Average ^{238}U, ^{232}Th, ^{40}K in typical rocks from the Alkaline Massif of Ditrău.

Type of Rock	Number of samples	Concentration U, Th (ppm) K (%)		
		^{238}U *Average*	^{232}Th *Average*	^{40}K *Average*
Hornblendite	R 17	2.2	12.8	1.4
Diorite	R 18	2.8	16.8	2.1
Syenite	R 19	4.3	19.2	4.6
Nepheline syenite	R 12	6.2	17.4	4.4
Monzonite	R 13	3.5	21.6	3.9
Granitoid	R 19	4.9	33.3	4.5
Aplite	R 11	4.3	31.9	3.3
Tinguaite	R 12	13.7	35.1	3.6
Lamprophyre	R 12	2.4	11.6	1.9
Metapelite	R 25	3.8	18.2	3.9

The detector was shielded from the background radiation using a 10 cm-thick lead wall that was internally lined with a 2 mm copper foil. The system was calibrated for energy using radioactive standards of known energies such as ^{152}Eu, ^{137}Cs and ^{60}Co. For the efficiency calibration, a multi-element standards containing radionuclides with known activities in 500 ml Marinelli beaker was used (IAEA – RGU-1, RGTh-1, RGK-1). The standard has the same size and geometry as the sample under study. Each sample was counted for 86,000 s. The background correction was accounted for by measuring a distilled water sample spectrum in the same geometry, and was subtracted from each spectrum. Each measured γ-ray spectrum has been analyzed offline by a dedicated software program (Gamma Vision-32), which performs a simultaneous fit to all the significant photopeaks appearing in the spectrum. Menu-driven reports are available for summaries including centroid channel, energy, net area count, background counts, intensity and width of identified and unidentified peaks in spectrum, as well as peak and average activity in $BqKg^{-1}$. The accuracy and precision of the results depend on many factors: the size and energy resolution of the detector; the mass and geometry of the sample; the shielding of laboratory background; counting time; data processing procedures; and the quality of the radioactive standards. The average concentration of ^{238}U, ^{232}Th and ^{40}K for samples of typical rocks are summarized in Table 1.

4. Results and discussion

The radioelement concentrations show an increase in average radioelement concentration with the increase of SiO_2, which is a typical behaviour of uranium and thorium in magmatic processes. Comparing the content data obtained for the Ditrău alkaline massif it can be observed an enrichment in thorium for all types of rocks.

The granitoids that occur in the north-east of the massif have the highest thorium content among all types of rocks. On the average, thorium (70.7 ppm) is two times higher than the average level of common granitic rocks (30.3 ppm) while the uranium content is within the range typical for granitic rocks. From the geochemical point of view, this is characteristic of radioactive elements (uranium and thorium) accumulation at the end of magmatic differentiation process (Tiepac et al., 1986). This accumulation is more obvious in rocks rich in potassium- and sodium-saturated volatile compounds. From those mentioned above, the empirical rule stating uranium concentration in magmas rich in potassium and thorium concentration in sodium-rich magmas can explain the enrichment of thorium in the massif Ditrău, dominated by Na-rich rocks. The contents of radioactive elements (Fig. 2) show that nepheline syenite, the richest in potassium have the highest content of uranium, while hornblendite, with the minimum concentration of potassium, have the lowest uranium content.

Another aspect of the geochemistry of radioactive elements is the spatial variation of the radioactiv elements content. The hornblendite and diorite from Jolotca area have lower average uranium and thorium contents than those determined in the Ghiduț area on the same types of rocks.

In Fig. 2, uranium and thorium values present large variation intervals. Syenite, nepheline syenite and lamprophyre show broader uranium variation, while diorite, aplite and lamprophyre display the largest

This difference in the distribution of radioactive elements is consistent with the concentration of both uranium and thorium mainly in accessory minerals (zircon, monazite, allanite, apatite, xenotime). The irregular distribution of the accessory minerals directly influences the oscillation range of uranium and thorium values. Although accessory minerals occur in small quantities in the rock mass, it should be considered that they have contents thousands of times higher compared with the main rock-forming minerals.

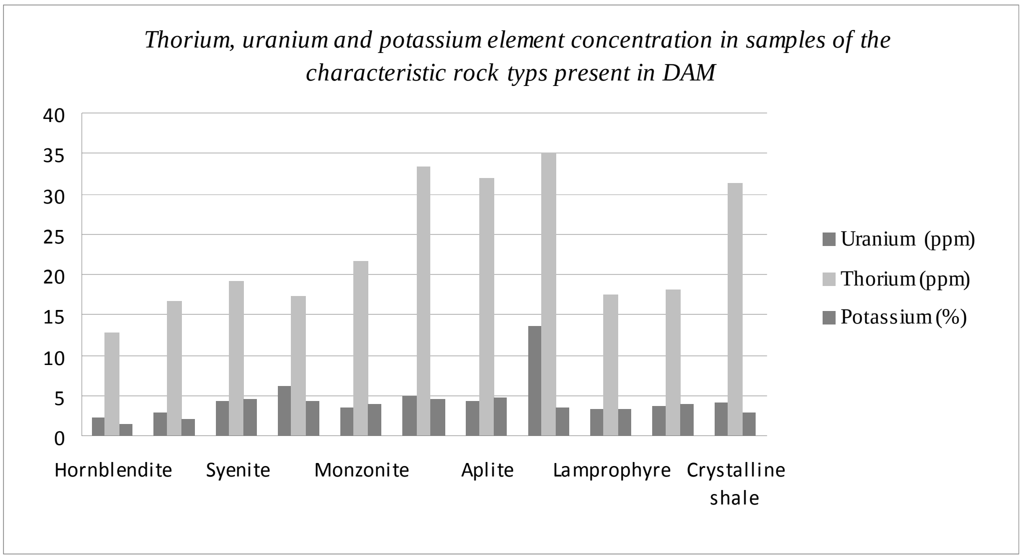

Fig. 2. Distribution of uranium, thorium and potassium in rocks. Hornblendite: Jolotca - 1.7 ppm U, 10 ppm Th; Ghiduț - 4.1 ppm U, 21.5 ppm Th. Diorite: Jolotca - 2.1 ppm U, 14.5 ppm Th; Ghiduț - 5.8 ppm U, 25.7 ppm Th.

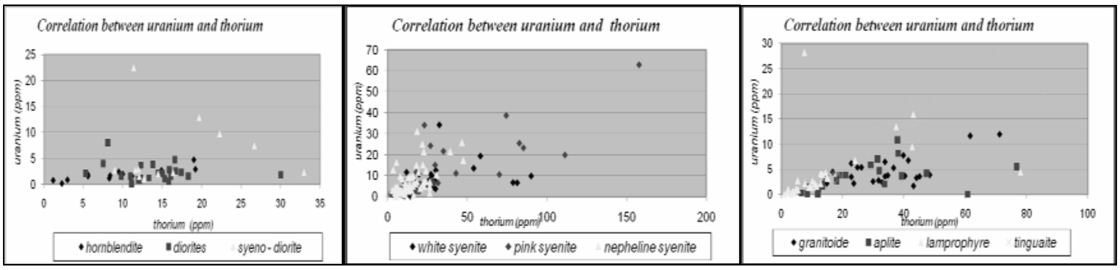

Fig. 3. *U-Th correlation in rocks from Ditrău area*

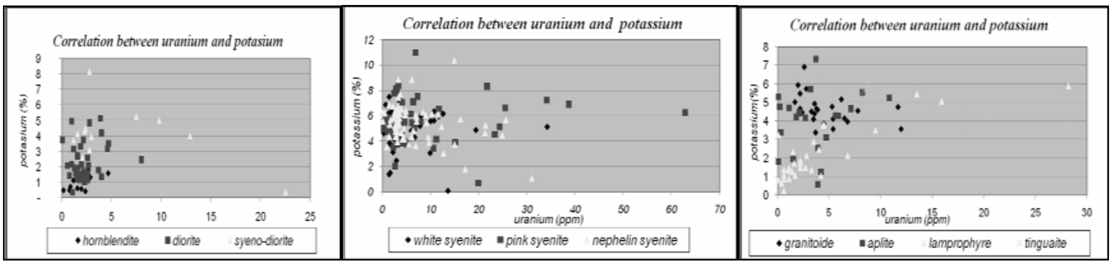

Fig. 4. *U-K correlation in rocks from Ditrău area*

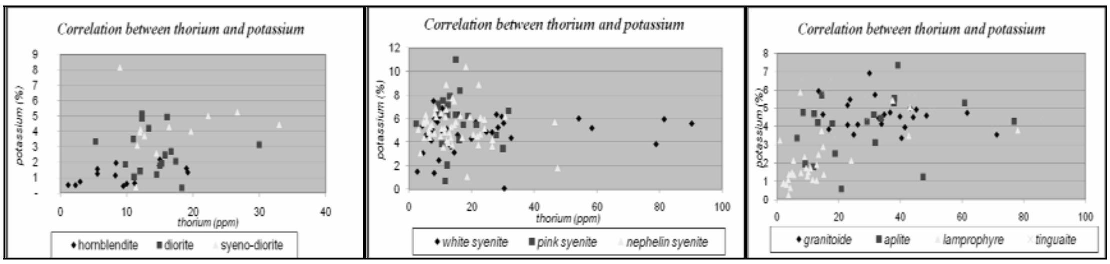

Fig. 5. *Th-K correlation in rocks from Ditrău area*

Correlation analysis U-Th (Fig. 3), U-K (Fig. 4) and Th-K (Fig. 5) reveals some aspects that can be summarized as follows:

(a) positive correlation of U-K and Th-K for dike rocks (aplite and lamprophyre), diorite, syenitdiorite and hornblendite;

(b) poor negative correlation, between U-K and Th–K in granitic rocks and marginal syenite;

(c) positive correlation between U and Th in almost all type of rocks.

These data indicate that potassic minerals do not control the accumulation of uranium and thorium in rocks.

5. Conclusions

The content of radioactive elements in the Ditrău massif increases from west to east and from north to south. Tinguaite and syenite from the center of the massif have higher uranium content, while the marginal areas of the Ditrău massif are enriched in thorium. Uranium and thorium contents present large variation limits for the same types of rocks in the study area. Uranium, thorium and potassium concentrations for the same type of rock vary with the location of the samples in the massif.

References

Anastasiu N., Constantinescu E., 1979. Structure and petrogenesis of the alkaline massif of Ditrău, Unpublished geological report, Archive of the IPEG "Harghita", Miercurea Ciuc.

Anastasiu N., Garbaşevschi N., Jakab G.,Vlad S., 1994. Mesozoic rift related magmatism / metallogeny at Ditrău. In Borcos, M., Vlad, S. (eds.). Plate tectonics and metallogeny in the East Charpatians and Apuseni Mts.. Field trip guide, IGCP Project No. 356 Bucharest, Geological Institute of Romania, 14-16.

Dallmeyer R.D., Kräutner H.G., Neubauer F., 1997. Middle-late Triassic $^{40}Ar/^{39}Ar$ hornblende age for early intrusions within the Ditrău Alkaline Massif, Romania: implications for Alpine rifting in the Carpatian orogene. Geologica Carpathica, 48, 347-352.

IAEA - TECDOC-1363, 2003. Guidelines for radioelement mapping using gamma-ray spectrometry data, Vienna. International Atomic Energy Agency, 45-51, 115-122.

Ion A., Anastase S., 2010. Natural radioactivity in soil samples from the area between Bistrita and Trotus valleys. Geology- Proceedings of the International Symposium–Geology of natural Systems – GeoIasi, Geologie Series, Al. I. Cuza University, 60-64.

Kräutner H.G. Bindea G., 1995. The Ditrău alkaline intrusive complex and its geological environment. In Guidebook to excursion E, (3rd Symposium on Mineralogy, Bucharest, Romanian Journal of Mineralogy, 77, 3, 18.

Kräutner H.G., Bindea G., 1998. Timing of the Ditrău Alkaline Intrusive Complex (Eastern Charpatians, Romana). Slovak Geological Magazine, 4, 213-221.

Morogan V., Upton B.G.J., Fitton J.G., 2000. The petrology of the Ditrău alkaline complex, Eastern Carpathians. Mineralogy and Petrology, 69, 227-275.

Tiepac I., Romanescu O.& Stoian M., 1986.Synthesis of geochemical data for radioactive elements and rare earth elements in Ditrău Massif. Unpublished geological report, Archive of the Geological Instititute of Romania.

SUSTAINABLE USES OF THE ECOLOGICAL POTENTIAL OF FORMAL PIT INTO NATURA 2000 SIT ARGES MIDDLE FLOODPLAIN

Andreia PETCU, Ionel URECHE
SC Lafarge Agregate Betoane SA Strada Modrogan 20 - 011826 -Bucuresti, sect 1, Romania;
andreia.petcu@lafarge.ro.

Abstract This paper presents the ability of ecologically rehabilitated areas to recruit and sustain new life, a true measure of their contribution to biodiversity conservation. The rehabilitation process may be accelerated by establishing combinations of forestation of native plant species, hydrological measures for new lakes and control of alien species. The study of alien species along five years conducted to specific measures.

Keywords: rehabilitation, sand and grave pit, Natura 2000, alien species.

1. Introduction

Historically used as an extraction point for aggregates since 1970, the Fusea area is located in the floodplain of the Arges River, part of the “Arges Middle Floodplain” Natura 2000 site. It is a mixed area of economical and natural value. The project area has around 100 hectares including former industrial sites, agricultural land, forests and lakes.

The area proposed for rehabilitation represents 2% of the Natura 2000 site and presents species of amphibians (1188 - *Bombina bombina*) and two types of habitats of European interest (91E0* - Alluvial forests with *Alnus glutinosa* and *Fraxinus excelsior* (*Alno-Padion, Alnion incanae, Salicion albae*) and 92A0 - *Salix alba* and *Populus alba* galleries).

The project was conducted in three phases aimed at achieving and implementing an integrated program of environmental rehabilitation of the affected area by mineral aggregate extraction activities.

2. Regional setting and geology of the study area

In terms of relief, Fusea natural area is located in the Romanian plain, in its subdivision Titu plain. This is a subsidence plain, formed due to the slow immersion of the surface, which generated meandered courses, puddles and swamps of Arges River. The natural area is located near the contact between the Romanian plain and the Cândesti piedmont (north direction). Minimum altitudes in this area are between 120 and 150 meters.

Basic soils characteristic in the investigated area is given by the Arges river meadow, where less evolved soils appear - protosoils and alluvial soils alternating with sand and gravel banks.

The analyzed area is characterized by the presence of a Quaternary alluvial complex (from the surface to a depth of 20-25 m) consisting by gravels with sand (ballast), in which are inserted thick clay lenses. Up to depths of 6-8 m and even 12 m it can be found a continuous ballast horizon, which was and continues to be (around the investigated area) the subject of exploitation within the gravel pits and sorting stations. Under these depths there are clay lenses irregularly distributed, with thicknesses ranging from 1-5 m to 7-9 m. At depths greater than 20 m are encountered clays formations and powder clays with fine sands areas, which may belong to Pre-quaternary formations. As appearance and characteristics these are similar to the lenticular clays from the upper alluvial complex.

Fusea Natural Area is located in Arges hydrographical basin, specifically in the lower valley of the river, on its left bank. Arges River has in this area an average multiannual flow of 40 m^3/s. Its riverbed is well individualized with banks that can reach 6 m in height. The river course is meandered and its width varies between 50 m (SE of the site) and 350 m (centre of the site). In table 1 the main coordinates of the area are presented.

Table 1. Geographical coordinates of the investigated area

Limit	Northern latitude	Eastern longitude
Western	44^0 38’ 33,00”	25^0 25’ 43,00”
Northern	44^0 38’ 53,34”	25^0 25’ 03,95”
Southern	44^0 38’ 07,23”	25^0 26’ 42,33”
Eastern	44^0 38’ 15,54”	25^0 27’ 00,86”

Maximum flows are recorded in spring (spring high foods: April - July) and minimum drainage is recorded in summer. During the warm season short-timed high floods occur, but with a great power of erosion and transport.

3. Materials and methods

Environmental status characterization in Fusea area was made by direct observation during field trips performed between summer 2007 - winter 2011; biological material sampling (plants and terrestrial invertebrates); measurements (hydrometry, physical-chemical parameters).

The investigated components were represented by:

• Terrestrial vegetation;
• Terrestrial invertebrates fauna;
• Birds;
• Limnic ecosystems characterization.

Direct observation activities of biotic components were accompanied by written records and photographic images that constitute an initial database regarding the investigated area.

The native species preserved typical galleries species such as: *Populus alba*,*Populus nigra*, *Salix alba, Salix fragilis*, *Alnus incana.* Also typical underbrush species (*Rubus caesius*, *Rubus hirtus*) and liana (*Clematis vitalba*, *Humulus lupus*) have been preserved. Of specific dune vegetation, two species of shrubs have been preserved: *Hippophae rhamnoides* and *Tamarix ramosissima*. The populations of these two species present a quite large number in relation to the investigated area. These are valuable, both for *Hippophae rhamnoides* whose populations at national level are decreasing and risk to be replaced with *Eleagnus angustifolia*, and for *Tamarix ramosissima* whose populations are also decreasing because their natural habitat is destroyed by sand extraction from the dunes where they vegetate.

Intense anthropogenic activity made some species, which typically don’t have their habitat here, to vegetate, grow and proliferate, for instance:

• fruit trees (some of them allochthonous): *Malus pumila, Pyrus pyraster, Prunus cerasifera, Juglans regia*, *Morus alba*, *Morus nigra*, *Cerasus avium*;
• invasive species: *Amorpha fruticosa, Phytolacca americana* , *Conyza canadensis, Echinocystis lobata, Erigeron annuus, Robinia pseudacacia, Gleditsia triacanthos*.

The invertebrate fauna in the area has a continuous spectacular development, both in terms of biological diversity and population effectives. This happens mainly because of their mobility, but also because of their smaller biological cycles, which, based on the reduction/ending of exploitation activities, allow them to have a more rapid colonization than in the case of vegetation.

In 2010, Lafarge and WWF experts have prepared a new ecological rehabilitation project in order to increase the value of ecological restoration of degraded floodplain and to ensure a community-based system of managing the environmental services in the area. Fig. 1 present project outlines in order to give a general view of the project. The main objectives of the project were:

- Develop and implement a plan for ecological restoration of the degraded areas from the Fusea site including biodiversity management, ecological enhancement and control of invasive species.
- Develop and implement a community based program for conservation and support of the natural development of the Fusea site

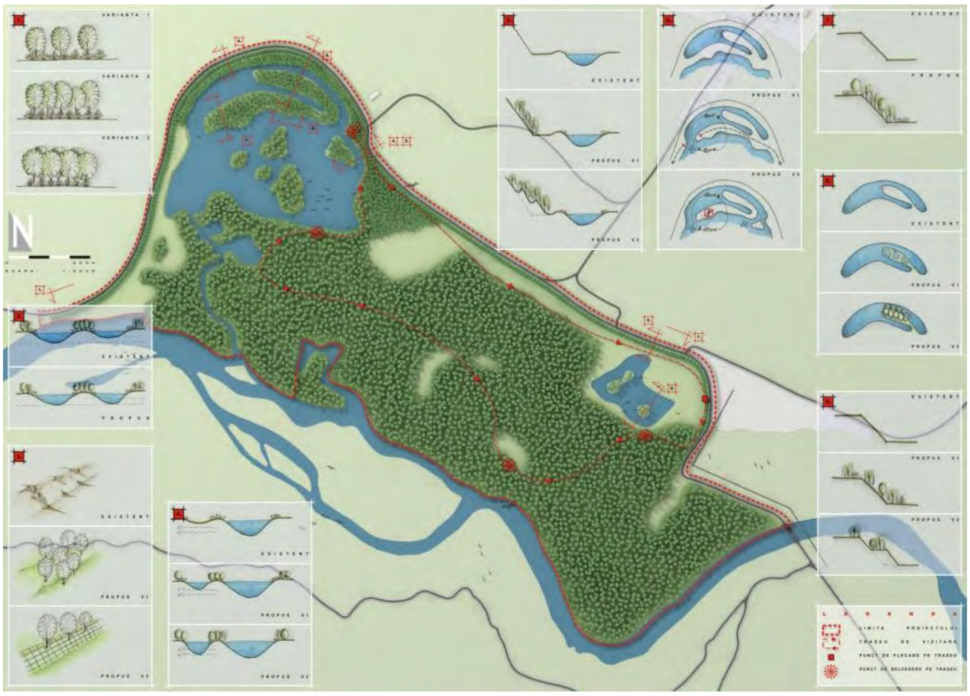

Fig. 1. Scheme of the rehabilitation project designed to carry out the ecological restoration of the degraded floodplain.

During the last 2 years, the project team implemented the ecological reconstruction works that could offer the proper conditions for ecosystems and species with high ecological value. The main activities were: creation of a large vegetation belt, creation of connectivity between two lakes, monitoring activities and a training concept (Fig. 2).

Fig. 2. A selection of pictures from key events in the area like stakeholders consultations process and rehabilitation works regarding connecting of lakes and environment training aspects.

4. Results

The direct benefit for nature and the community is understandable in restoring and enhancing the local species. There is also an indirect benefit for the people within the community – their engagement and ownership of the re-evaluation helps and change their behaviour and mind-set.

- A 5 year integrated plan for the ecological rehabilitation and management of the area that is based on the ecological characteristics of the area, including the high value species and habitats.
- Ecological rehabilitation works that have led to an increase in the number of bird species and to an extended surface of the aquatic habitats.
- Actions for eliminating the invasive alien species (e.g. *Amorpha*).

5. Conclusions

Studies have focused on many applications concerning revegetation operations in different conditions. The use of adapted species as well as native species has proven better efficiency in revegetation. We aimed at workable aspect, trying to position ourselves at the interface between theory, feasibility and practice activities.

This project was more than a "real scale" experiment and the results were not yet published. However the project give best practice example to formal sand and gravel pits restorations and contribute to conservation of biodiversity into Natura 2000 sit "Arges Middle Floodplain".

References

EPC Environment consultancy, 2008, Background study for the conservation and sustainable use of the ecological potential of Fusea natural area, p. 20-47, Bucharest;

EPC Environment consultancy, 2010, Memoriu de prezentare necesar obținerii acordului de mediu pentru reconstrucția ecologică a zonei Fusea - județul Dâmbovița, România -, pg 15-65, Bucharest;

GEOLOGICAL - METALLOGENETIC CONSIDERATIONS BASED ESPECIALLY ON GEOPHYSICAL DATA FOR BUCIUM - ROŞIA MONTANĂ – ROŞIA POIENI AREA

Justin ANDREI
Geological Institute of Romania, *paul.cristea@igr.ro*

Keywords: Bucium - Roşia Montană - Roşia Poieni batholith, geophysical-geological data, porphyry copper, epithermal gold-silver deposits

In January 2011, I decided to look for identification and geophysical investigation of unknown subvolcanic and hipabyssal bodies bearing rich gold-silver mineralization (indicative content 30g/t gold), in the Roşia Montană – Bucium mining district. Epithermal large deposits in the form of veins and stockwork exploited in this district (now exhausted) have been discovered since Roman antiquity, namely: Cetate, Cârnic, Igre – Văidoaia, Ţarina – Orlea, Jig, in Roşia Montană area, and Frasin hill and Bucium-Rodu, in Bucium area, north of the homonymous valley. All these deposits are located in the Kossovian subvolcanic dacite bodies or placed in the cap of such major structures (Ţarina – Orlea and Bucium-Rodu, respectively). Geological common sense suggests that the potential for gold-silver accumulation of this district is still very high. Highlighting the remarkable potential of this must take place on two levels: the "strategic" and "tactical".

On the **"strategic" level** the area of existence of gold-silver mineralization epithermal type, polymetallic ± gold-silver, respectively copper - gold - silver ± molybdenum porphyry copper type defined by Bucium – Roşia Montană – Roşia Poieni pluton. Unlike previous conceptions (Socolescu, fide Cristescu et al., 1970) this is not a granite pluton, even on the ground that the gravimetric image does not show a major regional minimum. Also surface geological data do not show the presence of some rhyolite subvolcanoes. Instead, according to these data, at surface appear volcanoes and subvolcanoes with quartziferous andesite and dacite composition. Therefore, the aforementioned pluton has a quartz diorite – granodiorite composition with a distinct metallogenetic specialization. Thus, quartz diorite component favored the existence of porphyry copper type deposits Roşia Poieni and Bucium Tarniţa. Opportunity to discover new porphyry copper deposits in this area is excluded because the interpretation of geophysical data (Andrei, Calotă, 1975; Andrei, 1983) eliminates the problem.

Delimitation of the Bucium – Roşia Montană – Roşia Poieni pluton I made it with high accuracy using high-quality regional geologic maps (Ghiţulescu, Socolescu, 1941; Bordea et al., 1979) and aero-magnetic images in research (Cristeascu et al., 1964) and detailed network (Cristescu et al., 1970), deciphered with petromagnetic investigations support (Andrei et al., 1972; Andrei, Nedelcu, 1974; Andrei, 1983). Fig. 1 show the outline obtained. This contour closes an area of $112km^2$, so the Bucium – Roşia Montană – Roşia Poieni quartz diorite - granodiorite pluton is a batholith. According to radiometric age determinations by K-Ar method (Roşu et al., 1997; Roşu et al., 2004) this batholith was put in place in Langhian (13.5 to 14.87 M.y.) as a result of the lithospheric expansion process. Subsequent eruptions of andesites with brown hornblende and pyroxene of Rotunda type-Pannonian age (9.3 M.y.), and basaltic andesites of Detunata were put in place to the Pannonian - Pontian limit (7.4 M.y.).

Epithermal gold-silver mineralization in the Bucium – Roşia Montană district is associated mainly with sub-volcanic dacite bodies. However in the Izbicioara valley - Boteş hill – Vâlcoi area, where gold-silver or polymetallic (Zn, Pb, Cu ± Au, Ag) veins occur, it seems that we are in the presence of peri-plutonic metal products, sometimes with significant economic value.

Parallel with Izbicioara valley - Boteş hill metallogenic fracture is known since ancient Roman the Corabia peak – Arama hill vein-system, east of Conţu hill (Vipere), associated with andesitic bodies and in the north with Conţu dacite. This vein-system is generally oriented NNW-SSE and has a length of 4km. It is the longest system veins in the Metaliferi Mountains, apparently compact, but gold and silver mineralization characterized essentially only the outer edges, with a major share in the Corabia group. In the median part the Arama, Argint, Aur and Nepomuc veins group has a diversified mineralization (Au, Ag, Cu with content of Ge). The significant presence of copper seems to be closely associated with the ENE plunge of porphyry copper Bucium Tarniţa structure. This plunge is strongly suggested by geophysical data (especially magnetometric and natural potential) (Andrei, Calotă, 1975), partially verified by drilling and attested by the presence of a mineralization in Arama vein's top, Bucium Tarniţa type (magnetite, pyrite, chalcopyrite), visible to the surface (Andrei, Andrei, 1974).

On **the "tactical" level**, share of geophysical methods to identify unknown gold-silver epithermal mineralization is decisive. Because, in essence, identifying gold-silver mineralization reduced to the discovery of unknown dacite bodies, in a first stage we must emphasize structures that do not intersect the current topographic relief. In this respect, note that all subvolcanic dacite bodies with gold-silver mineralization from Bucium – Roşia Montană mining district, which pierce at surface the Cretaceous sedimentary formations, determine the minimum gravity anomalies (Andrei et al., 1966).

For this purpose we filtered the detailed-network Bouguer gravimetric map, achieved by Prospecțiuni S.A. (Sava, 1970; Zorilescu, 1971) in type-level residual images.

By analyzing the gravimetrical results in the context of mining-geological, magnetometric, electrometric and pedogeochemical existing data (Ghițulescu, Socolescu, 1941; Andrei et al., 1972; Dinu et al., 2011) we selected ten residual gravity minima reflecting, very likely, mineralized dacite bodies which are below current topographic relief. Of these the most important are:

1) The gravity minimum south of Cetate quarry framed by Limpedea and Găuri creeks (right-tributaries of Corna brook) and bounded to the south of Corna fault. It has an extension comparable to the residual gravity minimum corresponding with the Cetate subvolcanic body. South Cetate (Corna) residual gravity minimum's area is fully covered by post-Rotunda sedimentary breccias with magnetite, which explains that the dacite sub-volcano is unknown to date. There are great chances to have to deal with the **most important structure with rich gold-silver mineralization found at Roșia Montană in the last two millennia**. Probably will provide underground mining for at least a century;

2) The strong residual gravity minimum from Valea Şesii (north of the Bucium Şasa's church) is located east of the Frasin hill sub-volcanic body, exploited for gold and silver from Roman antiquity. The Valea Șesii gravity minimum reflects the presence of another body, dacitic mineralized body, buried near the topographic surface. An impressive list of geological, electrometrical and pedogeochemical data, prove the metallogenetic character of the Valea Şesii sub-volcanic body;

3) North of Valea Şesii gravity minimum similar anomaly is placed, but elongated north-south, located on the right side of the Arsuri brook. Geological map suggests a not interesting situation, but the results of the pedogeochemical prospects are very encouraging;

4) Most spectacular result of gravity data processing is the alignment of residual minimum Ciungilor hill - Bucium Rodu mine field - south Bucium Muntari, with a length of 2.5 km. We are currently in the presence of the most important sub-volcanic system in the Metaliferi Mountains. The presence of the Bucium Rodu vein-field to the surface and indications provided by geological -mining data south of the Rodu brook and a remarkable volume of electrometrical and pedogeochemical data show that the sub-volcanic deep structure suggest **huge** gold-silver mineralization. Perhaps Bucium mining will be active in this area for some centuries.

These preliminary data will be supplemented by electromagnetic investigations (sounding), including controlled-source and induced polarization, directed and processed with high performance software, and gamma spectrometric, differential magnetometric, high precision gravimetric and oriented samples petromagnetic investigations.

Before concluding this preliminary note I mention that the top of the analyzed batholith four specialized metallogenetic poles are placed. Three of them: the porphyry copper Rosia Poieni, the "gold pole" of Bucium and the porphyry copper system Bucium – Tarnița, are rigorously placed on a major fracture NNW-SSE oriented. In addition, the two porphyry copper systems are placed in areas of crustal permeability (Andrei, Calotă, 1975; Andrei, 1983). The Poieni – Tarnița major fracture has the same orientation as most vein systems from the batholith area and perpendicular to the direction of extension of the crust (Roşu et al., 2004). The Bucium "gold pole" is placed at the intersection of the major fracture with a Mesozoic fault system, as emphasized by Ghitulescu and Socolescu (1935). This feature explains the metallogenetic potential of the Bucium "gold pole", slightly higher than the one from Roşia Montană.

The permeability areas of the crust are manifesting trough compact groups of volcanic and subvolcanic bodies surrounding the central subvolcanic andesitic-microdioritic body which bears the porphyry copper mineralization (like at Roșia Poieni) or on its eastern and western flanks (like at Bucium-Tarnița). In both cases the andesitic-microdioritic body presents a very pronounced fissuration till 1000 m depth.

Acknowledgements

The author expresses eternal gratitude to Professor Toma Petre Ghițulescu, founder of Applied Geophysics School at the Polytechnic University of Bucharest, one of those who laid the first brick building in geophysical prospecting Department of Geological Institute of Romania, under the lead of great geologist Ludovic Mrazec. Among other things the author learned from him that "deposits are found with ideas".

The author gratefully thanks all geophysicists and geologists from the Geological Institute of Romania who have supported the elaboration of this study and especially dr. eng. Anca-Marina Vâjdea, researcher II degree and tech. Gabriel Preda, who drew up the filtration for the residual gravimetric map in Bucium – Roşia Montană mining district.

References

Andrei, J., Calotă, C., Pătruţ, Şt. (1966), Consideraţii structurale asupra zonei erupţiunilor neogene de la Roşia Montană pe baza interpretării cantitative a datelor gravimetrice şi a corelării cu datele magnetometrice. Stud. cercet. Geol. Geof. Geogr. Geofizică, 4, 2, p. 317-336, Bucureşti.

Andrei, J., Calotă, C. (1975), Étude géophysique des corps andésitique de Roşia - Poieni et de Bucium – Tarniţa (Monts Métallifères) a l'aide du modelage des sources des champs potentiels. Rev. Roum. Géol. Géophy. Et Géogr – Géophysique, 19, 113-133, Bucharest. Work rewarded with „Gheorghe Murgoci" prize of the S.R.R. Academy in 1975.

Andrei, J., Ionescu, F., Ciucur, Elvira, Nedelcu-Ion, C. (1972), Sinteza lucrărilor geofizice din eruptivul Munţilor Metaliferi pentru mineralizaţii neferoase şi auro-argintifere (zona Runculeţe – Roşia Poieni), Arh. I.G.R., Bucharest

Andrei, J., Andrei, Cornelia (1974), Raport preliminar asupra studiului geologic şi petrofizic al mineralizaţiei de tip porfiric din D. Tarniţa (Calvaria) Munţii Metaliferi, Arh. I.G.R.- I.G.P.S.M.S., Bucharest

Andrei, J., Nedelcu-Ion, C. (1974), Studii petrofizice în Munţii Metaliferi pentru mineralizaţii cu magnetit, cu privire specială asupra zonei Roşia - Poieni, Arh. I.G.R., Bucureşti

Andrei, J. (1983), Considérations sur quelques indices de prospection des minéralisation type „porphyry copper" des Monts Metaliferi, An. Inst. Geol. Geof. – Geofizică, LXIII, 15-23, Bucharest

Bordea, S., Avram, Şt., Borcoş, M. (1979), Harta geologică a României la scara 1:50.000, foaia Abrud, Inst. Geol. Geof., Bucharest

Cristescu, T., Ştefănciuc, A., Enăchescu, M., Velicu, R. (2011), Prospecţiuni aeromagnetice de detaliu în Munţii Apuseni, Arh. I.G.P.S.M.S., Bucharest

Dinu, C., Stoica, M., Diaconescu, V., Manta, T. (1970), Condiţiile geologice şi seismo-tectonice care controlează seismicitatea lacului de acumulare Corna, Arh. Fac. Geol. Geof, Universitatea Bucureşti, Bucharest

Ghiţulescu, T.P., Socolescu, M. (1935), Relation entre la tectonique et la métallogènese dans le quadrilatere aurifère des Monts Apuseni (Romanie). Extrait du Congrès International des Mines, de la Métalurgie et de la Géologie appliquée, VIIe Session – Paris, 20-26 Octobre, 1935

Ghiţulescu, T.P., Socolescu, M. (1941), Étude géologique et minière des Monts Métallifères, An. Inst. Géol., Roum., XXI, Bucarest

Milu, Viorica (2006), Roşia Poieni ore deposit. Fifth National Symposium on Economic Geology, 2006, Albac, Alba, Romania

Petrulian, N. (1934), Étude chalcographique du gisement aurifère de Roşia Montană (Transylvanie, Roumanie), An. Inst. Géol. Roum., XVI, Bucharest

Roşu, E., Pecskay, Z., Ştefan, A., Popescu, Gh., Panaiotu, G., Panaiotu, Cristina Emilia. (1997), The evolution of Neogene volcanism in the Apuseni Mountains (Romania). Constrains for new K-Ar data. Geologica Carpatica, 48, 6, 353-359, Bratislava

Roşu, E., Seghedi, I., Downes, Hilary, Alderton, D., Szakács, A., Pecskay, Z., Panaiotu, C., Panaiotu, Cristina Emilia., Nedelcu, L. (2004), Extension-related Miocene calc-alcaline magmatism in the Apuseni Mountains, Romania: Origin of magmas. Schweizeriche Mineralogische und Petrographische Mitteilungen, 84, 153-172, Helvetia

Fig. 1. Geological map of Romania, scale 1:50.000, Abrud sheet (Bordea et al., 1979), with the contour (red line) of the Bucium – Rosia Montana – Rosia Poieni granodiorite – quartz diorite batholite, obtained from the geologic-metallogenetic and aeromagnetic maps.

ASPECTS OF THE PROCESS OF PRELIMINARY ASSESSMENT OF THE IMPACT ON THE ENVIRONMENT FOR THE ACTIVITY OF EXPLOITATION OF THE COPPER-GOLD ORE FROM THE ROVINA MINING PERIMETER

Mircea MĂNESCU[1], Sanda MĂNESCU[1], Sorin POP[2], Alexandru NICOLICI[3]

[1] S.C. ECOTERRA ING S.R.L. Baia Mare, ecoterraing@ymail.com

[2] S.C. TRIPART CONSULTING S.R.L. Baia Mare, geommed@gmail.com

[3] S.C. SAMAX ROMANIA S.R.L. Baia Mare, sasha@samax.ro

1. Introduction

The project of mining plant of the copper-gold ore from the Rovina mining perimeter (Rovina Mining Project) proposes activities of simultaneous exploit of the copper-gold deposits of Rovina, Colnic and Valea Gârzii-Cireşata through surface mining work (Rovina and Colnic quarries) and through undergroung mining work (Valea Gârzii-Cireşata mine), integrated with activities of preparation of the extracted ore.

The preliminary impact assessment on the environment was made in the period of elaboration/ finalisation of the Feasibility Study for the mining project, phase of designing that precedes the development of the Technical Project.

Certainly, the activity of exploitation of the natural resources through daily mining works and/ or through undergroung mining works is an activity with a high potential of impact on the environment. Here comes the necessity of the approach with lots of attention, accuracy and exigency of the relationship between the projected activity and it's impact over the environment, the impact assessment of the projected actions over the environment having to be made preponderant quantitative. Unfortunately, the data that might be used for quantitative environment assessment become available, in most cases, only in subsequent phases to projection, respectively after the finalisation of the Technical Project for the respective mining activity.

The mining projects have another particularity, too: the disponibility of the companies having mining projects to sustain the elaboration of some speciality studies that would define the initial state of the quality of environmental factors is minimum untill they have the certainty that the exploitation of the natural resources, as it was projected, is feasible and that, in principle, is accepted by the authorities/ institutions interested in the project. This leads to the fact that most of the evaluations relating to the initial state of the environment factors cannot be made other than quantitative, using only the existent public data. Currently, this kind of data have a high degree of generality and aren't enough actual.

The reduced availability of the companies to invest in environment assessments in this stage of the project is retrieved in the low number of concrete available elements for aplying some models that would allow the forecast over the evolution in time of the quality of environment factors.

In other words, the environment assessment for the mining project in the phase of elaboration of the Feasibility Study for the respective project, must be made starting from summary data about the quality of the environment factors at the moment of project elaboration and using a reduced number of elements in the shapings (pojections) regarding the evolution of the environment factors' quality.

At first sight, such an approach of an environment assessment seems a nonsense. Considering the fact that in the subsequent phases of the project lifetime the data needed for an adequate environment assessment will be certainly available, which is the usability of an environment assessment (in the phase of the feasibility analysis of the project) using, mostly, data with general character?

But, starting from the principle that environment assessment is a iterative and continuous process during the entire lifetime of a project, the role of the environment assessment in the phase of the feasibility analysis of a mining project starts to outline the gain.

In the case of the Rovina mining project, the role of an environment assessment in the early phase of the projection process was emphasized too by the manner in which S.C. SAMAX ROMANIA S.R.L. chose to approach the mining project, even from the phase in which the geological works were finished.

2. Specific problems

The most important data with public character refering to the results of the geological research were presented within public assemblies, where were invited all the inhabitants of the area in which the geological exploration works were carried on. The transition in the next stage, that of the feasibility study elaboration, was made only after the company that conducted the geological research work (S.C. SAMAX ROMANIA S.R.L.) and the inhabitants of the area agreed on: the opportunity of the transition from the geological research phase to the phase of expolitation of resources carried forth through the works of geological exploration; the functionality of the fields from the perimeter of mining exploitation after the end of the mining works.

Very important was the fact that both parties (the company and the area inhabitants) assumed the fact that the exploitation period of the copper-gold deposits might generate impacts over the environment and the inhabitants of the area, but that these impacts could also be avoided, minimized and/or compensated through adequate projection and administration of the mining works.

Starting from this phase, in the entire process of planning the future mining activity participated four important actors: the company, the specialty designers, the environment specialists and the community.

The final version of the project (the one analysed within the Feasibility Study and in the Report regarding the impact assessment on the environment) was chosen after many variants of the project were completed and analysed, each one with several technical solutions, chosing, for each project, the solutions that answered the demands of each party of the four involved.

From the perspective of all the parties involved, in this stage of the project's lifetime the first importance of the environment assessment consists in identification of the technological processes with impact over the environment, of the probable impact area and the environment factor/s on who will reverberate that impact. These first conclusions are:

- ➢ The main mining activities will unfold on four locations (Rovina quarry, Colnic quarry, V. Gârzii-Cireşata mine and the ore processing plant), but, for sustaining the main mining activities, other ground surfaces will also be covered (settling ponds, tailling dumps, ore deposit, plant soil deposit, access roads, pipelines trails, etc.).
- ➢ All the locations where activities of explotation of the ore and all the locations that support operating mining activities will be afected, from the perspective of the quality of the environment factors, of the activity undertaken.
- ➢ From the quality of soil perspective, the first areas of land afected will be those where will be built the Rovina and Colnic quarries, the settling ponds, the tailling dumps, the saracen ore deposit, the ore preparation plant, the industrial roads. For these areas of land, the impact over the soil will be direct, in principal, due to the removal of vegetable soil and the changing of the category of land use.
- ➢ In the area location of V. Gârzii-Cireşata mine, an important area of land will be affected by phenomens of immersion, due to the settlement of underground mining works.
- ➢ The quality of subsoil will be affected only in the area where the ore will be exploited. In Rovina and Colnic qarries and V. Gărzii-Cireşata mine, the ore extracted will be replaced entirely or partial with sterile material.
- ➢ The underground water and the surface water won't be significant affected by the projected activity.
- ➢ Installations are equipped in order to allow carrying out treatment of water unloaded in natural receptors, so that sensitive changes of their quality should not occur.
- ➢ The quality of the air will be affected by the particulate matter issued by pathways on motor transport and by plant ore processing. The area in which it will be felt particularly the influence of the designed activity over the air quality will be the area bounded to the North and South by Rovina and Colnic quarries. In this area are included also the farmhouses of the population from the West of Rovina and Merisor localities.

3. Main types of impacts

The general conclusions were separated for each particular environmental factor, as it follows:

3.1 The surface and underground water

- The mining activity in the perimeter of exploitation Rovina will not sensitively change the quality of surface water.
- Downstream of all mining constructions, the quality indicators of surface water will remain at approximately equal values with the actual values.
- It is foreseen a programme for monitoring the quality of water discharged into surface water courses and intervention measures are provided, in case the water originating from activities designed does not fall within acceptable limits.
- There are not foreseen quantitative or qualitative changes of the bodies of groundwater.
- There are not foreseen qualitative or quantitative changes to water sources in the area of the locality of exploitation.

3.2 Soil and subsoil

- The impact of mining activities on the quality of the soil will be felt during the period of the expoitation works and will consist, in particular, in the removal of soil from the areas intended for mining works. The impact will be local and will not extend on the soil surfaces from the exploitation perimeter that will not be efectively occupied by constructions/ objectives related to mining activities.
- The closure of mining works will also bring a reunification of land areas covered with soil, even if the destination of lands will no longer be the same as the initial.

3.3 Air

- The air quality will be clearly affected by the activities that will take place within the perimeter of Rovina exploitation.
- The main problems will be those related to the significant quantities of particulate matter and sedimentable dust which will be emitted to the atmosphere by all operations specific to mining activity, but mainly by truck transport operations of mining mass and the primary ore crushing operations.
- Throughout the period of exploitation strict measures will have to be applied in order to reduce emissions of particulate matter and stringent measures to monitor the effectiveness of measures applied for reducing atmospheric emissions of particulate.
- It is possible that, no matter how severe will be the measures to reduce air emissions of particulate matter, may not be able to ensure the maintenance of a proper quality of the air in the household area being at relatively small distances from transport industrial auto routes and from the Rovina and Colnic quarries.

3.4 Noise and vibrations

- The noise level generated by the future activity will be significant and will be clearly felt by at least some of the inhabitants of the settlements Rovina and Merişor.
- There will be necessary the application of a set of measures to restrict the noise level on the limits of the mining precinct and at the protected receptor's limit and the application of a monitoring program to verify the effectiveness of these measures.
- With all measures limiting the noise it is possible that, for some of the households located at small distances of industrial and transport routes and at small distances from the Colnic and Rovina quarries, might not be able to ensure an acceptable level of noise.
- Through the use of modern techniques for detonation of explosive materials used in quarries, the level of vibrations afferent to the use of explosive materials for breaking the rocks from the quarry can be kept within acceptable limits for the residents of the area.
- It is possible that, for some of the households located at small distances of the industrial transport routes and at small distances from the Colnic and Rovina quarries, the transport of ore and dump tips with high capacity might generate levels of vibrations higher than acceptable.

3.5 Vegetation and fauna

- Although environmental assessment is barely starting out, and further research must complete some inaccuracies or inconclusive data(some species occurring accidentally and/or which have not been observed in the early years of inventory), the main conclusion is that the project zone does not contain significant areas of habitat or important populations of species of national conservative or community interest. The impact on species and the majority of habitats are covered by measures to mitigate that impact. For those habitats mentioned in the chapter of flora and habitats, for which recreating will not be possible, a compensation plan must be realized.
- Detailed plans must be made for relocating the vertebrate species associated with damp habitats affected, of finding and closing the shelters of bats, of relocation of some species of fauna for which this has been proposed in the present document, to compensate for the loss of habitat types which will no longer be able to be recreated. The continuation of these studies, the permanent concern for finding solutions to reduce the impact and to compensate for this is a clear evidence of the company's policy, in order to achieve best practices for conservation the biodiversity of the areas potentially affected by the project and can become an example for other mining companies that would develop projects of this kind in Romania.

3.6 Polluted areas

- Preliminary estimates on the quality of environmental factors in populated areas after starting the mining activity show that, for the vast majority of the inhabitants in the area, the mining activity will not mean a decrease in the quality of the environment.
- However, a number of six households in the western extremity of the Rovina locality will have to relocate, as a result of the location of the Rovina dump on the field currently occupied by these households.
- For some of the households in the western part of the settlements Rovina and Merisor might not be possible to provide an acceptable level of noise, vibration and an acceptable level of atmospheric concentrations of particulate matter.
- From the point of view of the social and economic impact, although there were also identified possible negative effects, the majority effect will be a positive one, of growth of the standard of living of the population, of stabilization and of local and micro-regional economic growth.

The major conclusion resulting from the environmental impact assessment was that, for the most part of the perimeter of exploitation and for the majority of environmental factors considered, the impact of the activity of copper-gold ore exploitation within the perimeters of Rovina exploitation will fall within acceptable limits. The mining activities from Rovina and Colnic quarries and the ore and tips transport activity will generate a significant level of noise and vibration which might affect, over the maximum permissible limits, the population from the western part of the settlements Rovina and Merisor.

4. Identification of the actions to be followed

Having known possible effects of the planned activity on the quality of environmental factors, a first set of measures could be identified in order to avoid/mitigate the environmental impacts:

- location of targets at distances as great as possible from the inhabited places, in little visible spaces, as little visible from the localities and/or from the existing access driveways.
- construction of new roads that will run the activities of motor transport, located at distances as great as possible from the population houses.
- construction of distinct access roads for the use of the population in the area.
- maintaining a permanent good condition of the industrial roads, in order to minimize the amount of dust cleared, and to minimize noise and vibration level.
- use for all activities related to the project, only of some machines in perfect technical state of working.
- the use of effective techniques for minimising the atmospheric particulate emissions from activities in the quarries (breaking with explosive materials, broken materials loading, transport), from the transport activities, from the activities of self storage tips on overburden dumps and from processing activities of ore.
- the use of techniques of detonation of explosive materials/of breaking useful material and sterile from quarries and underground, which would minimize noise and vibration level.
- construction of plant protection curtains in areas in which the industrial activities will be held and at the borders of residential areas. Where will be the case, sound-absorbent panels will be fitted for reducing levels of noise to the limit of the protected receivers.
- reuse of a significant amount of water in the flow of ore processing technology.
- the application of appropriate techniques and procedures to maintain and control the technical condition of the installations used for carrying tips.
- Recirculating the exfiltration of water from the pond in the Lake of decanting. Exfiltration of water evacuation from the pond in surface water courses only during periods of frequent rainfall and only after a verification and an eventual quality correction.
- drainage and tubing of surface water courses (permanent and non-permanent) in the area of location of heaps of sterile, of poor ore deposit and settling ponds, to avoid the water contact of materials stored in mining deposits.
- arrangement of guard channels on the perimeter of heaps of sterile, of poor ore deposit and of settling ponds, to minimize the quantity of water possibly unpurified as a result of the contact with the materials stored in the mining deposits.
- ensure minimum salubrious flows for all surface water courses on which will be built settling ponds.

- the application of appropriate techniques and procedures for ensuring safety in the operation of exploitation/functioning of the decanting ponds, of dumps of heaps and of poor ore deposit.

5. Conclusions

Having known the results of preliminary assessments of the environmental impact and the main measures to avoid/mitigate the environmental impacts, the technical project that will establish the basis for future mining activity will be able to consider concrete technical measures which would lead to the elimination, reduction or compensation for each type of activity of the the impact on environmental factors.

The final characterisation of the impact of the mining activity that will run in the exploitation perimeter of Rovina on the quality of environmental factors may be realised after drafting the project/technical projects that will establish the basis for future business development.

– continued from the front cover –